

**DEVELOPING A METHOD FOR PROCESS DESIGN
USING LIMITED DATA: A FISCHER-TROPSCH
SYNTHESIS CASE STUDY**

Peter Mukoma

**DEVELOPING A METHOD FOR PROCESS DESIGN
USING LIMITED DATA: A FISCHER-TROPSCH
SYNTHESIS CASE STUDY**

Peter Mukoma

A thesis submitted to the Faculty of Engineering and the Built Environment,
University of the Witwatersrand, in fulfilment of the requirements for the degree
of Doctor of Philosophy.

Johannesburg, 2006

DECLARATION

I declare that this thesis is my own, unaided work, except where otherwise acknowledged. It is being submitted for the degree of Doctor of Philosophy at the University of the Witwatersrand, Johannesburg. This thesis has not been submitted before for any degree or examination at any other university.

Peter Mukoma

Signed this _____ day of _____ 20____

LIST OF PUBLICATIONS AND PRESENTATIONS

1. P. Mukoma, B.R. Jooste, H.C.M.Vosloo, Investigation of new materials for Direct Methanol Fuel Cell (DMFC) proton exchange membranes. 7th NorthWest/Botswana Universities Chemistry Symposium, 11th October, 2002, Gaborone, Botswana.
2. P. Mukoma, B.R. Jooste, H.C.M.Vosloo, Synthesis and characterization of cross-linked chitosan membranes for application as alternative proton exchange membrane materials in fuel cells. **Journal of Power Sources** 136 (2004) pp16- 23.
3. P. Mukoma, B.R. Jooste, H.C.M.Vosloo, A comparison of methanol permeability in Chitosan and Nafion 117 membranes at high to medium methanol concentrations. **Journal of Membrane Science** 243 (2004) pp 293 - 299 (refereed by a panel of experts).
4. T. Ngwenya, D. Hildebrandt, D. Glasser, N. Coville and P.Mukoma, **Fischer-Tropsch Results and their analysis for reactor synthesis**, Ind. Eng. Chem. Res. 2005, 44, 5987-5994.
5. P. Mukoma, V. Ngwenya, D. Hildebrandt, D. Glasser and N. Coville. **The Integration of Process Synthesis into an experimental program for Fischer-Tropsch Synthesis (FTS) chemistry**. Catalysis Conference 2003, Durban, 9 – 12 November.
6. P. Mukoma, V. Ngwenya, D. Hildebrandt, D. Glasser and N. Coville. **Fischer-Tropsch Results and their analysis for Process Synthesis**. AIChE Conference, Austin, Texas, USA, 7-12 Nov 2004.
7. P. Mukoma, D. Hildebrandt and D. Glasser. **The Integration of Process Synthesis into an experimental program for Fischer-Tropsch Synthesis (FTS) chemistry**. World Chemical Engineering Congress, Scotland, July 2005.
8. P. Mukoma, D. Hildebrandt and D. Glasser, **A Process Synthesis approach to investigate the effect of the probability of chain growth and conversion on the efficiency of the Fischer-Tropsch Process**, Ind. Eng. Chem. Res. 2006, 45, 5928 – 5935.

9. P. Mukoma, D. Hildebrandt and D. Glasser, **Synthesizing a Process from Experimental Results: A Fischer-Tropsch Case Study**, Ind. Eng. Chem. Res. 2007, 46, 156 – 167.

10. P. Mukoma, D. Hildebrandt and D. Glasser, **Screening the effect of the probability of chain growth on the efficiency of the Fischer-Tropsch Process Design**. AIChE Annual Meeting, Cincinnati, Ohio, USA, October 30 –November 4, 2005.

11. D. Brink, D. Hildebrandt, D. Glasser and P. Mukoma. **Determination of the effect of water and Carbon Dioxide addition into the reactor feed in Fischer-Tropsch Synthesis**. AIChE Annual Meeting, Cincinnati, Ohio, USA, October 30 –November 4, 2005.

12. P. Mukoma, D. Hildebrandt, D. Glasser, N. Coville, G. Jacobs and Burtron H. Davis, **Fischer – Tropsch Synthesis: A study of the effect of water on a cobalt catalyst**. Presented at the South African Chemical Engineering Congress (SACEC) September, 2006.

ABSTRACT

Most of the available tools and methods applied in the design of chemical processes are not effective at the critical early stages of design when the process data is very limited. Businesses are often under pressure to deliver products in shorter times and this in turn prevents the evaluation of options. Early identification of options will allow for the development of an experimental program that will support the design process.

The main objective of this work is to apply the Process Synthesis approach to develop a structured method of designing a process using mostly qualitative information based on limited experimental data, prior experience, literature and assumptions. Fischer-Tropsch (FT) synthesis of hydrocarbons from syngas generated by reforming natural gas and/or coal has been used as a case study to illustrate this method. Simple calculations based on experimental data and basic thermodynamics have been used to generate some FT Synthesis flowsheet models. The evaluation of different flowsheet models was done using carbon efficiency as a measure of process efficiency.

It was established that when choosing the optimal region for the operation and design of an FT Synthesis process, the influence of the system parameters must be well understood. This is only possible if the kinetics, reactor, and process design are done iteratively. It was recommend not to optimize the reactor independent of the process in which it is going to be used without understanding the impact of its operating conditions on the entire process. Operating an FT Synthesis process at low CO per-pass conversions was found to be more beneficial as this will avoid the generation of high amounts of methane which normally results in large recycles and compression costs.

Whether the process is run as a once-through or recycle process, the trend should be to minimize the formation of lighter gases by obtaining high α values because

carbon efficiency increases with the increase in α value. Experiments should be performed to obtain process operating conditions that will yield high α values.

However, if the aim is to maximize diesel production by hydrocracking long chain hydrocarbons (waxes), then an optimal α value should be targeted to avoid the cost of hydrocracking these very heavy waxes. The choice of the syngas generation technology has a direct impact on the carbon efficiency of an FT synthesis plant. This study has established that running an FT synthesis process with syngas obtained by steam reforming of natural gas with CO₂ addition can yield high carbon efficiencies especially in situations where CO₂ is readily available. In FT synthesis, CO₂ is normally produced during energy generation and its emission into the environment can be minimized by using it as feed during the steam reforming of natural gas to produce syngas.

ACKNOWLEDGEMENTS

Thanks be to God, the most high.

I wish to sincerely thank my supervisors, Professor Diane Hildebrandt, Professor David Glasser and Professor Neil Coville, for their guidance, inspiration and sound advice throughout the period of my study. It has been a privilege for me to study under their supervision.

At the Center for Applied Energy Research (CAER), University of Kentucky, Lexington, USA, I would like to thank Burtron Davis and his research group for giving me an opportunity to work in their catalysis laboratory.

I am very grateful to the staff and post grad students at COMPS for providing a stimulating and fun environment in which to learn and grow. Thank you guys in Richard Ward 310(Bilal Patel, Geoffrey Ngigi, Tshepo Modise, Olufemi Fasemore and Mr Tabrizi) for all the discussions and good company.

Finally, I would like to thank all my friends and family, particularly my mum and dad, for their support. A special thank you to Alex and his wife Vili, their kids Kaluba and AJ, for their love and hospitality. I could not have finished writing this thesis without the support of my wife Musa, honey, thank you for believing in me.

CONTENTS

DECLARATION.....	II
LIST OF PUBLICATIONS AND PRESENTATIONS.....	III
ABSTRACT.....	V
ACKNOWLEDGEMENTS.....	VII
CONTENTS.....	VIII
LIST OF FIGURES.....	XI
LIST OF TABLES.....	XVIII
LIST OF SYMBOLS AND ABBREVIATIONS.....	XIX
1 INTRODUCTION.....	1
1.1 MOTIVATION.....	1
1.2 THESIS OUTLINE.....	2
1.3 REFERENCES.....	4
2 FISCHER-TROPSCH RESULTS AND THEIR ANALYSIS FOR REACTOR SYNTHESIS.....	5
2.1 INTRODUCTION.....	6
2.2 EXPERIMENTAL.....	7
2.2.1 Catalysts preparation.....	7
2.2.2 Experimental set-up and procedure.....	7
2.2.3 Product analysis.....	10
2.3 RESULTS AND DISCUSSION.....	11
2.3.1 Influence of Partial Pressures and Feed Ratios of H ₂ /CO on the Rate of CO Consumption.....	11
2.3.2 The effect of Partial Pressures and Feed Ratios of H ₂ /CO on the Rate of CH ₄ production.....	18
2.3.3 The Effect of the Partial Pressures and Feed Ratios of H ₂ /CO on the Rate of Hydrocarbon Production per mole of CO consumed.....	24

2.4	CONCLUSION.....	30
2.5	REFERENCES.....	32
3	SYNTHESIZING A PROCESS FROM EXPERIMENTAL RESULTS: A FISCHER-TROPSCH CASE STUDY.....	34
3.1	INTRODUCTION.....	36
3.2	RATIONALE.....	37
3.3	METHODOLOGY.....	39
3.4	SYSTEM DESCRIPTION.....	40
3.5	PROCESS MODELLING - FLOWSHEET DEVELOPMENT.....	42
3.5.1	Air separation and synthesis gas generation.....	42
3.5.2	Fischer –Tropsch Synthesis.....	49
3.6	CONCLUSION.....	67
3.7	REFERENCES.....	68
4	A PROCESS SYNTHESIS APPROACH TO INVESTIGATE THE EFFECT OF THE PROBABILITY OF CHAIN GROWTH ON THE EFFICIENCY OF THE FISCHER-TROPSCH SYNTHESIS.....	71
4.1	INTRODUCTION.....	73
4.2	PRODUCT SELECTIVITY.....	78
4.3	CO CONVERSION.....	80
4.4	DESIGN BASIS.....	80
4.4.1	Reforming Model.....	81
4.5	CARBON EFFICIENCY.....	82
4.6	RESULTS.....	84
4.6.1	The Once Through Process Consisting of Reforming and FT Synthesis Sections.....	84
4.6.2	The Recycle Process.....	86

4.7	WAX HYDROCRACKING.....	89
4.7.1	Carbon efficiency of the once - through and recycle FT process with Hydrocracking of heavier products to diesel.....	91
4.8	CONCLUSION.....	94
4.9	REFERENCES.....	96
5	A COMPARISION OF COAL AND NATURAL GAS FEED MATERIAL FOR FISCHER-TROPSCH SYNTHESIS.....	98
5.1	INTRODUCTION.....	100
5.2	PROCESS FLOWSHEET DESCRIPTION.....	103
5.2.1	Natural gas based Design.....	104
5.2.2	Coal based Design.....	121
5.3	CONCLUSION.....	129
5.4	REFERENCES.....	130
6	OVERALL CONCLUSION.....	131
	APPENDIX I.....	133
	APPENDIX II.....	151

LIST OF FIGURES

Figure	Page
2.1	Schematic diagram of the experimental setup.....9
2.2A	The rate of CO consumption at 220 °C at various partial pressures of CO and H ₂ for 3 different feed ratios. The numbers indicate the rate of CO consumption in μmoles CO/g _{cat} 's. The feed ratio for each set of experiments is indicated on the associated line.....12
2.2B	The rate of CO consumption at 250 °C at various partial pressures of CO and H ₂ for 3 different feed ratios. The numbers indicate the rate of CO consumption in μmoles CO/g _{cat} 's. The feed ratio for each set of experiments is indicated on the associated line.....13
2.3A	A plot of (1/r _{CO}) versus partial pressure of H ₂ at 220 °C. Each curve corresponds to a different feed ratio of H ₂ /CO as indicated in the legend. The dimensions of the rate of CO consumption are μmoles CO/g _{cat} 's.....15
2.3B	A plot of (1/r _{CO}) versus partial pressure of H ₂ at 250°C. Each curve corresponds to a different feed ratio of H ₂ /CO as indicated in the legend. The dimensions of the rate of CO consumption are μmoles CO/g _{cat} 's.....16
2.4A	The rate of CH ₄ production at 220 °C at various partial pressures of CO and H ₂ for 3 different feed ratios. The numbers indicate the rate of CH ₄ production in μmoles CH ₄ /g _{cat} 's. The feed ratio for each set of experiments is indicated on the associated line.....19

2.4B	The rate of CH ₄ production at 250 °C at various partial pressures of CO and H ₂ for 3 different feed ratios. The numbers indicate the rate of CH ₄ production in μmoles CH ₄ /g _{cat} ·s. The feed ratio for each set of experiments is indicated on the associated line.....	20
2.5A	A plot of (1/r _{CH₄}) versus partial pressure of H ₂ at 220 °C. Each curve corresponds to a different feed ratio of H ₂ /CO as indicated in the legend. The dimensions of the rate of CH ₄ consumption are μmoles CH ₄ /g _{cat} s.....	22
2.5B	A plot of (1/r _{CH₄}) versus partial pressure of H ₂ at 250 °C. Each curve corresponds to a different feed ratio of H ₂ /CO as indicated in the legend. The dimensions of the rate of CH ₄ consumption are μmoles CH ₄ /g _{cat} s.....	23
2.6A	Effect of the partial pressures and feed ratios of H ₂ and CO on hydrocarbon selectivity at 220 °C. The numbers on the graph indicate hydrocarbon selectivity = (r _{CO} - r _{CH₄})/r _{CO} × 100	25
2.6B	Effect of the partial pressures and feed ratios of H ₂ and CO on hydrocarbon selectivity at 250 °C. The numbers on the graph indicate hydrocarbon selectivity = (r _{CO} - r _{CH₄})/r _{CO} × 100	26
2.7A	A plot of (-r _{CO} /r _{CH₂}) vs partial pressure of H ₂ at 220 °C. Each curve corresponds to a different feed ratio of H ₂ /CO as indicated in the legend.....	28

2.7B	A plot of $(-r_{CO} / r_{CH_2})$ vs partial pressure of H_2 at $250\text{ }^\circ\text{C}$. Each curve corresponds to a different feed ratio of H_2/CO as indicated in the legend.....	29
3.1	Flow sheet for syngas production and air separation.....	44
3.2	Distillation process modelled as a set of heat engines.....	45
3.3	Detailed flowsheet for air separation modelled as thermodynamic engines.....	47
3.4	Process flow sheet showing air separation and syngas generation stages.....	48
3.5	Flowsheet with air separation, syngas synthesis, and FTS reactor.....	53
3.6	Rates of CO conversion measured at various space velocities for $P=8\text{ bar}$ and $T=220\text{ }^\circ\text{C}$ (The lines on the graphs have no significance other than to group the points together that have the same feed concentration).....	54
3.7	Product molar flow rates at various CO conversions for the reaction at $220\text{ }^\circ\text{C}$ and 8 bar	55
3.8	Product molar flow rates at various CO conversions for the reaction at $250\text{ }^\circ\text{C}$ and 8 bar	57
3.9	Flowsheet with ideal separation and perfect reforming.....	58

3.10.	Carbon Efficiency for the process assuming Perfect Reforming and Ideal Separation at 220 °C.....	59
3.11	Flowsheet development by assuming ideal separation, Perfect Reforming and Compression of the recycle stream.....	61
3.12	Carbon Efficiency for the process assuming Perfect Reforming, Ideal Separation and Compression.....	63
3.13	Flowsheet with CH ₄ /-CH ₂ - separation, compression, air separation and reforming.....	63
3.14	Carbon efficiency for the process with the incorporation of the CH ₄ /-CH ₂ - separation unit.....	64
3.15	Percentage energy demands for the various operations at various space velocities, CO conversions and H ₂ : CO =1:1 at 220 °C.....	65
3.16	Carbon efficiency as a function of methane formation.....	66
4.1	Probability of chain growth (α) as a function of the weight factor.....	79
4.2	Simple model showing variables considered in carbon efficiency Calculations.....	82
4.3	Fischer-Tropsch Synthesis (FTS) flowsheet in a once-through process with 100% conversion.....	85
4.4	Carbon Efficiency and moles of lighter gases formed as a function of alpha for the once through process, 100 % overall carbon efficiency.....	86

4.5	FTS flowsheet with a lighter gas recycle stream.....	87
4.6	Comparison of carbon efficiencies at different α values in once-through and recycle processes at 100% conversion.....	88
4.7	FTS flowsheet with a lighter gas recycle stream and wax (C ₁₉₊) hydrocracking.....	92
4.8	Carbon efficiency as a function of α in a once-through and recycle process.....	93
5.1	A once-through FT Process flowsheet utilizing syngas from steam reforming of natural gas with a CO ₂ feed without wax hydrocracking.....	106
5.2	A once-through FT process model based on syngas obtained from the partial oxidation (POX) of natural gas using compressed air without wax hydrocracking.....	106
5.3	Carbon efficiencies at various α values in a once-through FT process based on syngas production from natural gas using two different processes at 100% CO conversion.....	108
5.4	A once – through FT Synthesis process flowsheet with wax (C ₁₉₊) hydrocracking	110
5.5	Carbon efficiencies at various α values in a once-through FT process based on the two syngas production processes at 100% CO conversion.....	111
5.6	A separation process driven by heat input.....	113

5.7	A distillation process modelled as a heat engine.....	115
5.8	Carbon efficiency at various α values for a once-through FT Process with wax hydrocracking at 100% CO conversion.....	116
5.9	An FT synthesis process flowsheet for a recycle process with syngas obtained from steam reforming of natural gas with CO ₂	117
5.10	FT synthesis process flow model for a recycle process with syngas obtained by partial oxidation of natural gas using oxygen obtained from an oxygen plant.....	118
5.11	Carbon efficiency at various α values for the recycle FT process without hydrocracking.....	119
5.12	Carbon efficiency at various α values in the recycle process with wax hydrocracking at 100% CO conversion.....	120
5.13	Process flow model for a once-through FT synthesis process based on syngas obtained by coal reforming with compressed air.....	122
5.14	FT synthesis process flowsheet for a recycle process with syngas obtained by steam reforming of coal using oxygen obtained from an oxygen plant.....	123
5.15	A comparison of carbon efficiencies at various α values in the once-through FT process based on coal and natural gas reforming without wax hydrocracking.....	124

5.16	A comparison of carbon efficiency at various alpha values in the once-through FT process based on coal and natural gas reforming with wax hydrocracking.....	125
5.17	A comparison of carbon efficiencies at various α values in the recycle FT process based on coal and natural gas reforming without wax hydrocracking.....	127
5.18	A comparison of carbon efficiencies at various alpha values in the recycle FT process based on coal and natural gas reforming with wax hydrocracking.....	128

LIST OF TABLES

Table	Page
2.1A Operating conditions for the optimal reactor and the resulting process for converting a given amount of CO in the smallest possible reactor.....	18
2.1B Operating conditions for the optimal reactor and the resulting process for minimizing the production of CH ₄ for a given amount of CO converted.....	24
2.1C Operating conditions for the optimal reactor and the resulting process for maximizing hydrocarbon selectivity.....	30

LIST OF SYMBOLS AND ABBREVIATIONS

ASU	Air Separation Unit
BET	Brunauer-Emmet-Teller
BHJ	Barrett-Joyner-Halenda
CE	Carbon efficiency
C_p	Heat capacity at constant pressure (J/mol.K)
CPO	Catalytic Partial Oxidation
CSB	Continuously Stirred Basket
CSTR	Continuously Stirred Tank Reactor
C_v	Heat capacity at constant volume (J/mol.K)
C_n	Carbon number n
FID	Flame Ionization Detector
FTS	Fischer-Tropsch Synthesis
GC	Gas Chromatography
i.d	Internal diameter (mm)
M	Molar flow rate (mol/s)
m_{cat}	Mass of catalysts (g)
N	Number of moles (mol)
P	Pressure (bar)
PF	Plug Flow
Q	Volumetric flow rate (m^3/s)
R	Gas constant (J/mol.K)
r_{CO}	Rate of CO consumption ($\mu mol/g_{cat}\cdot s$)
r_{CH_2}	Rate of hydrocarbon formation ($\mu mol/g_{cat}\cdot s$)
r_{CH_4}	Rate of methane formation ($\mu mol/g_{cat}\cdot s$)
rpm	revolution per minute
SL	Standard Liter
T	Absolute temperature (Kelvin, K)
T_c	Cold temperature (K)
TCD	Thermal Conductivity Detector

T_H	Hot temperature (K)
TPD	Temperature Programmed Desorption
TPR	Temperature Programmed Reduction
W	Work done (J/s)
WGS	Water Gas Shift
wt %	Weight percentage
XRD	X-Ray Diffraction
ΔH	Change in Enthalpy (J/mol)
ΔG	Change in Gibbs free energy (J/mol)
ΔS	Change in Entropy (J/mol)
α	Probability of chain growth
ε_i	Extent of reaction for species i
η	Efficiency
χ_i	Molar fraction of component i

1

INTRODUCTION

1.1 MOTIVATION

Process development usually takes place in an evolutionary way, in which the process flowsheet is developed based on experience and proven best practice rather than on a systematic framework that can generate process alternatives. Although this approach yields useful designs quickly and reliably, it does not promote the use of novel approaches, nor does it allow for the comparison of alternative designs. Since most important decisions regarding product and process development are made early in the life of a project – in the absence of detailed data, the danger of using the traditional approach is that of jumping to a solution before the problem is really understood.

The main objective of this work is to apply the Process Synthesis approach to develop a structured method of designing a process using mostly qualitative information based on limited experimental data, prior experience, literature and assumptions. The generation of simple qualitative models in the early stages of design can help in the identification of alternatives and also help to steer future experimental and process development programs. The identification of a potential process alternative is not in itself a guarantee that it can be made to work, but that experimental work will be required to support the suggested alternatives.

During process design the designer makes a selection of the various process units and how to interconnect them to create a flowsheet. Process Synthesis is an act of determining the optimal interconnections of these process units as well as the optimal type and design of the units within a process system of interest. Although some publications existed earlier, Process Synthesis was largely ignored as a research area until the late 1960's when Rudd and his students sought to create a computer program

called AIDES, which could, with limited information, develop almost automatically the structure of a preliminary process flowsheet (Rudd, 1968). Early reviews on the field of process synthesis can be found in Hendry et al., 1973), Westerberg (1980), Nishida et al., 1981, Umeda (1983) and Stephanopoulos and Townsend (1986).

Fischer-Tropsch (FT) Synthesis has been used as a case study to demonstrate how this proposed method can be used to synthesize alternative process configurations. The FT Synthesis reaction produces environmentally clean fuels and chemicals from a gas mixture of carbon monoxide and hydrogen commonly called synthesis gas using various process configurations and operating conditions. Synthesis gas is normally obtained by reforming coal and/or natural gas. Although fairly standard, the main process steps can vary depending on the feed stock, syngas synthesis methods and desired products. Depending on their objective functions, each process will have its own constraints and drivers. One way of evaluating the viability of a process under development is by costing its energy, work, and material (feedstock) requirements. The methodology adopted in this study which mostly relies on basic mass and energy relations, thermodynamic principles and available rate and process data, has been developed in our research group (COMPS) and it has been applied before in the optimization of ammonia and methanol production. The rate data used in this study was obtained in our laboratory by a previous postgraduate student (Themba Ngwenya).

1.2 THESIS OUTLINE

Chapter 2 is a study that examined the effects of various reaction conditions such as flow rates, temperatures and CO/H₂ feed ratios on the performance of a Fischer – Tropsch Synthesis process using a cobalt-based catalyst. Process Synthesis concepts were used to investigate the interaction between the optimum regions for reactor operation and experimental results. The effect of various objectives on the optimal

operating regions was also investigated, and its implication for the process design and further experimental program was considered.

A method of synthesizing a FT Synthesis process from experimental results is presented in Chapter 3. The impact of the various unit operations on the entire FT Synthesis process has been studied by turning all their material, energy, and work requirements into one variable, namely carbon efficiency. This will enable us to identify which among the process operations has the biggest impact on plant carbon efficiency. In doing so, bad options will be identified and alternatives developed.

The effect of designing an FT Synthesis process targeting a particular value of the probability of chain growth (also referred to as α value) has been studied in Chapter 4 using simplified FT flowsheet models. This study allows for the screening of the process carbon efficiencies at various α values. Two process configurations –namely, the once-through and recycle processes - have been compared.

In Chapter 5, minimum information has been used to synthesize and compare two possible FT synthesis processes, one based on the coal feed and the other one based on natural gas feed. The carbon efficiencies of the two processes have been compared at the same α values.

An investigation on the effect of water on the catalytic activity of an FT synthesis cobalt catalyst was done experimentally. If suitable process operating conditions and product selectivity are to be obtained to yield high α values, then it is important to know the effects of by-products such as water on the catalytic activity. Since the developed methodology of process synthesis was not applied to this study, it was decided to include it in this thesis as Appendix I.

1.3 REFERENCES

Hendry, J. E., Rudd, D. F and Seader, J. D. (1973), Synthesis in the Design of Chemical Processes, AIChE Journal., 19 (1), pp. 1-15.

Nishida N., Stephanopoulos, G and Westerberg, A. W. (1981), A review of process synthesis, AIChE Journal. 27, pp. 321- 351.

Rudd, D. F. (1968), The Synthesis of System Designs, I: Elementary Decomposition Theory, AIChE Journal., 14, pp. 348.

Stephanopoulos, G and Townsend, D. (1986), Synthesis in process development, Chem Eng Res Des, 64, 160-174.

Umeda, T. (1983), Computer aided process synthesis, Comp Chem Eng, 7 (4), pp. 279-309.

Westerberg, A. W. (1980), A review of process synthesis, In Squires, R. G and Reklaitis, G. V (Eds.), Computer application to chemical engineering process design and simulation, ACS Symp Serial No. 124 (pp. 53 -87), American Chemical Society, Washington D C.

**FISCHER-TROPSCH RESULTS AND THEIR ANALYSIS
FOR REACTOR SYNTHESIS**

This paper has been published in the *Industrial & Engineering Chemistry Research*
2005, 44, 5987 – 5994.

Fischer-Tropsch Results and their Analysis for Reactor Synthesis

Themba Ngwenya¹, Peter Mukoma¹, David Glasser¹, Diane Hildebrandt¹ and Neil Coville²

¹COMPS, School of Chemical and Metallurgical Engineering

²School of Chemistry

University of the Witwatersrand, Johannesburg, Private Bag 3, WITS 2050.

Abstract

The rate of Fischer-Tropsch reaction was studied for various flow rates, temperatures and H₂/CO feed ratios using a cobalt-based catalyst. Process synthesis concepts were used to investigate the interaction between the optimum regions for reactor operation and the experimental results. The effect of various objectives on the optimal operating region was also investigated and the implication of this for the process design and further experimental program was considered.

2.1 INTRODUCTION

Fischer-Tropsch Synthesis is a process in which synthesis gas (H₂ and CO) is converted into a complex multi-component mixture consisting of linear and branched hydrocarbons and oxygenated products. These products are produced in the presence of an iron-based or cobalt-based catalyst.

A literature survey revealed a large volume of literature available on the subject of Fischer-Tropsch Synthesis. In most of the literature, emphasis is placed on reaction and catalysts optimisation (preparation, pre-treatment, metal dispersion, active sites

and support) while the effect of reaction conditions and reactor design has received less attention.

In this paper, the effect of various reaction conditions such as flow rates, reaction temperatures and H₂: CO feed ratios on a cobalt based catalyst were studied in a stirred basket reactor. The data collected from the kinetic studies was used to study the optimum region for the operation of a Fischer-Tropsch reactor. Furthermore, the influence of various objectives on the optimal regions for reactor operation and design was also investigated. The approach used in this study is from the ideas of a new approach to process synthesis (Glasser et al. (1999)).

2.2 EXPERIMENTAL

2.2.1 Catalyst preparation

A 0.25 wt % Ru/10 wt % Co/TiO₂ catalyst was prepared by incipient wetness impregnation of a TiO₂ support with cobalt nitrate and a ruthenium complex (Richardson, 1989). The ruthenium source was loaded as [Ru₃O(OCOCH₃)₆(H₂O)₃][OCOCH₃], which was prepared according to the method described by Spencer & Wilkinson (1972). The catalyst was then dried at 120°C for an hour and thereafter calcined at 400 °C and atmospheric pressure for 16 h. For convenience, 0.25 wt % Ru/10 wt % Co/TiO₂ will be referred to as the Ru/Co/TiO₂ catalyst.

2.2.2 Experimental set-up and procedure

The kinetic studies of the Ru/Co/TiO₂ catalyst were performed on an experimental set-up consisting of feed, reactor and analysis section. A schematic diagram for the experimental set-up is shown in Figure 2.1.

Feed gases were ultra high purity H₂, CO and N₂, which were supplied from individual cylinders. These gases were mixed to a required feed composition of H₂, CO and N₂. The H₂ and CO ratio was varied from 1:1 to 4:1, while the N₂ was kept constant at a composition of 10 vol %. The total gas flow rates for each feed composition were also varied. For the H₂:CO feed ratio of 4:1, the total gas flow rates were varied from 0.31 to 0.95 mL/s, while the total flow rates for the feed ratios of H₂:CO = 2:1 and 1:1 were varied from 0.19 to 0.95 mL/s and 0.12 to 0.95 mL/s, respectively. The N₂ gas was used for mass balance purposes. The reaction temperatures used for the reaction were 220 °C and 250 °C.

A continuously stirred basket (CSB) reactor whose design is similar to the Berty reactor (Berty, 1974) was used. A detailed description of this reactor is available in the work of Price (1994). The baskets of the CSB reactor were loaded with 3.58 g of Ru/Co/TiO₂ (calcined) catalyst, with a particle sizes ranging from 850 to 1180 μm.

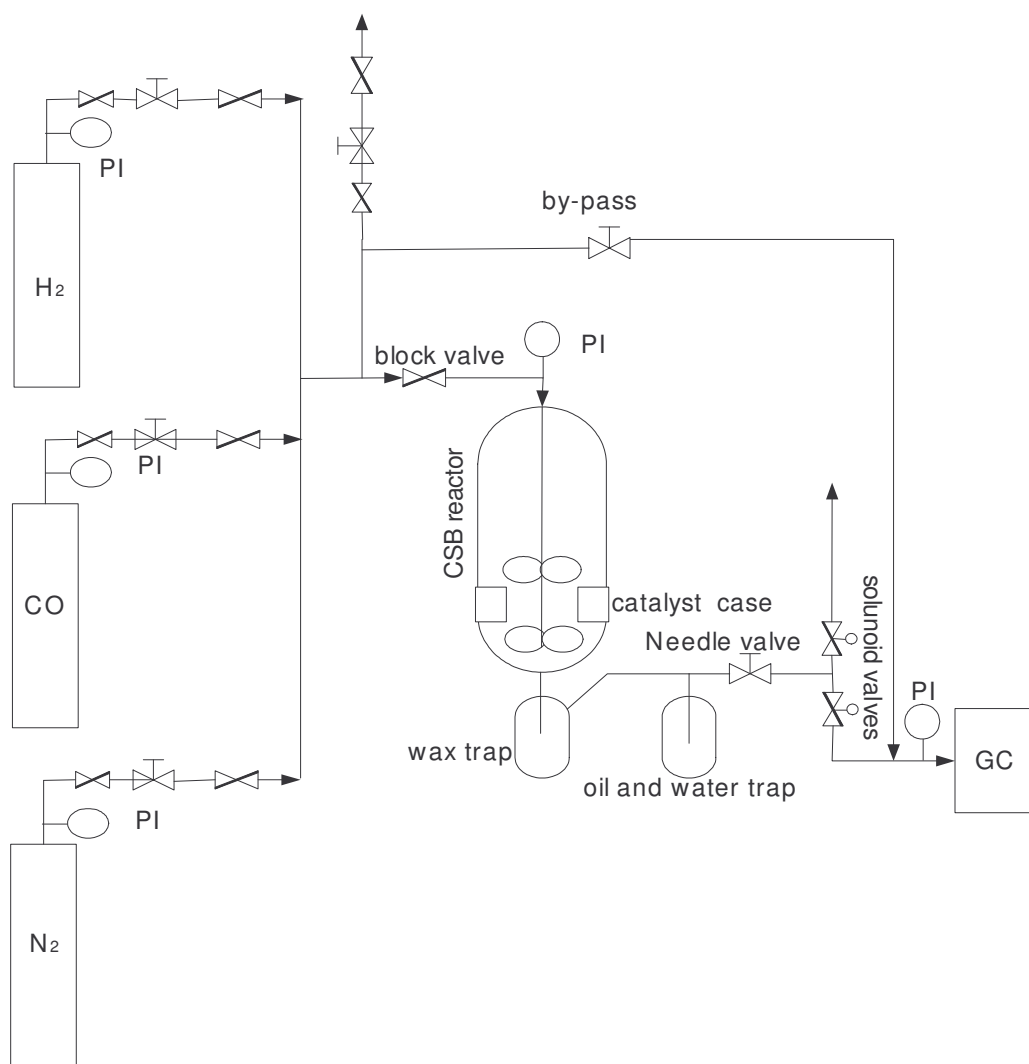


Figure 2.1 Schematic diagram of the experimental setup.

Catalyst reduction was performed at 250°C under atmospheric pressure using an ultra high purity H₂ with a space velocity of 500 h⁻¹ for a period of 16 h. After the catalyst reduction was completed, the synthesis gas was introduced to the reactor at the desired flow rate and composition. The reactor, at standard conditions, was operated at 8 bar and an impeller speed of 900 rpm. A residence distribution time test

had been performed by Chronis (1999), which indicated that at impeller speed of 700 rpm and above there were no gas phase mass transfer limitations.

Wax products were collected in the wax pot located at the bottom of the reactor, and the remaining condensables (oil and water) were collected in the oil trap. The wax trap and all the down stream lines were heated to 150 °C while the oil trap was kept at ambient temperature. At the beginning of the experimental run, wax and oil pots were emptied and the total gas flow rate was re-measured. Each experimental run was performed for at least 48 h. A mass balance was also performed at the end of each run to test for accuracy and consistency.

2.2.3 Product analysis

The product stream is split into gas, oil, wax and water. The gaseous products and reactants were analyzed online using flame ionization detector (FID) and thermal conductivity detector (TCD) gas chromatographs (GCs), respectively. These analyses were carried out regularly using solenoid valves, which were programmed to autosample these gasses at a specific time. The TCD GC was fitted with a carbosieve S-II packed column (2 m x 1/8 in. stainless steel), which was used for separating H₂, CO (reactants) and N₂ (tracer). Ultra high purity argon gas was used as a carrier gas in this GC. The FID GC was fitted with a Zebron ZB-1 capillary column, which was able to separate paraffins and olefins in the range of C₁-C₁₇. This capillary column is a 30 m x 0.53mm i.d. 5µm film thickness, which uses 100% methylpolysiloxane stationary phase. Ultra high purity nitrogen gas was used as a carrier gas in this column. A single integrator connected to both TCD and FID was able to pick up the desired signals. An offline FID GC was fitted with a BP-5 capillary column (30 m x 0.25 mm i.d.), which was used for analyzing oil and wax products.

2.3. RESULTS AND DISCUSSION

The experimental data was used to calculate the rates of CO consumption, CH₄ production and hydrocarbon production at various experimental conditions and the results are reported below.

2.3.1 Influence of Partial Pressures and Feed Ratios of H₂/CO on the Rate of CO Consumption.

To illustrate the application of process synthesis to optimizing the reactor design, we will initially consider a simple objective (which is possibly quite unrealistic). We consider that we wish to react a given amount of CO in the smallest possible reactor. In order to do this, we need to consider the rate of CO consumption and what it depends on.

The partial pressures of H₂ and CO represent those in the reactor, and were calculated from the exit stream conditions. The rate of CO consumption was determined from:

$$-r_{CO} = (N_{CO,in} - N_{CO,out}) / g_{cat} \quad (2.1)$$

where $-r_{CO}$ is the rate of CO consumption ($\mu\text{mol}/\text{g}_{cat}\text{s}$), $N_{CO,in}$ and $N_{CO,out}$ are the CO molar flow-rates ($\mu\text{mol}/\text{g}_{cat}\text{s}$), in the reactor feed and exit stream, respectively and g_{cat} is the catalyst mass (g).

The set of outputs for a fixed feed composition and varying residence time are given in Figures 2.2A and B for the reaction temperatures of 220 °C and 250 °C

respectively. The points with the same fixed feed composition are indicated by a line that has no other significance to help group them for ease of interpretation. The composition of the feed gas is shown for each set. The measured rate of CO consumption at the associated outlet partial pressures are the numbers indicated on the graph. The values of the outlet partial pressures of H₂ and CO are the result of varying the feed flow rates and hence the conversion in the reactor. The total pressure is constant for all points in Figures 2.2A and B and was not considered as a variable in this paper. However, the ideas described below could be extended to investigate the effect of total pressure on the reactor design if experimental data at other pressures was measured.

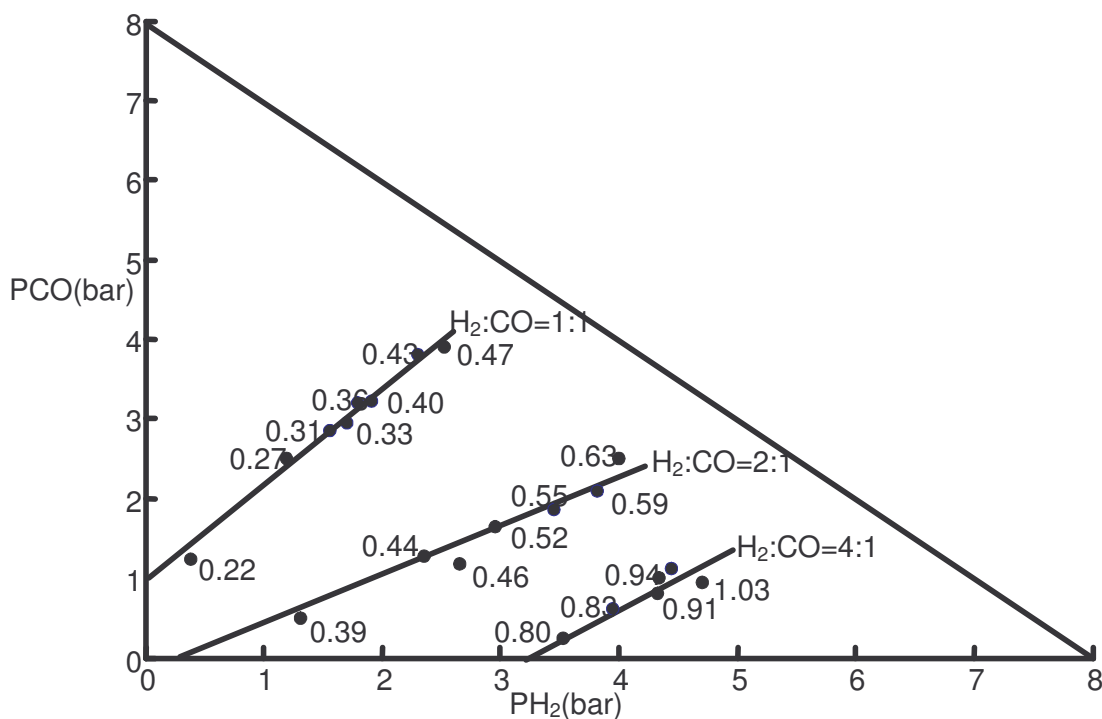


Figure 2.2A: The rate of CO consumption at 220 °C at various partial pressures of CO and H₂ for 3 different feed ratios. The numbers indicate the rate of CO consumption in $\mu\text{moles CO/g}_{\text{cat}}\cdot\text{s}$. The feed ratio for each set of experiments is indicated on the associated line.

We observed that by increasing the feed flow rates, the rate of CO consumption increases. A similar trend in the increase of the rate of CO consumption with the increase in flow rates was observed by Henrice-Olive & Olive (1984). The variation in the rate of CO consumption at various flow rates is associated with the concentration effect of CO and H₂ on the catalyst surface (Levenspiel, O., 1972) as the Fischer-Tropsch reactions are known to be surface reactions. At low CO conversion (high flow-rates), the concentration of the bulk H₂ and CO on the catalyst surface is high, hence the overall rate of CO consumption is high. In contrast, high conversion (low flow-rates) will result in a low concentration of the bulk H₂ and CO on the catalyst surface, hence a low overall rate of CO consumption will be obtained.

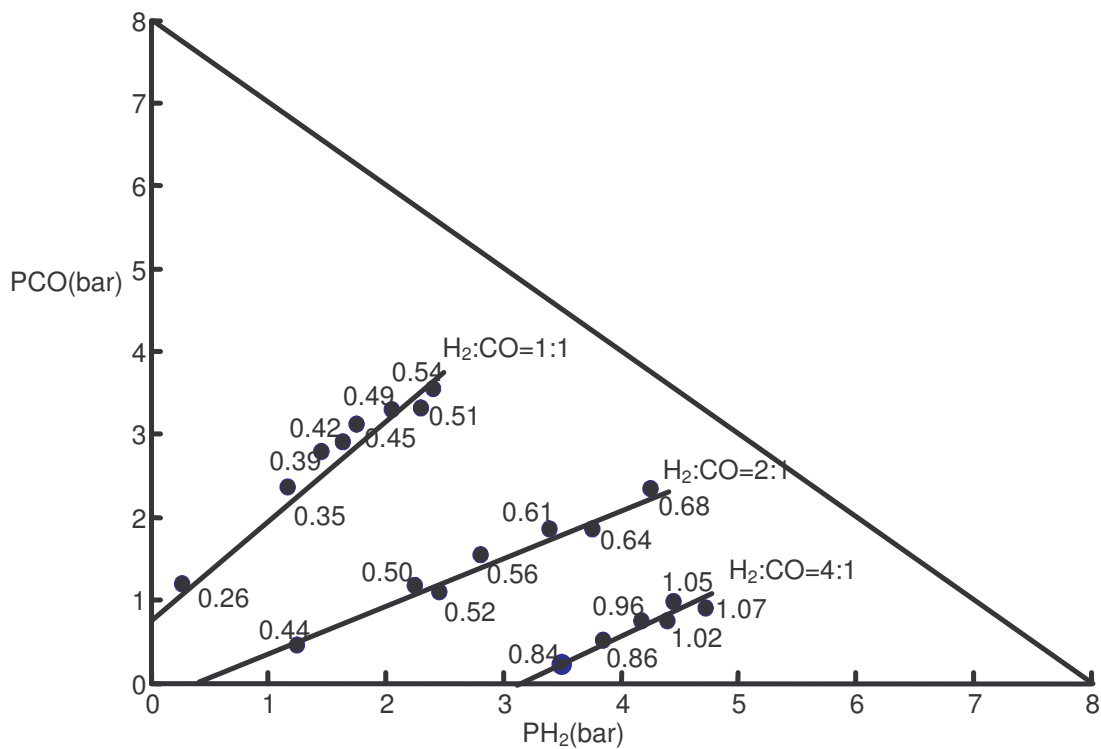


Figure 2.2B: The rate of CO consumption at 250 °C at various partial pressures of CO and H₂ for 3 different feed ratios. The numbers indicate the rate of CO consumption in μmoles CO/g_{cat}·s. The feed ratio for each set of experiments is indicated on the associated line.

The trend shown in Figures 2.2A and B is that for each set of experiments with a fixed H₂/CO feed ratio, the rate of CO consumption decreases monotonically as the partial pressures of H₂ and CO decreases. Furthermore, an increase in the partial pressures of H₂ and a decrease in the partial pressure of CO favor high rates of CO consumption.

Wojciechowski (1988) also reported a similar trend. A proposed explanation for this is that the CO is more strongly adsorbed on the catalyst surface than H₂ (Wojciechowski, 1988; Dry, 1981). At lower ratios of H₂/CO the CO saturates the catalyst surface excluding the H₂, and hence the rate of CO consumption decreases.

When comparing the rates of CO consumption from Figures 2.2A and B it can be seen that the rate has increased as the reaction temperatures was increased from 220 to 250 °C. In the work of Keyser et al. (2000), Chronis (1999) and Niemell et al. (1997) a similar behaviour for similar cobalt Fischer-Tropsch catalyst was observed.

If we now consider the objective function that we proposed, namely to react a given amount of CO in the smallest reactor, we can see that this would be equivalent to operating the reactor at the highest rate of CO consumption. The highest rates of CO consumption for a fixed feed composition are obtained at high partial pressures of H₂ and CO and high temperatures. The reactor should thus be operated at low conversions and higher reaction temperatures. If the above objective is applied in a situation where there is flexibility of changing the H₂/CO feed ratios, the reactor should rather be operated in a region of high H₂/CO feed ratios. For the data shown this would correspond to a H₂/CO feed ratio of 4:1.

The optimal reactor structure for the implementation of the above objective can be obtained from a Levenspiel plot (Levenspiel, 1972). The best reactor is chosen from a plot of the reciprocal rate ($1/\text{rate}$) versus concentration. For the purpose of answering the question of how to convert a given amount CO in the smallest possible reactor, we plotted the reciprocal rate of CO consumption ($1/-r_{CO}$) at various partial pressures of H_2 and at different H_2/CO feed ratios and reaction temperatures as indicated in Figures 2.3A and B.

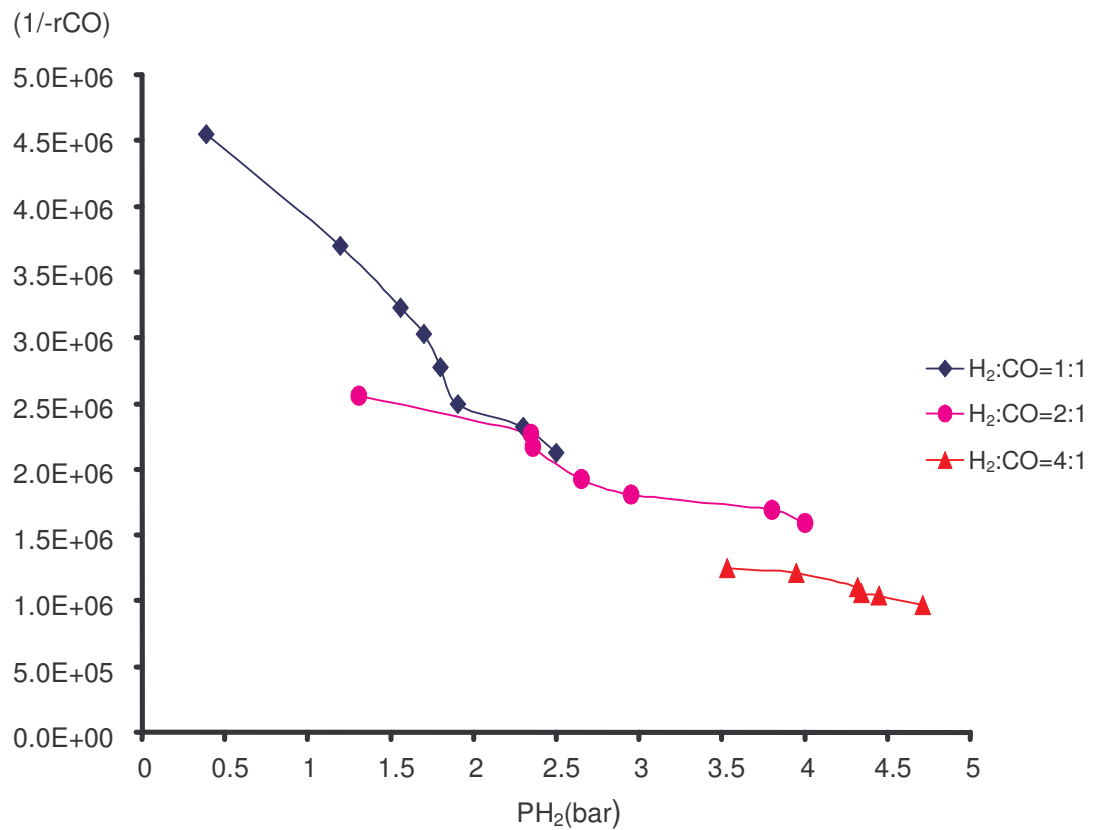


Figure 2.3A: A plot of $(1/r_{CO})$ versus partial pressure of H_2 at 220 °C. Each curve corresponds to a different feed ratio of H_2/CO as indicated in the legend. The dimensions of the rate of CO consumption are $\mu\text{moles CO/g}_{\text{cat}}\text{s}$.

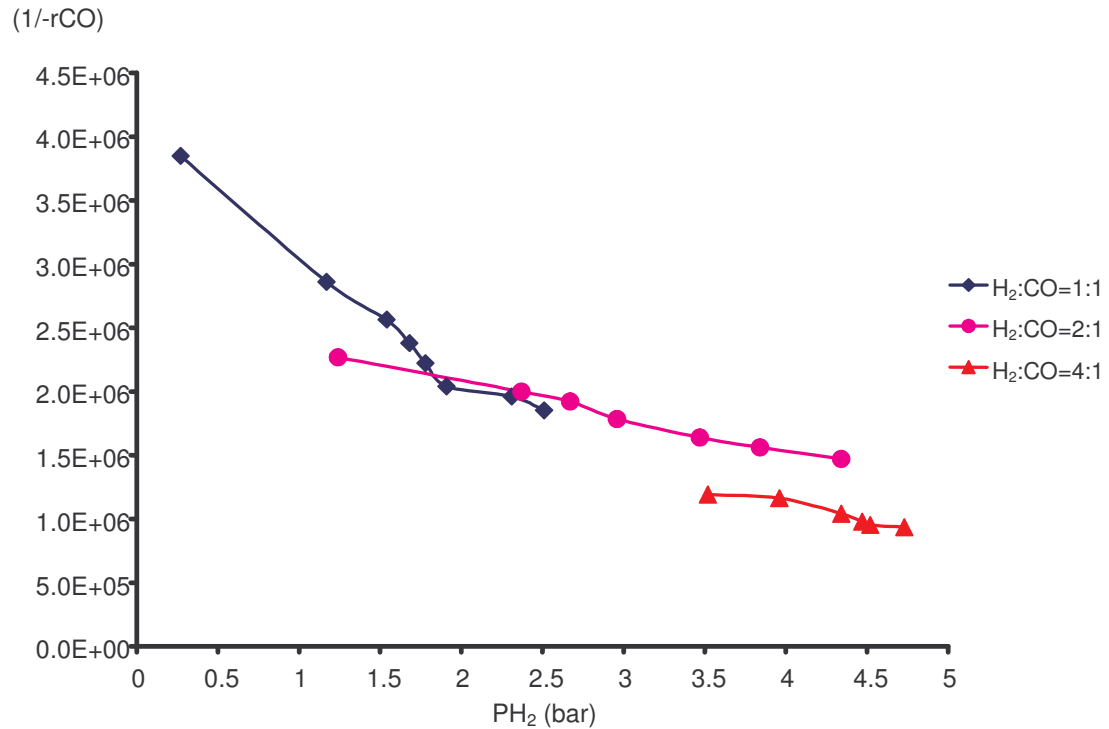


Figure 2.3B: A plot of $(1/r_{CO})$ versus partial pressure of H_2 at $250^\circ C$. Each curve corresponds to a different feed ratio of H_2/CO as indicated in the legend. The dimensions of the rate of CO consumption are $\mu\text{moles CO}/g_{\text{cat}} \text{ s}$.

It can be seen from Figures 2.3A and B that $(1/-r_{CO})$ increases monotonically as the partial pressure of H_2 decreases (because the flow-rate decreases and hence conversion increases) for each of the experimental sets with different H_2/CO feed ratios. This trend indicates that the optimum reactor structure to be used is a plug flow reactor (Levenspiel, O., 1972, Doraiswamy & Sharma, 1984). High rates of CO consumption are obtained in the region of high partial pressure of H_2 and low partial pressure of CO, thus a plug flow reactor with an H_2 rich feed would give the optimum reactor structure for this simple objective. This could be achieved by designing a process with a large H_2 rich recycle stream around a plug flow reactor as shown in Table 2.1A.

Table 2.1A: Operating conditions for the optimal reactor and the resulting process for converting a given amount of CO in the smallest possible reactor.

Objective : Convert a given amount of CO in smallest possible reactor
Optimal Reactor Structure : Plug flow reactor with a H ₂ rich feed, Low per pass conversion, High temperature
Process Implementation

The diagram illustrates a process for converting CO. It starts with a 'Feed' stream where the H₂:CO ratio is 4:1. This feed enters a 'PF reactor' (Plug Flow reactor), which is represented by a cylinder with a hatched section. The output of the reactor goes to a 'Separator'. From the separator, a portion of the stream is recycled back to the reactor inlet as an 'H₂ rich recycle' stream. The remaining stream from the separator exits the process.

There are two factors that we need to consider at this stage. At first sight it seems we would need to do further experiments at even higher H₂/CO feed ratios, lower conversions and higher reaction temperatures in order to see if the trend of the reaction rate continues increasing and where the highest rates occur. Hence we can see that we should design an experimental program so that the interpretation of the experimental results and implications on design are incorporated into the planning.

However, the objective of minimizing the reactor volume is going to result in a process with a large recycle. The recycle stream would be a H₂ rich stream as described in Table 2.1A. Its implication on the process is that, because of the large recycle stream, the recycle compression costs would be large leading to correspondingly large operating costs. Thus, although the reactor volume may be

minimized, it is at the expense of the process itself. At this stage we would need to do calculations to examine the trade off between reducing the reactor volume and increasing the process operating and capital costs due to compression and separator costs. The results of these calculations could modify the decision as to where to perform further experiments. However, rather than continue with this objective, we shall rather consider the effect on the reactor design, experimental program and process design when we change the objective function.

2.3.2 The effect of Partial Pressures and Feed Ratios of H₂ to CO on the Rate of CH₄ production.

Let us assume that we change the objective and now wish to minimize the production of methane. To consider this new objective, we need to consider the rate of CH₄ production and in particular, what it depends on. The numbers on Figures 2.4A and B show the measured rate of methane production at various partial pressures of CO and H₂ for different H₂/CO feed ratios and reaction temperatures. Again the only significance of the lines in the Figures 2.4A and B is to group the reactor outputs together which correspond to the same feed composition. The trend shown in Figures 2.4A and B is that the rate of CH₄ production increases as the partial pressures of H₂ and CO decreases for all H₂/CO feed ratios. Dry, M. E (1981) found that a high linear gas velocity (low residence time) decreases the temperature rise in the fixed bed reactor, with the benefit of increasing wax selectivity. This agrees with the findings in this work, as low residence times would correspond to low conversions and hence high partial pressures of H₂ and CO. As the H₂/CO feed ratio is decreased from 4:1 to 1:1, a considerable decrease in the rate of CH₄ production is observed. Generally, it is accepted that high H₂/CO feed ratios favors high rates of CH₄ production (Dry, M.E (1981), Iglesia, E (1997), Bartholomew & Lee (2000), Bertole & Mims (1999)). Price, J.G (1994) and Chronis, T (1999) observed a similar trend when they used the same (Ru/CO/TiO₂) catalyst.

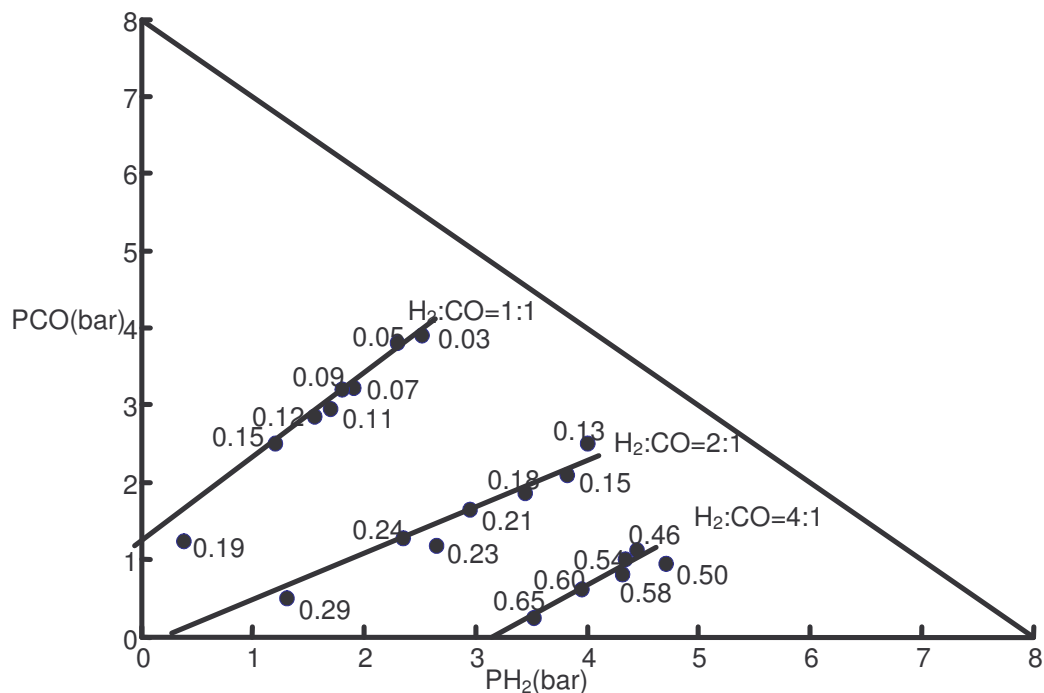


Figure 2.4A: The rate of CH₄ production at 220 °C at various partial pressures of CO and H₂ for 3 different feed ratios. The numbers indicate the rate of CH₄ production in μmoles CH₄/g_{cat}·s. The feed ratio for each set of experiments is indicated on the associated line.

When comparing the results in Figures 2.4A and B, we notice that, at a reaction temperature of 250 °C, the rate of CH₄ production increased significantly relative to that measured at 220 °C. Higher reaction temperatures have always been found to favor higher rates of CH₄ production and a decrease in the probability of chain growth (Iglesia, E (1997), Iglesia, E (1992), Dry, M.E (1996)). The increase in the rate of CH₄ production at higher reaction temperatures is thought to be due to the increase in the hydrogenation rate of the individual -CH₂- units available on the catalyst surface, and

hence leads to lower chain growth (Dry, M. E., 1996). Consequently, higher rates of CH₄ production and low rates of production of long chain hydrocarbon result.

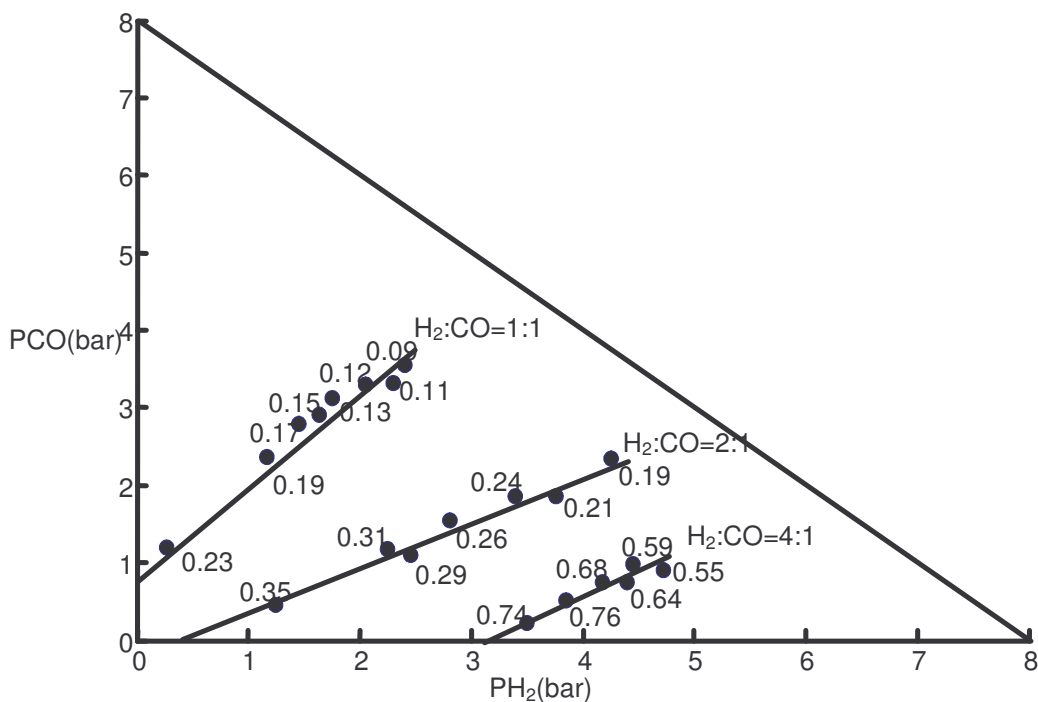


Figure 2.4B: The rate of CH₄ production at 250 °C at various partial pressures of CO and H₂ for 3 different feed ratios. The numbers indicate the rate of CH₄ production in μmoles CH₄/g_{cat}·s. The feed ratio for each set of experiments is indicated on the associated line.

When the results (Figures 2.4A and B) are looked at from a process synthesis view, it can be seen that if we wish to minimize the production of CH₄ for a given H₂/CO feed ratio, we would design the reactor to incorporate regions where the rates of CH₄ production are low. Hence, we would operate the reactor at low conversions and reaction temperatures. If there is flexibility in choosing the H₂/CO feed ratios, we would rather operate the reactor at low H₂/CO feed ratios as well as low conversions.

If we were to consider the implications of these reactor design decisions on the process itself, we would see that we would implement the desired operating conditions by having a process with a large CO rich recycle. We would again need to consider the compressor and separation costs when deciding on the trade offs on how low the reactor conversion should be and how much excess CO we should feed to the reactor. The implications on the experimental program is that one might need to do further experiments at even lower H₂/CO feed ratios and reaction temperatures in order to decide on the trade offs between reduced CH₄ production and increased plant costs.

For this new objective of minimising the rate of CH₄ production, the optimum reactor structure was also determined from the Levenspiel plot (Levenspiel, O., 1972). Figure 2.5A and B show the plots of the inverse rate of CH₄ production ($1/r_{CH_4}$) at various partial pressures of H₂ for each set of H₂/CO feed ratios and reaction temperatures. It can be seen that ($1/r_{CH_4}$) increases monotonically as the partial pressures of H₂ increases for each of the H₂/CO feed ratios.

The trend shown by the $1/r_{CH_4}$ plot is an indication that a continuously stirred tank reactor would be optimal for the maximization of CH₄ production but because our objective is to minimize the production of CH₄, the optimal structure will be that of a plug flow reactor (Doraiswamy & Sharma, 1984; Levenspiel, O., 1979). As we previously discussed, the optimal operating region for suppressing the production of CH₄ requires high partial pressures of CO and low partial pressures of H₂. Thus, to implement these results would require a process as shown in Table 2B with a plug-flow reactor and a (large) CO-rich recycle stream.

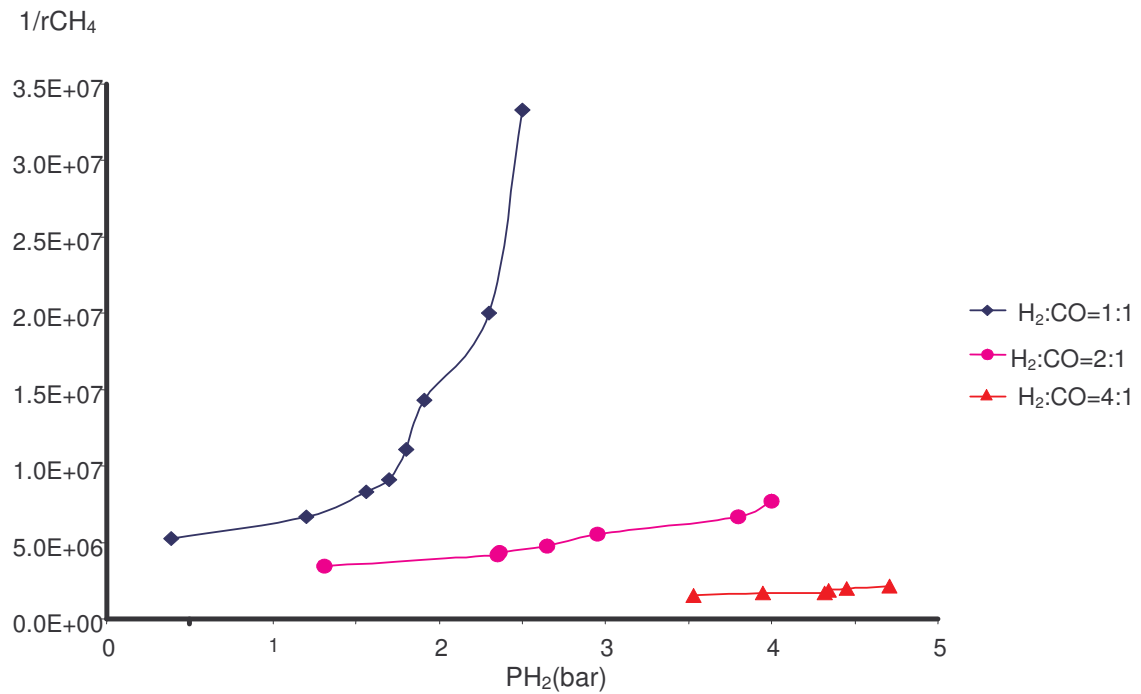


Figure 2.5A: A plot of $(1/r_{CH_4})$ versus partial pressure of H_2 at 220 °C. Each curve corresponds to a different feed ratio of H_2/CO as indicated in the legend. The dimensions of the rate of CH_4 consumption are $\mu\text{moles } CH_4/g_{\text{cat}} \text{ s}$.

If we consider the two previous objectives we see that we obtain similar results in that the reactor conversion should be kept low in order to have a high reaction rate of CO and a low rate of CH_4 production. There is however a conflict as to whether to operate a reactor with a H_2 rich feed at high temperatures in order to increase the rate of CO consumption or a CO rich feed at low temperatures to decrease the rate of CH_4 production. There is also a conflict of where further experiments need to be performed. We shall next consider a more realistic objective function that tries to balance these two factors.

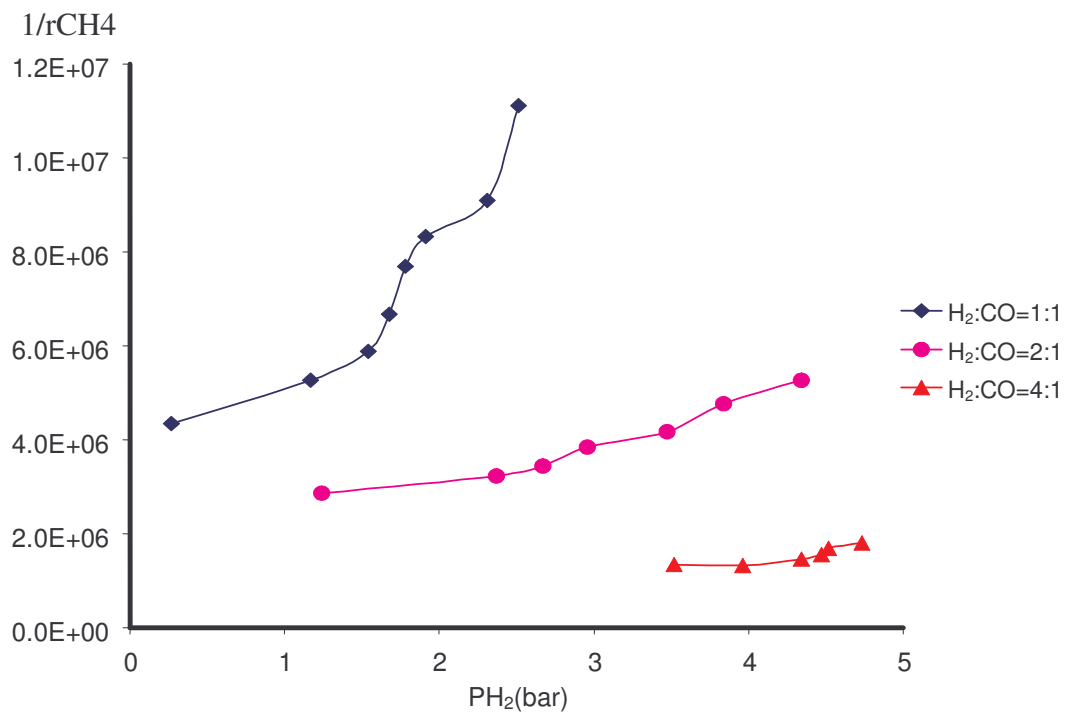
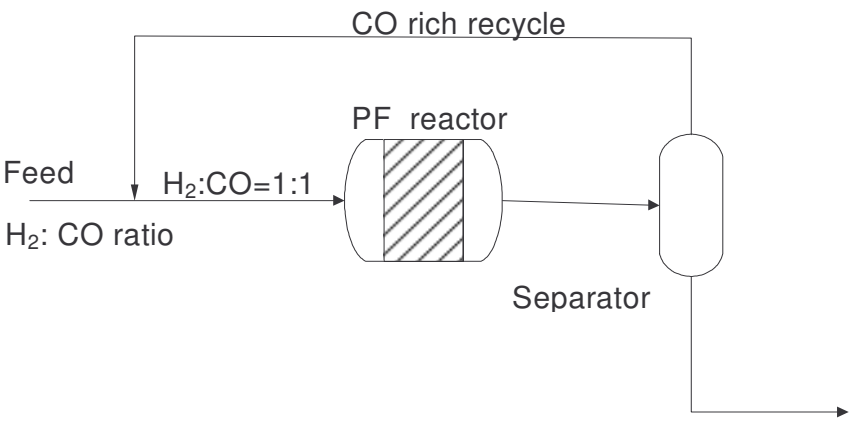


Figure 2.5B: A plot of $(1/r_{CH_4})$ versus partial pressure of H_2 at 250 °C. Each curve corresponds to a different feed ratio of H_2/CO as indicated in the legend. The dimensions of the rate of CH_4 consumption are $\mu\text{moles } CH_4/\text{g}_{\text{cat}}\text{s}$.

Table 2.1B: Operating conditions for the optimal reactor and the resulting process for minimizing the production of CH₄ for a given amount of CO converted.

<p>Objective : Minimize the production of CH₄ for a given amount of CO converted</p>
<p>Optimal Reactor Structure : Plug flow reactor with a CO rich feed , Low per pass conversion, Low temperature</p>
<p>Process Implementation</p>  <p>The diagram illustrates a process flow. On the left, a 'Feed' stream with an 'H₂: CO ratio' of 1:1 enters a 'PF reactor' (represented by a cylinder with diagonal hatching). The output of the reactor goes to a 'Separator' (represented by a vertical cylinder). From the top of the separator, a 'CO rich recycle' stream is drawn and fed back into the reactor. From the bottom of the separator, an outlet stream exits the process.</p>

2.3.3 The Effect of the Partial Pressures and Feed Ratios of H₂/CO on the Rate of Hydrocarbon Production per mole of CO consumed.

If we wish to maximize the selectivity towards hydrocarbons other than CH₄ we would look at maximizing the rate of hydrocarbon production relative to the rate of CO consumption. The rate of hydrocarbon production per mole of CO consumed (hydrocarbon selectivity) is defined by

$$\frac{r_{CH_2}}{-r_{CO}} = \frac{-r_{CO} - r_{CH_4}}{-r_{CO}} \quad (1.2)$$

where, r_{CH_2} is the rate of hydrocarbon formation ($\mu\text{mol}/(\text{g}_{\text{Cat}} \text{s})$) excluding r_{CH_4} (the rate of methane formation ($\mu\text{mol}/(\text{g}_{\text{Cat}} \text{s})$). This will allow us to discriminate between a decrease in the production of CH_4 and an increase in a rate of CO consumption. The values of the hydrocarbon selectivity were calculated from the experimental data and the results in Figures 2.6A and B show the values of the hydrocarbon selectivity at various partial pressures of H_2 and CO and at different H_2/CO feed ratios and reaction temperatures. Again the lines in Figure 2.6A and B group the reactor outputs together which correspond to the same feed composition.

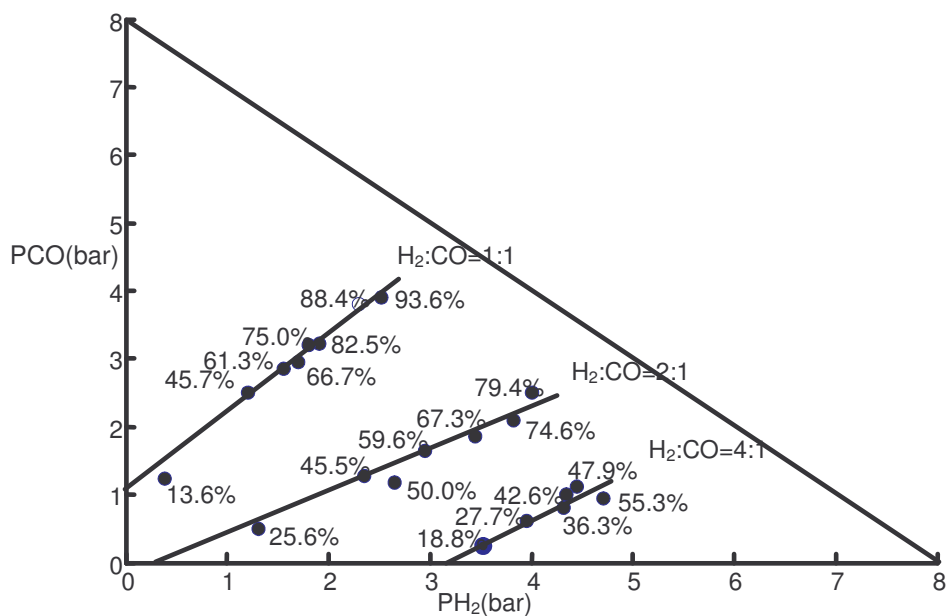


Figure 2.6A: Effect of the partial pressures and feed ratios of H_2 and CO on hydrocarbon selectivity at $220\text{ }^\circ\text{C}$. The numbers on the graph indicate hydrocarbon selectivity $= (r_{CO} - r_{CH_4}) / r_{CO} \times 100$.

As the partial pressures of H₂ and CO decreases for a given amount of H₂ and CO in the feed, the hydrocarbon selectivity decreases substantially. Furthermore, high hydrocarbon selectivity is favored in the region of high partial pressures of CO and low partial pressures of H₂. This trend of increase in the hydrocarbon selectivity with a decrease in the H₂/CO feed ratios agrees with the hypothesis that the probability of the formation of long chain hydrocarbon products is favored at low ratios of H₂/CO (Dry, M. E., 1981). However this is said to be dependent on a catalyst type, reaction conditions and type of reactor.

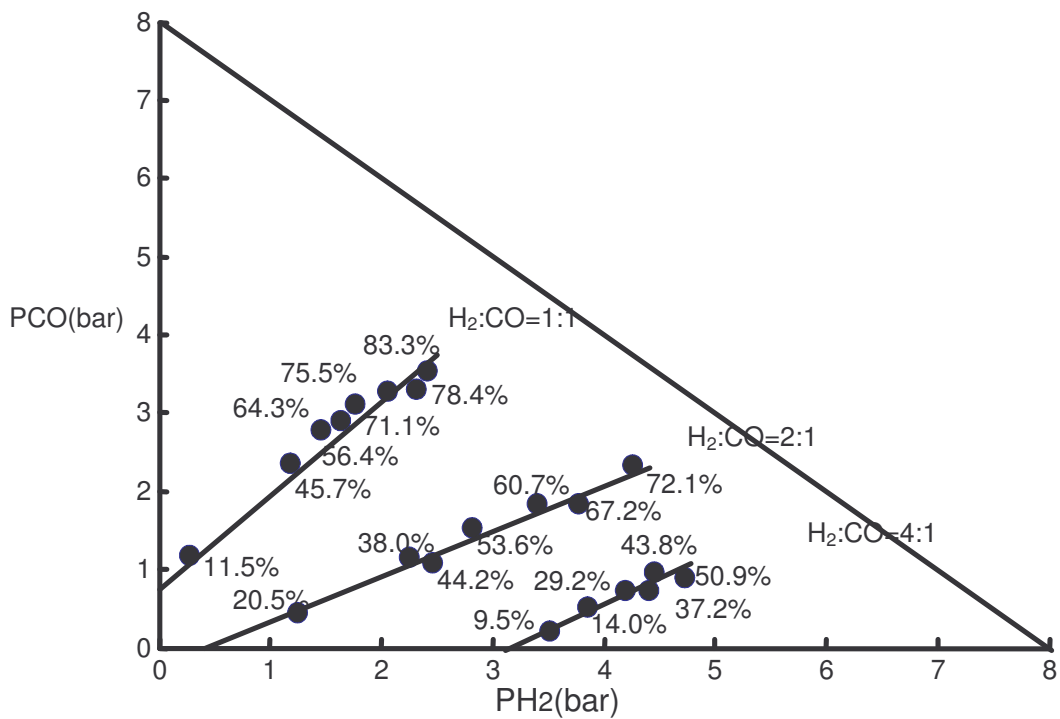


Figure 2.6B: Effect of the partial pressures and feed ratios of H₂ and CO on hydrocarbon selectivity at 250 °C. The numbers on the graph indicate hydrocarbon selectivity = $(r_{CO} - r_{CH_4}) / r_{CO} \times 100$.

When comparing the results in both Figures 2.6A and B, we can see that as the reaction temperature increases the hydrocarbon selectivity decreases. This decrease in the hydrocarbon selectivity at higher temperatures is expected, since higher temperatures have been observed to favour high rates of CH₄ production (section 2.3.2).

If we now consider an objective function in which we wish to produce the most hydrocarbons per mole of CO consumed for a given amount of H₂ and CO in the feed, we would wish to operate the reactor in the region of high hydrocarbon selectivity. Thus the reactor would be operated at low conversion and reaction temperatures. If there is flexibility in changing the H₂/CO feed ratios, the reactor will be operated at low H₂/CO feed ratios. However, one needs to do further experiments at even lower H₂/CO feed ratios and lower conversions to see if the trend in the increase in the hydrocarbon selectivity continues and where the highest hydrocarbon selectivity occurs. These experiments might also be performed at even lower reaction temperatures in order to see how the temperature will influence the hydrocarbon selectivity.

The optimum reactor structure for maximisation of hydrocarbon selectivity is also determined from the Levenspiel plot (Levenspiel, O., 1972). Figures 2.7A and B show the inverse of hydrocarbon selectivity (r_{CO}/r_{CH_2}) at various partial pressures of H₂ and at different H₂/CO feed ratios and reaction temperatures. It can be seen that (r_{CO}/r_{CH_2}) decreases monotonically as the partial pressures of H₂ increases. This trend shown by (r_{CO}/r_{CH_2}) is an indication that a plug flow reactor would be required for maximising the hydrocarbon selectivity.

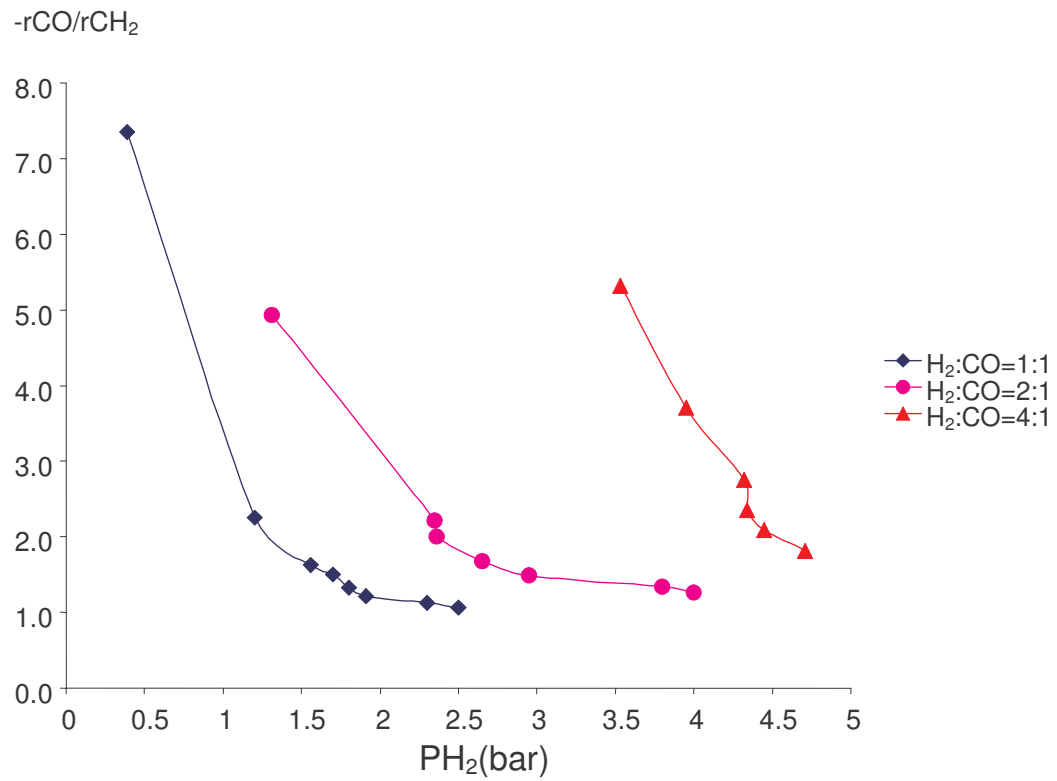


Figure 2.7A: A plot of $(-r_{CO}/r_{CH_2})$ vs partial pressure of H_2 at 220 °C. Each curve corresponds to a different feed ratio of H_2/CO as indicated in the legend.

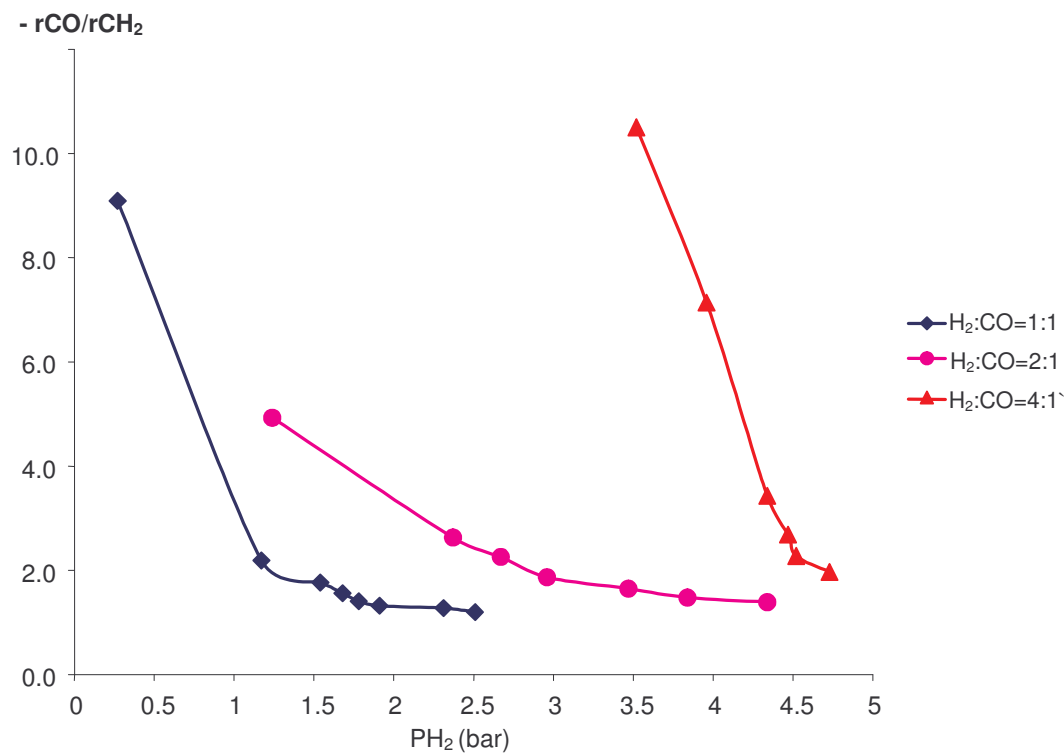


Figure 2.7B: A plot of $(-r_{CO}/r_{CH_2})$ vs partial pressure of H₂ at 250 °C. Each curve corresponds to a different feed ratio of H₂/CO as indicated in the legend.

Thus, if we consider the process that has a reactor operating at high hydrocarbon selectivity, we can see that this would be achieved if the partial pressures of CO in the reactor feed was high and the partial pressure of H₂ low (Figures 2.6A and B). One can conclude that a plug flow reactor with a CO rich recycle stream (Table 2.1C) operating at low temperature should be used to achieve the above objective.

Table 2.1C: Operating conditions for the optimal reactor and the resulting process for maximizing hydrocarbon selectivity.

Objective : Maximum hydrocarbon selectivity
Optimal Reactor Structure : Plug flow reactor with a CO rich feed , Low per pass conversion, Low temperature
<p>Process Implementation</p>

2.4 CONCLUSION

The results presented in this study have shown how the Ru/Co/TiO₂ catalyst behaves under various reaction conditions when used in a stirred basket reactor.

The general trends observed indicate that high partial pressures of H₂ and CO, which correspond to short residence times, give highest rates of CO consumption, lowest rates of CH₄ production and highest selectivity towards hydrocarbons. As the H₂/CO feed ratio is increased, the rate of CO consumption and the rate of CH₄ production increases while the hydrocarbon selectivity decreases. High reaction temperatures favour high rates of CO

consumption and CH₄ production and low selectivity towards hydrocarbon. Interestingly, all of these conclusions can be arrived at without modelling any of the kinetics.

Choosing the optimal region for the operation and design of a Fischer-Tropsch reactor differs for different objectives. Therefore one needs to be sure about what one is trying to optimise and set as system parameters. In order to be able to do this, one needs to choose the operational objectives and system parameters carefully. Furthermore, the influence of the system parameters on the optimal operating region needs to be understood. This can only be done if the kinetics, reactor and process design is done iteratively. This suggests that it would be desirable to integrate the experimental program with the process design. This is one of the important aspects of what we call process synthesis.

Probably one of the most important results is that in all cases implementing the optimal reactor operating conditions resulted in processes with large recycles and hence large operating and capital costs. This shows that one should not optimise the reactor independently of the process in which the reactor is going to be used. This point will be addressed in a subsequent paper where it will be shown why it is desirable for the process design and laboratory programme to be done interactively. Furthermore we will look at quick, simple calculations that can be used to optimise the process at the earliest design stages.

ACKNOWLEDGEMENTS

David Glasser thanks the Oppenheimer Trust for the award of the Harry Oppenheimer Memorial Fellowship that allowed the recipient to spend a period at the Chemical Engineering Department at the University of Sydney during which period some of this work was done. We would also like to thank the NRF and THRIP for funding that made this project possible.

2.5 REFERENCES

Bartholomew, C.H & Lee, W.H. (2000), Effects of Support on Methane Selectivity in Cobalt-catalysed F-T synthesis: A kinetic Model, *Studies in Surface Science Catalysis*, 130, 1151- 1156.

Bertole, C.J and Mims, C.A. (1999), Dynamic Isotope Tracing: Role of subsurface Oxygen in Ethylene Epoxidation on silver, *Journal of Catalysis*, 184, 224-235.

Berty J.M. (1974), Reactor for Vapor-Phase Catalytic Studies, *Chemical Engineering Progress*, 70, 5, 78.

Chronis, T. (1999), PhD Thesis, A Fischer-Tropsch study of Co/Ru catalysts, University of the Witwatersrand, South Africa.

Doraiswamy, L.K and Sharma, M.M. (1984), Heterogeneous reactions: Analysis, Examples and Reactor Design, John Wiley and Son, New York, 283-288.

Dry. M.E. (1981), in Anderson,. J.R and Boudert,. M, *Catalysis Science and Technology*, Springer-Verlag, New York, Chapter 4.

Dry, M.E. (1996), Practical and Theoretical aspects of the catalytic Fischer- Tropsch process, *Applied Catalysis A: General* 138, 319-344.

Glasser, D., Hildebrandt, D & McGregor, C. (199), TRIZ Course – Theory of inventive problem solving, 5th International conference on Foundation of Computer Aided Process Design, Breckenridge, Colorado.

Henrice-Olive, G and Olive, S. (1984), The Chemistry of the Catalysed Hydrogenation of Carbon Monoxide, Springer-Verlag Berlin, Heidelberg: Berlin, p179.

Iglesia, E. (1997), Design, synthesis and use of cobalt-based Fischer-Tropsch synthesis catalysts, *Applied Catalysis A: General* 161, 59-78.

Iglesia, E., Soled, S.L and Fiato, R.A. (1992), Fischer-Tropsch synthesis on cobalt and ruthenium, Metal dispersion and support effects on reaction rate and selectivity, *Journal of Catalysis* 137, 212-224.

Keyser, M.J., Everson, R.C and Espinoza, R.L. (2000), Fischer-Tropsch kinetic studies with cobalt-manganese oxide catalysts, *Industrial & Engineering Chemistry Research* 39, 48.

Levenspiel, O. (1972), *Chemical Reaction Engineering*, 2nd Edition, Wiley.

Levenspiel, O. (1979), *The Chemical Reactor Omnibook*, Corvallis, Oregon, Chap 5.

Niemell, M.K., Backman, L., Krause, A.O.I and Vaara, T.(1997), The activity of the Co/SiO₂ catalyst in relation to pre-treatment, *Applied Catalysis A: General*, 156 319-333.

Price, J.G. (1994), PhD Thesis, An Investigation into Novel Bimetallic Catalysts for Use in the Fischer-Tropsch Reaction, University of the Witwatersrand, South Africa.

Richardson, J.T. (1989), *Principles of Catalyst Development*, Plenum Press, New York, NY, 111- 112.

Spencer, A and Wilkinson, G. (1972), μ - Oxo-triruthenium carboxylate complexes, *Journal of the Chemical Society, Dalton Transactions*, 1570.

Wojciechowski, B. W. (1988), The Kinetics of the Fischer-Tropsch Synthesis, *Catalysis Reviews – Science and Engineering*, 30 (4), 629-702.

**SYNTHESIZING A PROCESS FROM EXPERIMENTAL
RESULTS: A FISCHER-TROPSCH CASE STUDY**

This paper has been accepted for publication in the *Industrial & Engineering Chemistry Research* 2007, 46, 156 – 167. Part of this work was presented at the following conferences:

- CATSA conference, Durban, November 9 – 12, 2003.
- AIChE Meeting, Austin, Texas, USA, November 7 – 12, 2004.

Synthesizing a Process from Experimental Results: A Fischer-Tropsch Case Study

Peter Mukoma¹, Diane Hildebrandt¹, David Glasser¹ and Neil Coville².

¹COMPS, School of Chemical and Metallurgical Engineering

²School of Chemistry

University of the Witwatersrand, Johannesburg, Private Bag 3, WITS 2050.

Abstract

When industrial laboratory experiments are done, it is important to keep in mind the objectives of the study. This is because the experiments that will be required are critically dependent on these objectives. In order to decide what these objectives are one need to have a rudimentary design for the process that highlights the key issues and drivers for the economics of the process. We address this by doing a case study on a Fischer-Tropsch (FT) Process.

A method of synthesizing an FT flowsheet incorporating syngas generation, air separation, hydrocarbon synthesis, product workup, recycling and reforming is presented. The impact of these unit operations on the entire FT synthesis process has been studied by turning all their material, energy and work requirements into one variable namely carbon efficiency. Preliminary experimental data on an FT catalyst is used to demonstrate the method. From this analysis the effect of the H₂: CO ratios, space velocities and the feed partial pressures in the FT synthesis loop on the overall plant carbon efficiency are investigated. The implication of the results on further flowsheet development and experimental program is considered.

3.1 INTRODUCTION

When performing experiments in an industrial laboratory program, we believe it is important to have realistic objectives in mind. Often when doing these experiments the laboratory personnel try to maximize properties such as yield and selectivity because they are not given very clear directions of what to look for. We believe that based on minimal information one may actually devise the outline of a process. Once this has been done, one is then in a position to do simple calculations to see what the important drivers for the process are. By this we mean which of the process unit operations have the biggest effect on the efficiency of the process. It is difficult to explain these in words and so we have rather chosen to demonstrate the methods using an example based on an experimental program. The example chosen relates to the Fischer-Tropsch synthesis of hydrocarbons from synthesis gas. In particular we will examine the influence of all the unit operations on the efficiency of the proposed plant and in so doing actually synthesize an overall flowsheet.

Results from a recent study and analysis of Fischer-Tropsch (FT) synthesis experimental data for reactor synthesis using cobalt-based catalysts showed that choosing the optimal reactor conditions for the design and operation of an FT plant is subject to the designer's objective function. Each objective function shifts the operating regions and sets its own system parameters. There is nothing wrong with optimizing the reactor design conditions and parameters, the problem is that optimizing the reactor alone independent of the process in which the reactor is going to be used may not be very useful since each optimized reactor configuration has an effect on the efficiency of the rest of the process (Ngwenya et al., 2005). In a multi-step process such as FT synthesis, one cannot afford to take a narrow view and look only at the process of hydrocarbon production (reactor alone). There is a need to consider the impact that the other steps such as syngas generation, compression, recycling, separation and reforming have on the production of the desired product.

This needs to be done at the earliest stages of the process design and if possible before and during the experimental program so that insights into the reactor design and catalyst performance and how they influence the overall process efficiency can be incorporated into the experimental program.

At the early stages of the synthesis of a process and in particular, during the experimental program, it is important to be able to set up simple models of the major process units and the interconnections between them. These models must characterize the inherent or target efficiencies of the units so that a wide range of operating parameters and flow sheets can be scanned quickly and efficiently. A method of developing a preliminary process flow sheet and the analysis of this process incorporating syngas production, FT synthesis, product separation and recycling/reforming of methane and unconverted syngas is presented in this paper. This method makes it possible for process designers to have a feel for the process and the implications of its operating regions and parameters of the reactor and catalyst on the entire plant. Since most of the information for process design purposes is obtained from the laboratory, the designer will be able to identify the experiments that need to be done that facilitate a better understanding of the plant. Espinoza et al. (1999) advised that, due to the complexity of FT synthesis and the variety of rate expressions found in the literature, kinetic studies for design purposes should be performed on the specific catalyst under consideration covering the envisaged commercial operating conditions. This has the effect of minimizing the experimental program and getting the results necessary to do the subsequent design as quickly and efficiently as possible.

3.2 RATIONALE

When planning and performing experiments for developing a chemical process, there is a need to have the objectives for the system clearly in mind. These objectives will

clearly be different from those normally used when only trying to understand the chemistry and the mechanisms. Furthermore, if the program is to produce results quickly and efficiently the objectives of the program need to be known and understood very early in the program when there is minimum information at hand. In this paper, we will develop a methodology to do this. We will illustrate it by looking at results from the Fischer-Tropsch (FT) reaction system.

In an earlier paper on this topic we looked at results from an experimental program on FT Synthesis (FTS) on a cobalt catalyst and showed that the continuation of the program would be very different depending on the objective that was chosen in order to optimize the reactor. Furthermore we showed that at that stage, if we only looked at the reactor, we were not in a position to choose the objective rationally. We therefore made the case that one could only really define the objective if we took the whole plant into account. The problem at that stage is that one is not in a position nor is it desirable, to try to do too detailed a costing exercise as we only require semiquantitative information about where to perform the next set of experiments (Ngwenya et al., 2005).

It is the purpose of this paper to illustrate how one can use simple concepts and calculations to synthesize the process and thereby identify the main issues and drivers that will determine the economics and the environmental impact of the process. The purpose is to be able to do the calculations at the earliest stage of the program in order to drive it to get the required results as quickly and cheaply as possible. Thus the purpose is not to get an accurate costing but to make sure that at the completion of the experimental programme, if the decision to go ahead is made, the designers have the required information to the required accuracy to do the more detailed design and costing. Clearly, as many more programs will be undertaken than are actually commercialized, it is important that one gets to this stage as efficiently as possible.

To do this efficiently, we propose that the process design (synthesis) be done interactively with the experimental program so that as experimental results become available the synthesized process flowsheet can be upgraded and these results are then used to inform the decisions of how the experimental program is to proceed. If this is to be possible then the process models need to be simple and perhaps more difficult the laboratory and the design teams need to work together!

Various process configurations and operating conditions can be used in the conversion of syngas to hydrocarbon products using FTS technology. Although fairly standard, the main process steps can vary depending on the feed stock, syngas synthesis methods and desired products. As a proven technology capable of producing hydrocarbon fuels and chemicals, FT synthesis can be coal-based, natural gas-based and even biomass-based (Larson & Jin, 1999). Depending on their objective functions, each process will have its own constraints and drivers. One way of evaluating the viability of a process under development is by costing its energy, work, and material (i.e., feedstock) requirements. An FT synthesis plant can be made up a number of unit operations (to be referred to as processes), and each of these processes can employ a variety of equipment in order to accomplish a particular operation. All of these processes have been developed and optimized individually and predicting the efficiency of their combined application in the most cost-effective manner is a big challenge to process designers (Vosloo, 2004). In this paper, a method of developing a process and then systematically evaluating it with a view of identifying the major economic drivers is presented.

3.3 METHODOLOGY

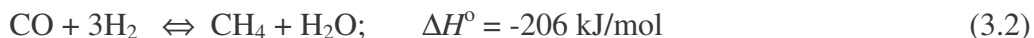
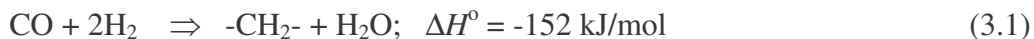
A method of combining major processes in a plant and then collectively costing them has been developed in this work. This is an exercise that needs to be done at an early stage of process development using only basic information. This should be done without taking into account detailed capital expenditure and operating costs. We have

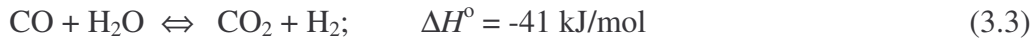
decided for this particular process to turn all the various process activities into one common variable and therefore, the economic drivers will be evaluated in terms of the plant carbon efficiency. Although the concept of carbon efficiency is commonly used in evaluating the efficiency of a process in terms of turning feed stocks into desired products, it is applied differently in this paper. The various pieces of process equipment will be added to the flowsheet as the process develops (is synthesized) and their impact on the overall carbon efficiency of the plant will be evaluated. This will enable us to identify which among the process operations has the biggest impact on plant carbon efficiency. By so doing, bad options will be identified and alternatives developed and insights and understanding gained.

We call this new approach to process design “process synthesis” and it has been applied to develop the flow sheet using basic information about the raw materials, the desired products, and the reaction route. Process synthesis is a tool that process designers can use to develop better and cheaper process concepts quickly. It helps in the selection of cost-effective alternatives from a wide variety of options and these can be integrated in a technically feasible and low cost process concept (PDC, 2004).

3.4 SYSTEM DESCRIPTION

The FT reaction produces hydrocarbons of various chain lengths from a gas mixture of carbon monoxide and hydrogen commonly called synthesis gas. Synthesis gas is normally obtained by the reforming of coal and/ or natural gas. The FT synthesis can be summarized by the following reactions:





Equations 3.1 and 3.2 describe the formation of higher hydrocarbons and methane, respectively. Carbon monoxide can also react with water vapor formed in eqs 3.1 and 3.2 to form Carbon dioxide and hydrogen via the water-gas-shift (WGS) reaction. Note that for simplicity we have chosen to lump together all hydrocarbons of longer chain length than methane as a single entity.

The $-\text{CH}_2-$ is the building block for longer hydrocarbons. One of the most significant performance parameters of the FT synthesis is the product selectivity of the process. The product selectivity is determined by the so-called “chain growth probability”. This is the probability that a hydrocarbon chain grows with another $-\text{CH}_2-$ group, instead of terminating. For instance, a high C_{5+} selectivity is necessary to obtain a maximum amount of long hydrocarbon chains as the product yield in the C_1 – C_4 range decreases with increasing C_{5+} selectivity.

Product selectivity is influenced by a number of factors. These factors can be either catalyst dependent or noncatalyst dependent. The catalyst dependent factors are: type of catalyst metal (iron or cobalt), support, preparation (technique, loading, dispersion, promoters, etc) pre-conditioning and age of catalyst. The noncatalyst dependent factors are: H_2/CO ratio of the feed gas, temperature, pressure, and reactor type. The rate of FT synthesis for iron catalysts is more related to the absolute pressure of the reactants while for cobalt catalysts, it is more dependent on the ratio of the partial pressures of H_2/CO (Espinoza et al., 1999).

For optimal FT reactor design purposes, the type of catalyst to be used must be taken into consideration. The rate of reaction decreases with conversion for reaction systems catalyzed by iron. While this may be explained by the consumption of the reactants in the reactor, one of the main reasons is the formation of reaction products, water and CO_2 (from the water gas shift reaction). Water and/or CO_2 has an inhibiting effect on the FT kinetics of iron based catalysts. Generally speaking, water has no

negative effect on the kinetics of cobalt based catalysts. Therefore, from a kinetic point of view, by using cobalt catalysts there is a likelihood of achieving a higher per pass conversion than by using iron catalysts (Jager & Espinoza, 1995).

In his publication, Vosloo (2004), emphasized that in the design of hydro-processing unit, a balance must be struck between the per-pass conversion in the reactor and the product properties. The higher the per-pass conversion, the smaller the processing unit will be. This is due to the fact that there will be less recycle of material back to the unit. Generally speaking, if the per-pass conversion is low, there will be a cost associated with recycling the unconverted material back to the reactor.

3.5. PROCESS MODELING (FLOW SHEET DEVELOPMENT)

As we want to perform the calculations for the purposes of process synthesis at a very early stage of the process development, we will be using the simplest methods available to perform the calculations. These will generally be thermodynamic calculations based on heat engines. If we wished to refine these calculations with extra information at a later stage this would of course be possible. However, until we have determined the magnitudes of the contributions of the various sub-processes we are adding, this is not justified.

3.5.1 Air separation and Synthesis gas generation

A number of synthesis gas reforming technologies have been developed. These are: steam reforming, autothermal reforming, and catalytic and noncatalytic partial oxidation. It has been reported that synthesis gas generation may account for approximately 60% of the required investments in large scale gas conversion plants based on natural gas (Rostrup-Nielsen, 2002). The choice of the syngas generation technology and the size of the syngas plant will have a direct impact on the carbon efficiency of the entire plant. It is, therefore, important that the choice of the syngas

reforming technology be made by taking into consideration the effect it will have on the rest of this multi-step operation.

The FT synthesis studies in this paper are based on cobalt catalysts. In this low-temperature FT synthesis the cobalt catalyst is taken not to be active for the water-gas shift reaction and as such, apart from H₂, CO is the only reactant. The desirable composition of the syngas from a mass balance point of view for this low-temperature FT synthesis corresponds to a ratio H₂/CO ratio of approximately 2. This can be achieved by the catalytic partial oxidation (CPO) of methane through reaction 3.4. It has been shown that by CPO, high H₂ and CO selectivity above 90% can be obtained from CH₄ at a conversion above 90% (Bodke et al., 1998).



$$\Delta H_{298}^{\circ} = -38 \text{ kJ/mol}; \quad \Delta G_{298}^{\circ} = -86.5 \text{ kJ/mol}$$

Up to 40% of the main costs of a syngas plant based on partial oxidation are related to the oxygen plant. There have been suggestions of using air directly for syngas generation thereby eliminating the cryogenic air separation plant. The use of air in the process stream is only feasible in once-through synthesis schemes in order to avoid the accumulation of nitrogen (the syngas will contain about 50 vol % N₂). The use of air instead of oxygen will result in big reformer volumes and consequently big feed/effluent heat exchangers and compressors. This may also result in big purge gas streams leading to energy and material waste (Jess et al., 1999). Synthesis gas generation in our studies will be by partial oxidation and oxygen will be supplied from an air separation unit. Other alternatives could be considered using the same approach. However, as the aim of this paper is to demonstrate the process synthesis methodology, at this stage it is not necessary to compare syngas production

alternatives. Figure 3.1 shows the flow sheet of syngas generation with oxygen from the air separation unit.

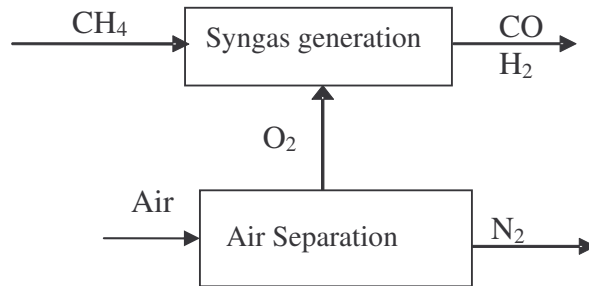


Figure 3.1 Flowsheet for syngas production and air separation.

As in any commercial cryogenic Air Separation Units (ASUs), separation of O_2 from N_2 is achieved by distillation because these gases have different boiling points. While we do not dispute the values of the minimum work of separation used for ASUs that exist in the literature, we have decided to look at a typical distillation process and determine the minimum separation work using a fundamental approach based on thermodynamics. Since distillation is a separation process driven by heat input (King, 1971), Carnot engines have been used to perform heat interactions with the surroundings to determine the minimum work (Figure 3.2). This is because all our other calculations will be done in a similar way, and we are looking for not absolute values but relative ones.

Taking heat from the surroundings, the distillation column has been modeled as a heat pump while the refrigeration process that has to provide condensation has been modeled as a Carnot heat engine. The work of refrigeration will be provided through the normal steam cycle, which converts heat generated by the burning of methane into work. The minimum work of separation is the net result of all the maximum possible work output delivered by Carnot heat engines and the maximum possible work input required by the Carnot heat pumps. This type of analysis has been done

before to determine the minimum work requirement for distillation processes (Cerci, 2002).

This minimum work of separation represents a lower bound on the energy that must be consumed by a separation process. This is very important at the early stages of process design because it gives an indication of the relative difficulties of the separation. In some processes the separation must be carried out with energy consumption close to the minimum work of separation in order to be economical.

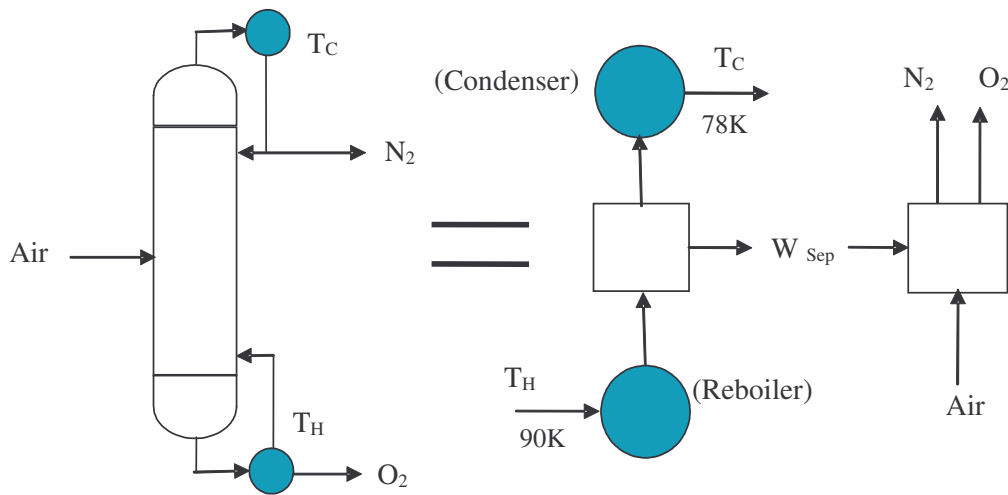


Figure 3.2 Distillation process modeled as a set of heat engines.

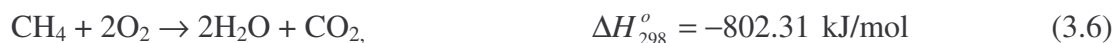
For a fixed production rate of hydrocarbons per day, the daily oxygen requirements will be calculated from the following overall reaction:



The boiling points for oxygen and nitrogen at atmospheric pressure are 90 and 78 K, respectively. We could of course look at the air separation process in more detail such

as considering doing it at higher pressure. The effect of this would be that we would have to take into account the work that is put in by compression relative to the fact that we would run the Carnot engines between different temperatures. This however is a separate exercise and we will not be doing it in the present paper. For the distillation process, we shall supply heat to the reboiler of the column at 90 K and then removed it from the condenser at 78 K. Heat could be supplied to the reboiler by the surroundings, but we need to consider how heat could be rejected in the condenser.

The removal of heat from the condenser at 78 K will need to be done via refrigeration which will absorb the heat from the condenser at 78 K and reject it to the atmosphere at 298 K. However, for the refrigeration process to proceed, we need to provide energy to the system. It is proposed that we relate this energy requirement to the amount of methane that would need to be combusted to generate the heat that is required (eq 2.6).



This heat will be converted to work using a normal steam power cycle. The heat from combustion will be assumed to be absorbed as steam at 573 K and the steam will be run through a turbine to generate the work for the refrigeration process. This turbine (modeled as a heat engine) will take in heat at 573 K and release it to the atmosphere at 298 K. The three processes (Distillation, Refrigeration and Power generation) needed for air separation have all been modeled as thermodynamic heat engines and this is shown in an integrated flow sheet in Figure 3.3.

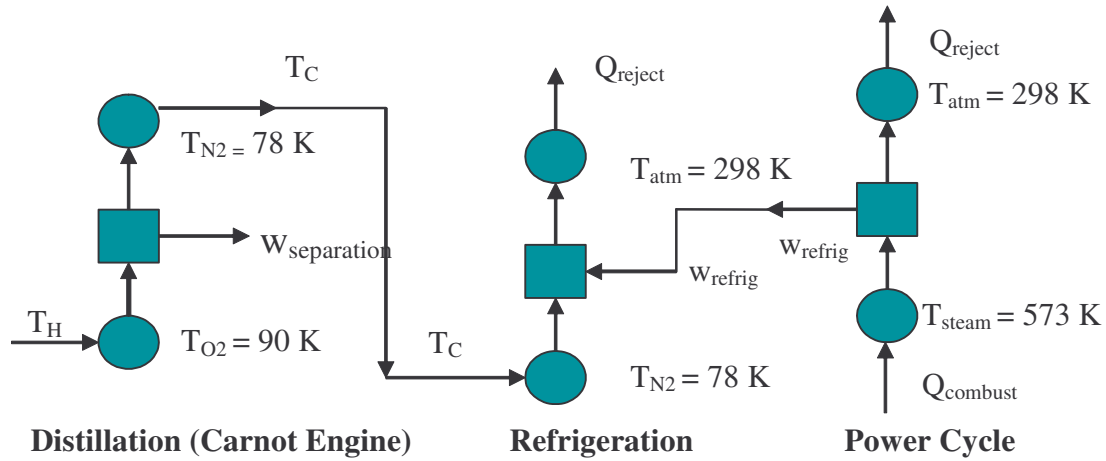


Figure 3.3 Detailed flowsheet for air separation modeled as thermodynamic engines.

The minimum isothermal work of separation is also equal to the increase in Gibbs free energy (G) of the products over the feed. The Gibbs free energy is defined as $G = H - TS$. Therefore

$$\Delta G = W_{\min,T} = \Delta H - T\Delta S \quad (3.7)$$

Where T = the absolute temperature, ΔH = the enthalpy of the products minus the enthalpy of the feed and ΔS = the entropy of the products minus the entropy of the feed. For the isothermal separation of a mixture of ideal gases $\Delta H = 0$ and therefore the minimum work for a reversible separation process separating products at the same temperature and pressure as the feed is:

$$W_{\min,T} = -T\Delta S = -RT \sum_{i=1}^N x_i \ln(x_i) \quad (3.8)$$

where, $W_{\min,T}$ is the reversible work of separation (kJ/(K mol)) at temperature T , R is the gas constant (kJ/(K mol)), T is the ambient temperature (K), and x_i is the mole fraction of component i in the mixture (in this case O_2 and N_2 only).

The work of separation ($W_{\text{separation}}$ in unit of kJ/day) was determined by multiplying W_{min} by the daily flow rate of the air.

$$W_{\text{separation}} = W_{\text{min}} \times N_{\text{Air flow rate}} \quad (3.9)$$

It is known that Air Separation Units (ASUs) are highly inefficient and as such the actual work of separation is much higher than the minimum work, but what we have done here suffices for our purposes at this stage. At a later stage when more accurate calculations become necessary these factors could be taken into account.

Calculations of the efficiencies of the thermodynamic engines required for the separation i.e., the Carnot and Refrigeration engines are given in appendix II. A process flow sheet incorporating air separation and syngas generation is shown in Figure 3.4

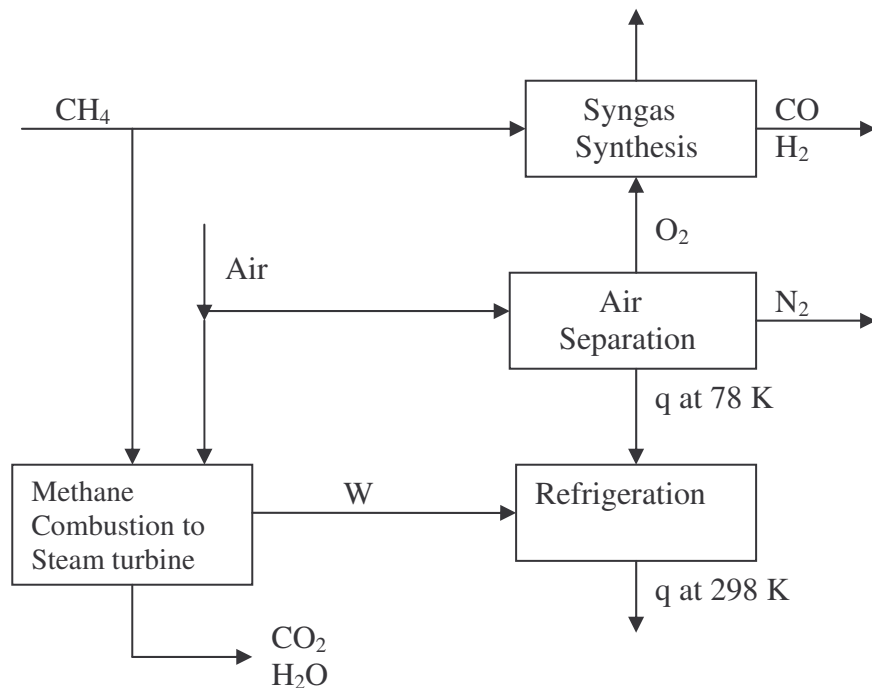


Figure 3.4 Process flowsheet showing air separation and syngas generation stages.

Note that we have not tried to take into account the real efficiency of the processes as we are really first looking for those that have the major impact on the overall process. Once we have identified these drivers we could try to refine the calculations, but this is not justified at this stage of the process synthesis.

There is enough evidence in the literature that apart from reducing the partial pressures of the feed gas to the reactor, CO₂ which is produced during the syngas synthesis does not have any inhibiting effect on the rate of FT synthesis for cobalt catalysts that are not active for the water gas shift reaction (Espinoza et al. (1999), and for this reason, it was decided not to include the CO₂ removal section in this analysis.

3.5.2 Fischer-Tropsch Synthesis

The FT synthesis was modelled on the basis of the experimental data obtained from the laboratory. The experiments were conducted in a continuously stirred basket (CSB) reactor on a cobalt-based catalyst. The total reactor pressure was 8 bar, and the reactions were run at 220 and 250 °C. The main objectives of these runs were to obtain basic information on the activity and selectivity of the catalyst as a function of space velocity and H₂ to CO feed ratio. Space velocity was used as a variable because it is known to have an impact on the degree of CO conversion. CO conversion is also a good indicator of catalyst activity and can easily be measured. The more active the catalyst is, the higher the CO conversion at constant temperature and space velocity (Cerci, 2002). The variation in temperature and H₂ to CO feed ratio were also expected to have an effect on product selectivity. The partial pressures of H₂ and CO in the exit stream and the rate of methane formation were therefore also measured.

While it is clear in the literature that pressure drop constraints are a reality in fixed bed operations for catalysts with larger particle sizes ($d > 1$ mm) and that for

particles of this size, intraparticle diffusion can be a limiting factor for the overall reaction rate (Sie & Krishna, 1998), the cobalt-based catalyst that was used in this study was chosen to obtain kinetic data to be used for design purposes only. For this reason, the analysis was not done with respect to kinetic expressions and intraparticle diffusion limitations that are inherent. The objective was, to use this laboratory data to develop a simple flowsheet model for FT synthesis that includes major process units so as to identify the major drivers in the process. Thus, for the purpose of this study, the results obtained from the laboratory using the chosen catalyst are real and the design of the process will depend on them. This is in accordance with recommendations in the literature that kinetic studies for design purposes should be performed on the specific catalyst under consideration for use for commercial purposes (Espinoza et al. (1999)).

The trend of increasing CO conversion with decreasing space velocity was in line with results that have been reported in the literature (Lampert et al., 1983; Kuipers et al., 1996). As expected, it was observed that the highest rates of CO conversion, lowest rates of methane formation and highest selectivity toward hydrocarbons were obtained in the regions of high partial pressures of H₂ and CO. The measured rates of CO conversion and CH₄ formation, and as the CSB is essentially a CSTR, the partial pressures of H₂ and CO in the exit stream will be used in the calculations.

To obtain sufficient information for the process synthesis, simple calculations were done using the data from the laboratory. No model was fitted to the kinetic data so the results obtained are essentially model-free. Equations 2.1 and 2.2 will be expressed in terms of reaction extents 1 (ϵ_1) and 2 (ϵ_2), respectively.

Assuming that the above reactions are taking place simultaneously and using the reaction extents (ϵ_i), we can calculate the flow rates of various components in the exit streams.

The molar flow rates of the hydrocarbon and methane formed will be equal to ε_1 and ε_2 , respectively. The molar flow rate of water formed is $N_{H_2O} = \varepsilon_1 + \varepsilon_2$. The molar flow rate of CO converted is $N_{CO}^o - N_{COout} = \varepsilon_1 + \varepsilon_2$, while that of H₂ converted will be $N_{H_2}^o - N_{H_2out} = 2\varepsilon_1 + 3\varepsilon_2$.

Using the reaction rates of CO conversion (r_{CO}) and methane formation (r_{CH_4}) measured in the laboratory, the rate of hydrocarbon formation (r_{CH_2}) was calculated as

$$r_{CH_2} \text{ (mol/s*g)} = r_{CO} - r_{CH_4} \quad (3.10)$$

To get a value of N_{CH_2} , an assumption of the mean molecular mass of the hydrocarbons produced (other than methane) had to be made. A value of 6 carbon chain length was used. It was however, shown that the results were very insensitive to this value. If the product distribution was measured this value could be calculated.

Since the amount of hydrocarbons to be formed is fixed (the plant's production rate), the rate of their formation can be calculated from eq 3.10. The mass of catalyst required for this reaction will be:

$$m_{cat} \text{ (g)} = \frac{N_{CH_2}}{r_{CH_2}} \quad (3.11)$$

and using the same amount of catalyst calculated in eq 2.11, the molar flow rate of methane formed is

$$N_{CH_4} = r_{CH_4} m_{cat} = \varepsilon_2 \quad (3.12)$$

The amount of CO converted can also be calculated using the amount of catalyst for the reaction:

$$N_{CO} \text{ (mol/s)} = r_{CO} m_{cat} = N_{CO}^o - N_{COout} = \varepsilon_1 + \varepsilon_2 \quad (3.13)$$

The compositions of CO and H₂ in the exit stream were measured in the laboratory and since the total reactor pressure (P_{Total}) is known and in this study 8 bar was used, the partial pressures of CH₄, CH₂ and H₂O will be calculated taking into account the 10% inert gas in the feed and exit streams, using the following equation:

$$P_{Total} = P_{CO} + P_{H_2} + P_{N_2} + \left(\frac{N_{CH_2}}{N_{Total}} P_{Total}\right) + \left(\frac{N_{CH_4}}{N_{Total}} P_{Total}\right) + \left(\frac{N_{H_2O}}{N_{Total}} P_{Total}\right) \quad (3.14)$$

The total molar flow rate and the volumetric flow rate in the exit stream are:

$$N_{Total} = \frac{(N_{CH_2} + N_{CH_4} + N_{H_2O})P_{Total}}{P_{Total} - (P_{CO} + P_{H_2} + P_{N_2})} \quad \text{and} \quad Q_{Total} = \frac{N_{Total}RT}{P_{Total}}, \text{ respectively.}$$

R is the gas constant (kJ/K mol) and T is the reactor temperature (K). Using the value of Q_{total} in the exit stream, the molar flow rates of CO, H₂ and N₂ in the exit streams were calculated from the expression $N_{x_{out}} = \frac{Q_{Total} P_{x_{out}}}{RT}$, and the flow rates in the feed stream $N_{COin} = \varepsilon_1 + \varepsilon_2 + N_{COout}$ for CO and $N_{H_2in} = 2\varepsilon_1 + 3\varepsilon_2 + N_{H_2out}$ for H₂. (Assuming that $N_{N_2in} = N_{N_2out}$).

Using the information on the rates of CO conversion and CH₄ formation and also the exit partial pressures of CO and H₂, the flow rates of the products formed CH₂, CH₄, H₂O and the unreacted CO and H₂ were calculated. The above calculations were repeated for the various space velocities and H₂ to CO feed ratios considered in this study. Figure 3.5 shows the revised flowsheet with the FTS reactor incorporated in it.

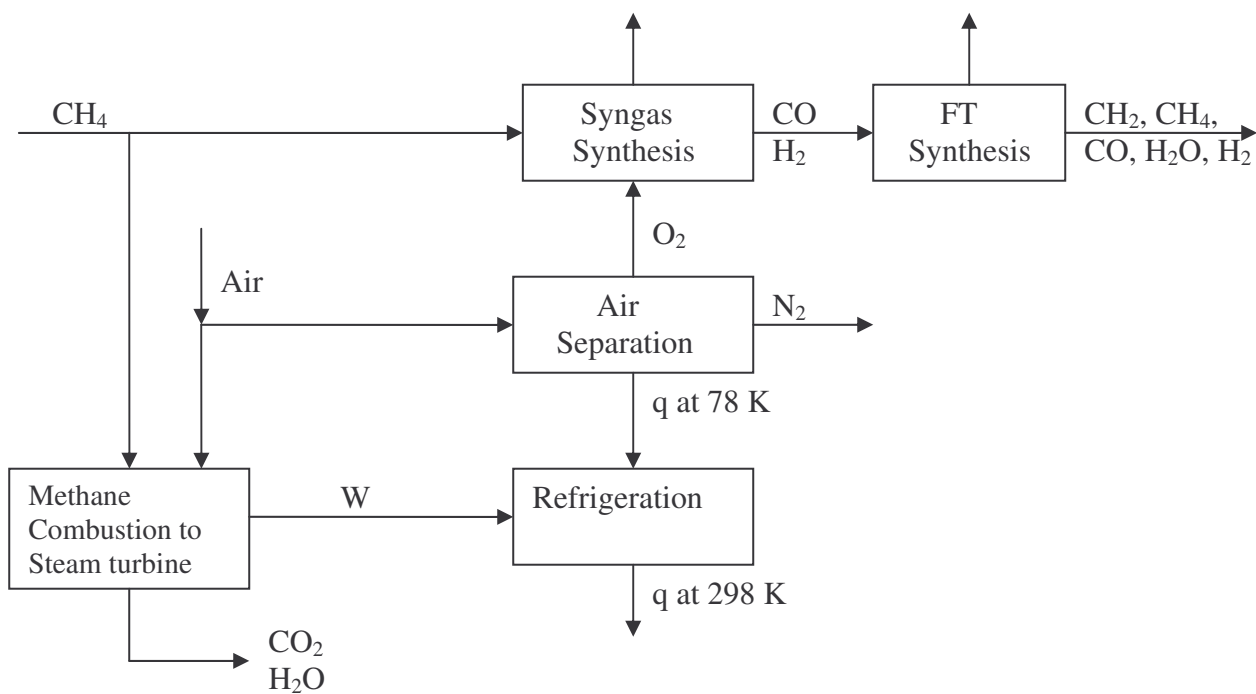


Figure 3.5 Flowsheet with air separation, syngas synthesis, and FTS reactor.

The rates of CO conversion at various space velocities for experiments done at 8 bar and $T = 220\text{ }^{\circ}\text{C}$ using different feed ratios of H_2/CO are shown in Figure 3.6.

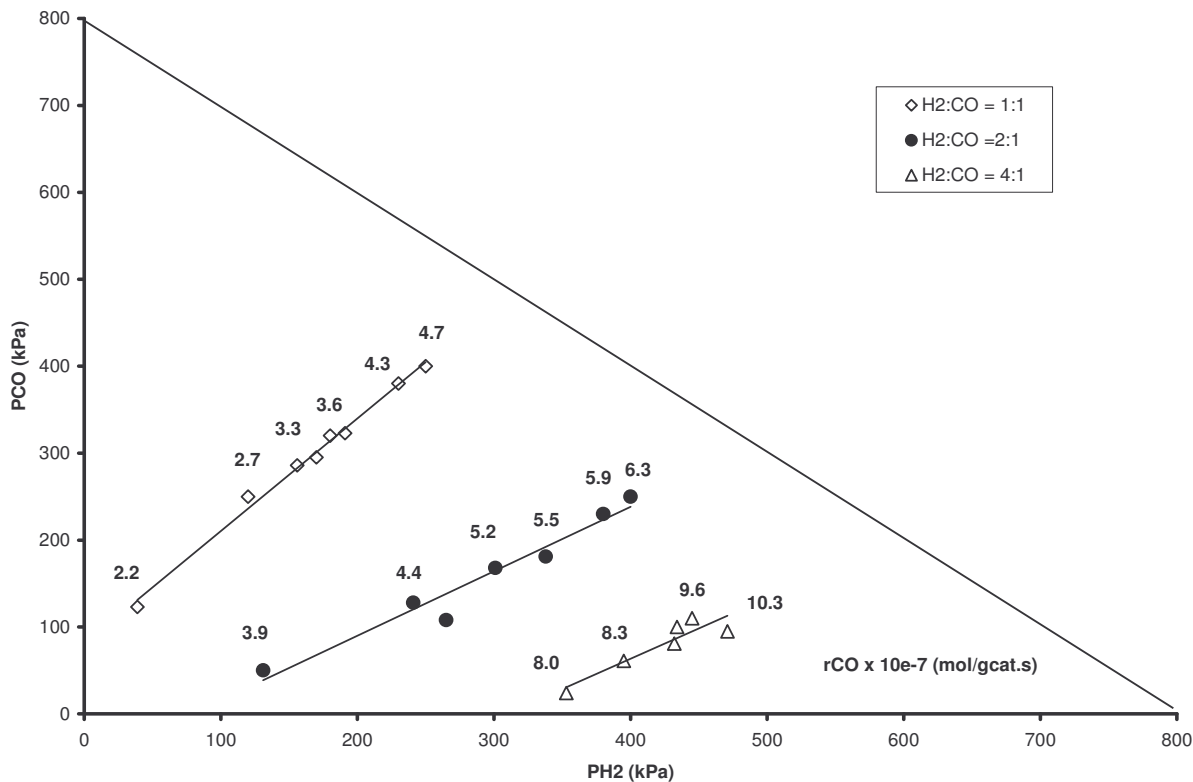


Figure 3.6 Rates of CO conversion measured at various space velocities for $P=8$ bar and $T=220$ °C (The lines on the graphs have no significance other than to group the points together that have the same feed concentration).

Figure 3.7 shows the molar flow rates of $\text{-CH}_2\text{-}$, CH_4 , and H_2O calculated for each amount of CO converted for the three H_2 : CO ratios (1:1; 2:1; 4:1) and various space velocities investigated at 220 °C and 8 bar. According to eqs 3.1 and 3.2, for all three cases of H_2 : CO ratios, the amount of hydrocarbon formed was fixed while the amount of water formed was equal to the amount of hydrocarbon and methane put together. The rate of methane formation was lowest at the lowest CO conversions. Both CH_4 and H_2O formation increased with CO conversion.

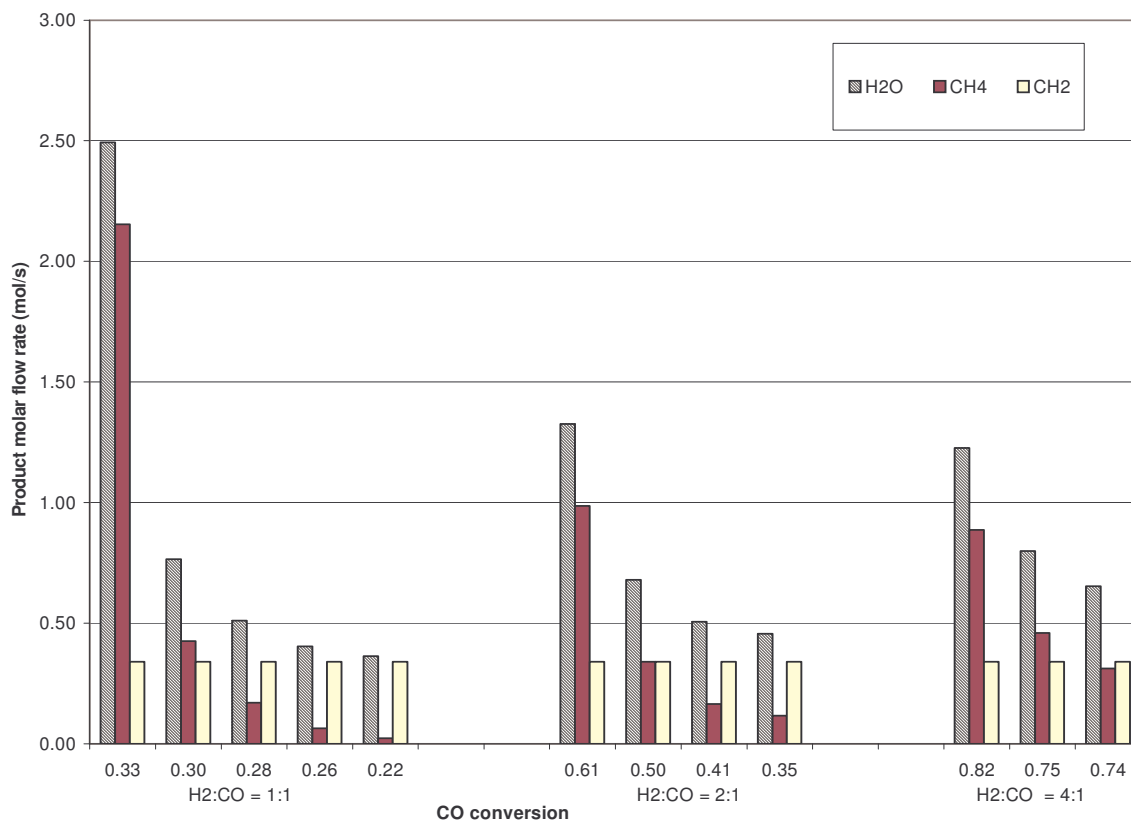


Figure 3.7 Product molar flow rates at various CO conversions for the reaction at 220 °C and 8 bar.

The same trend is observed in Figure 3.8 where the reaction took place at 250 °C and 8 bar. The most striking difference between the two graphs is that there was more methane and water formed at 250 °C than at 200 °C. It has been reported that the operating temperature depends on whether the catalyst used is cobalt or iron based, but usually it is below 250 °C in order to minimize unwanted methane production and to maximize wax selectivity (Madon et al., 1991).

Once the synthesis gas has been converted to liquid hydrocarbons in the FT reactor, the products are fed to the workup unit to separate the liquid hydrocarbons from the gaseous products. Normally, these gaseous products consist of unreacted H₂ and CO, methane, ethane, propane and butane. In this study, ethane, propane, and butane have

been lumped with methane. Assuming that the process employs the use of an ideal separator separating hydrocarbons from the unreacted CO and H₂, methane, and H₂O and that all the methane formed will have to be recycled and reformed with a stoichiometric amount of H₂O, a new flow sheet shown in Figure 3.9 was developed taking into account the separation and reforming. For the purpose of illustration, the second reforming unit has been used to reform methane using steam while the first reforming unit for syngas production used partial oxidation without any steam. The amount of recycled methane and water will determine the composition of the syngas leaving the reformer.

Again, in order to convert all the heat requirements back to one variable, it will be assumed that methane combustion will be used as the only source of energy for those processes that require energy. The quantity of methane required to produce energy $Q_{\text{combustion}}$ is given by the following expression:

$$N_{CH_4} = \frac{Q_{\text{combustion}}}{\Delta H} \quad (3.15)$$

Where ΔH is the enthalpy of methane combustion (802.31 kJ/mol).

Energy for running the air separation plant is obtained from the combustion of methane and so is the energy for the reforming process.

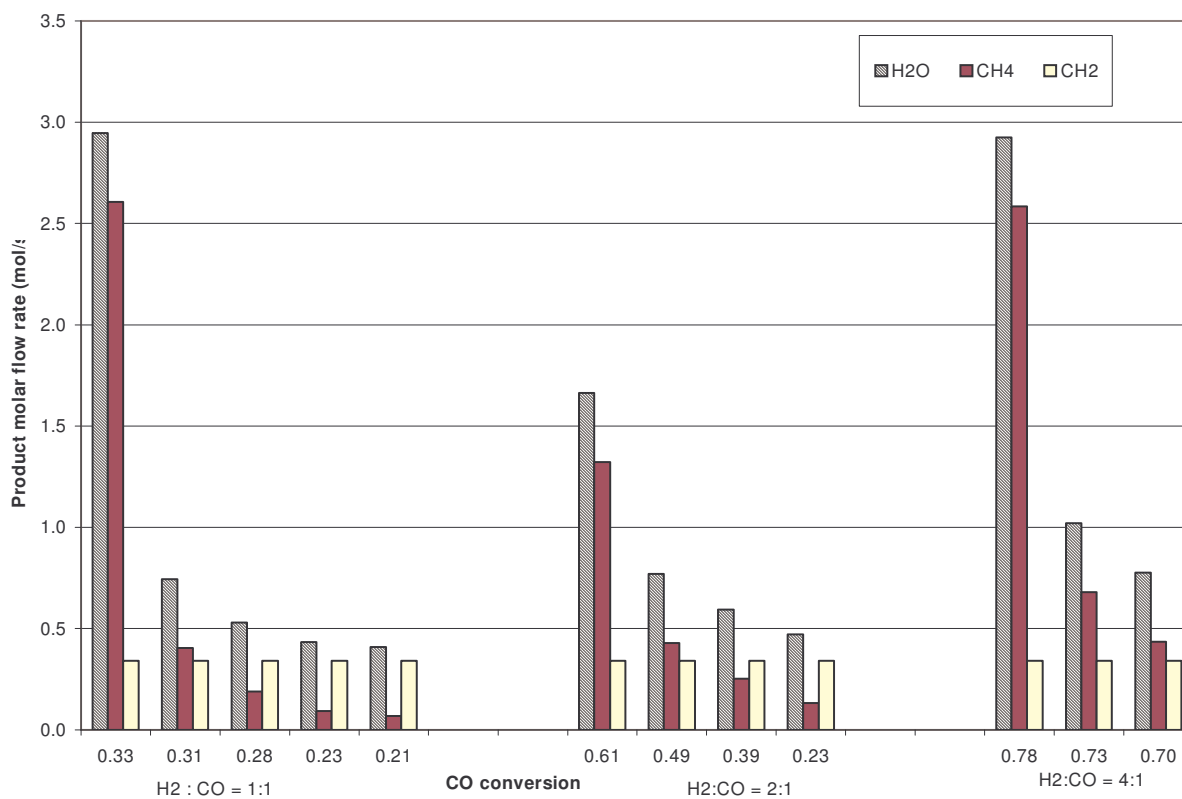


Figure 3.8 Product molar flow rates at various CO conversions for the reaction at 250°C and 8 bar.

The flowsheet in Figure 3.9 shows that the carbon required for the process will be in the methane feed to reformer 1 and methane used for supplying energy for air separation and reformer 2.

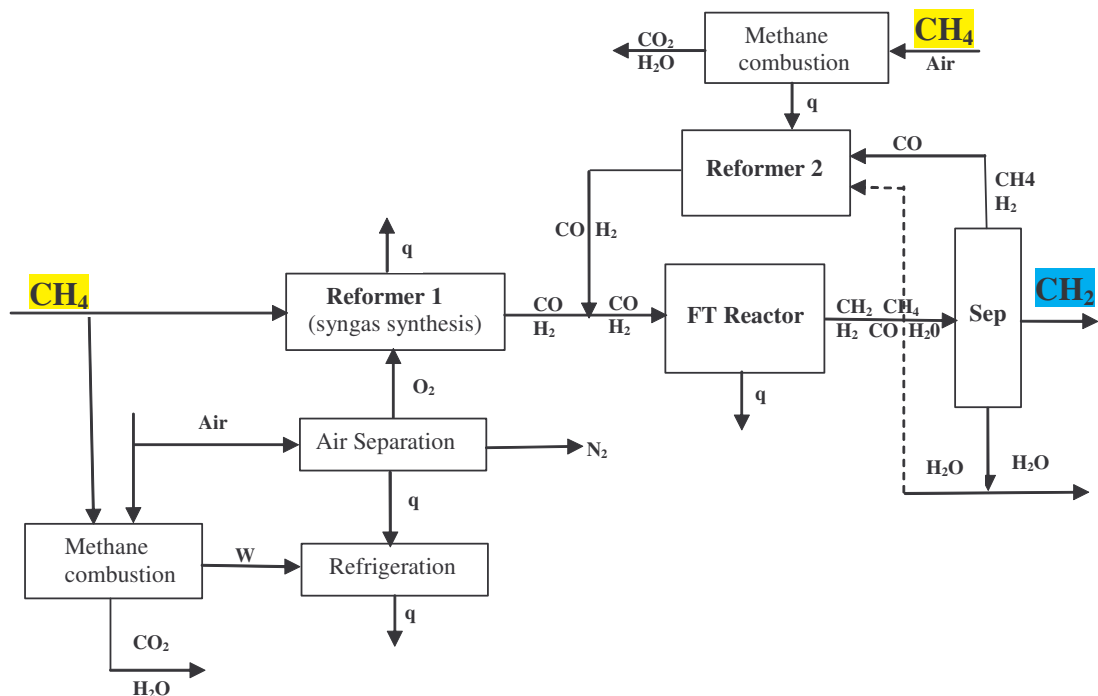


Figure 3.9 Flowsheet with ideal separation and perfect reforming.

It is stated in the methodology section that all the various activities in the process will be turned into one common variable called “carbon efficiency”. As a key measure of the plant’s operating economics, carbon efficiency (CE) is calculated as follows:

CE =

$$\frac{\text{Carbon in hydrocarbon products}}{\text{Carbon fed to process including C in any necessary fuel}}$$

Carbon efficiency was calculated for all the runs at various space velocities and plotted in the CO and H_2 partial pressure space shown in Figure 3.10.

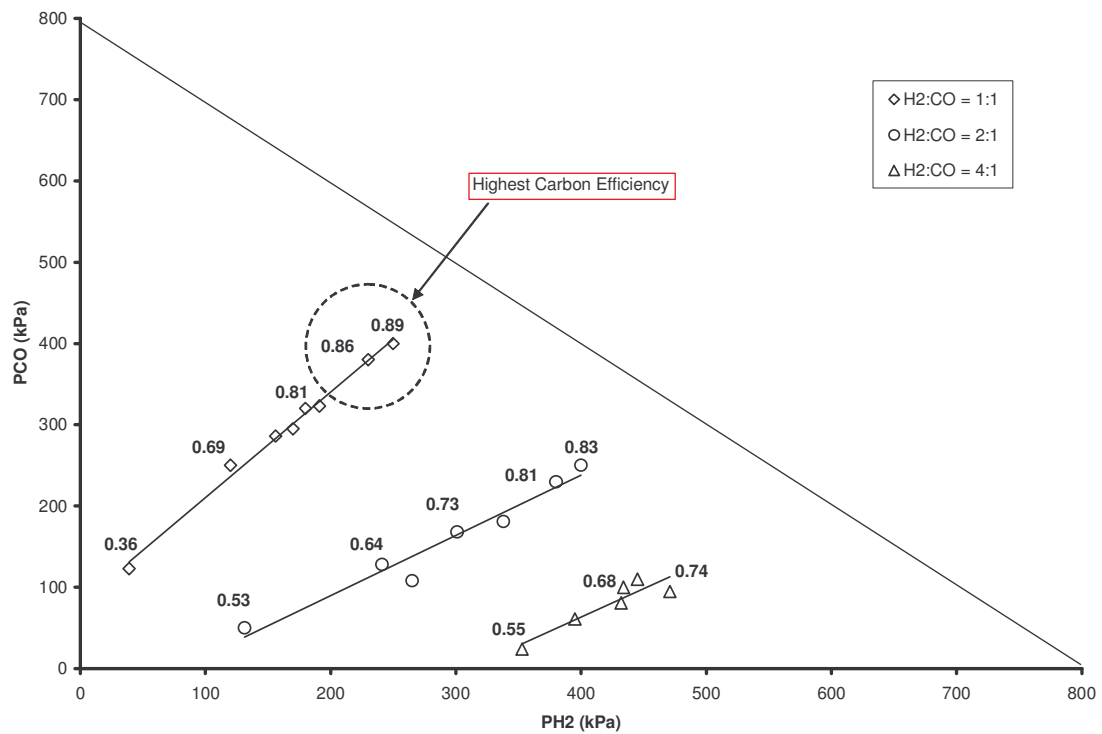


Figure 3.10. Carbon Efficiency for the process assuming Perfect Reforming and Ideal Separation at 220 °C.

Figure 3.10 shows that the carbon efficiency is higher at lower rates of CH₄ formation, lower CO conversion and shorter residence times. In all the three ratios of CO: H₂ investigated, carbon efficiency increases with the increase in CO and H₂ partial pressures. The highest value of carbon efficiency was obtained in the experiment running with a CO rich feed, i.e., H₂: CO = 1:1 at the lowest residence time. Carbon efficiency was also calculated for the experiments done at 250 °C and it was found that Carbon Efficiency was slightly lower than that obtained at 220 °C by about 5% on average. This is because of the higher production rates of methane at 250 °C. Hence as the suppression of methane production is a key driver. We can see that to increase carbon efficiency we need to run the process at low rates of methane formation which corresponds to low temperature.

If we choose to run the process in the region of higher carbon efficiency the result will be a process with large recycles because these are also regions of low conversions. Because it is important to take into consideration these recycles, a compressor will be introduced to compress the recycled CH₄, CO and H₂ to the reformer. A 10% pressure drop in the loop has been assumed. This process drop is actually in the hands of the designer of the equipment. The value chosen is a typical value. If this proves to be an important assumption then calculations can be repeated for other values. Two other compressors will be considered. One compressor will be used to compress the methane feed to reformer 1 while the other one will compress syngas feed to the FT reactor. The new flow sheet developed with the three compressors in it is shown in Figure 3.11. The three compressors will require energy by way of compressor work and this will be provided for by burning methane. Carbon efficiency will be calculated for this new flow sheet in order to see the effect of compressors on the overall carbon efficiency of the process.

The compression work (W_s) was calculated by assuming that the compressor work isothermally (eq 3.16) and the energy for this compression work was obtained from combustion of methane (reaction 3.6). Equation 3.17 shows how the quantity of methane needed to provide this energy for compression work was calculated.

$$W_s = \left(\frac{\gamma}{\gamma - 1} \right) MRT_1 \left[\left(\frac{P_2}{P_1} \right)^{\frac{\gamma - 1}{\gamma}} - 1 \right] \quad (3.16)$$

Where W_s = adiabatic work [kW], T_1 = compressor feed temperature (K), P_1 = feed pressure to compressor, P_2 = exit pressure from compressor, M = molar flow rate of the gas to the compressor [kmol/s], $\gamma = C_p / C_v = 1.4$ (C_p is heat capacity at constant pressure and C_v is heat capacity at constant volume).

$$N_{CH_4}(Comp) = \frac{|W_s|}{\eta \Delta H_{combustion}}, \quad \eta = 0.48 \quad (3.17)$$

Where, N_{CH_4} is the number of moles of methane required for compression, W_s is the work of compression calculated in eq 3.16, $\eta = 0.48$ is the compression efficiency and $\Delta H_{combustion}$ is the enthalpy of methane combustion in reaction 3.6.

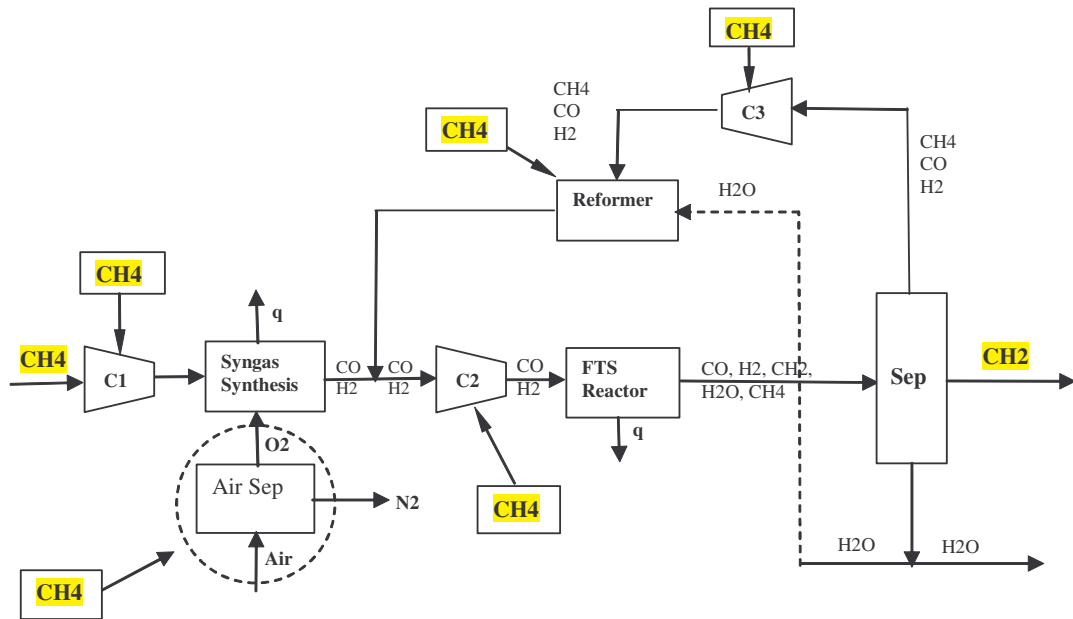


Figure 3.11 Flowsheet developed by assuming ideal separation, Perfect Reforming and Compression of the recycle stream.

From the calculations and the picture in Figure 3.12, there was an average reduction of about 2% in carbon efficiency due to the addition of these compressors to the process. Therefore, it is reasonable at this stage to say that the three compressors did not have a major impact on the carbon efficiency of the overall process.

Instead of assuming perfect separation, distillation will be assumed to be used in separating the liquid hydrocarbons from other gaseous products and this unit will be incorporated in the flowsheet. The calculations will be based on separating the average hydrocarbon products from methane. The distillation process has again been modelled as a set of heat engines. The energy for refrigeration in the distillation unit will be provided for by the combustion of methane. A new flow sheet that includes syngas generation, air separation, FT synthesis, product separation, compression and reforming has been developed in Figure 3.13.

Results of the carbon efficiency analysis for this modified flowsheet are shown in Figure 3.14. Addition of a separation unit did not have any impact on the overall carbon efficiency of the plant. The results are virtually the same as those in Figure 3.12.

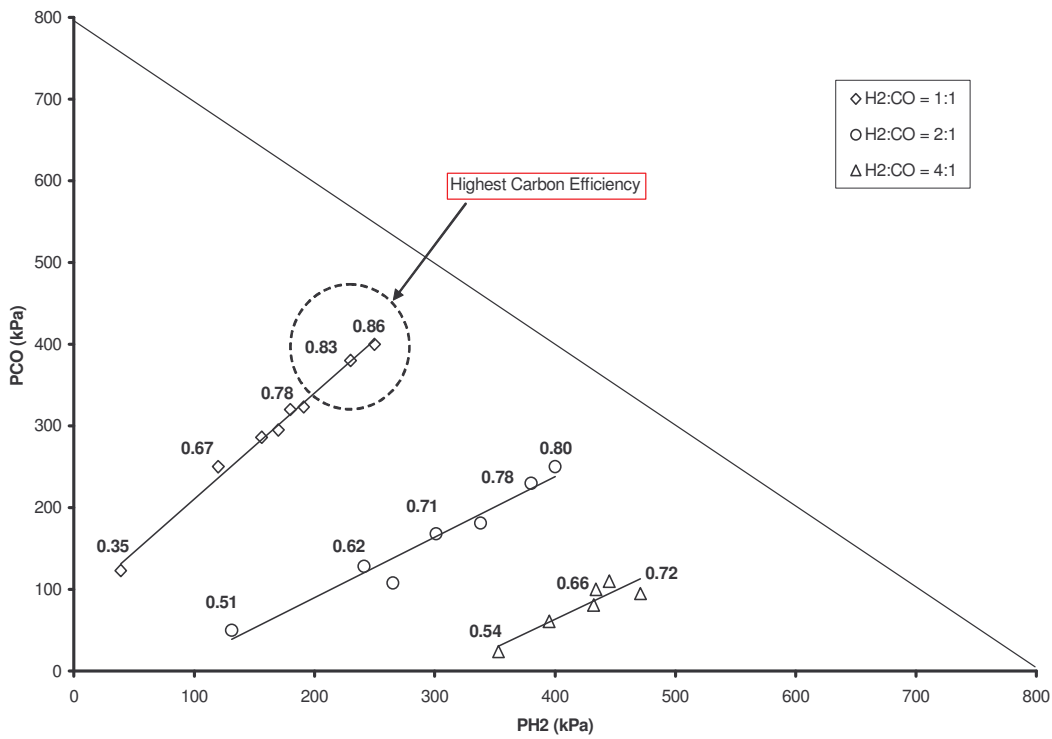


Figure 3.12 Carbon Efficiency for the process assuming Perfect Reforming, Ideal Separation and Compression.

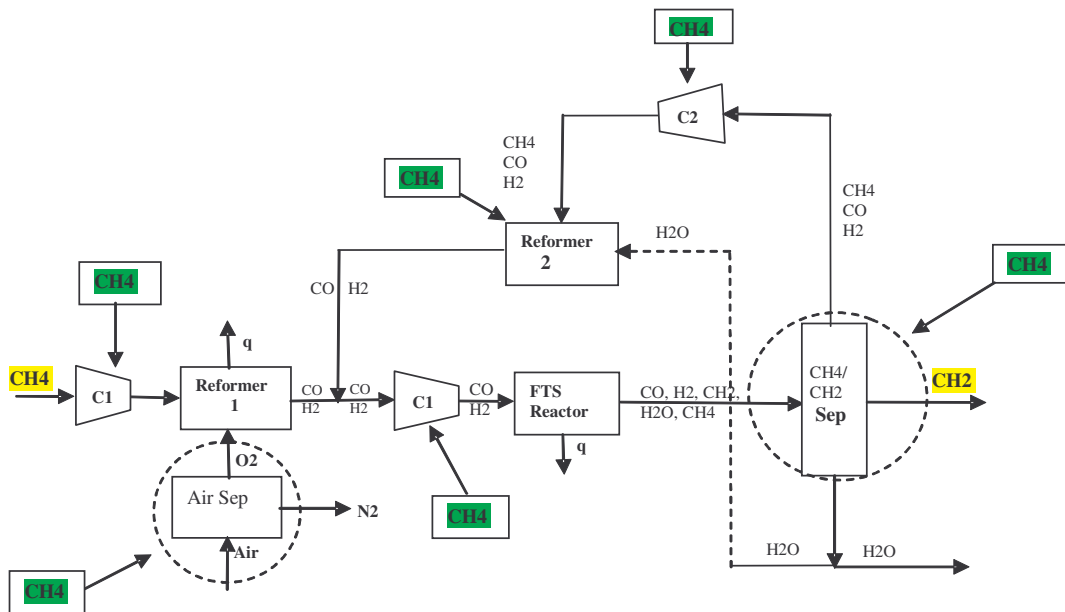


Figure 3.13 Flowsheet with CH₄/CH₂- separation, compression, air separation and reforming.

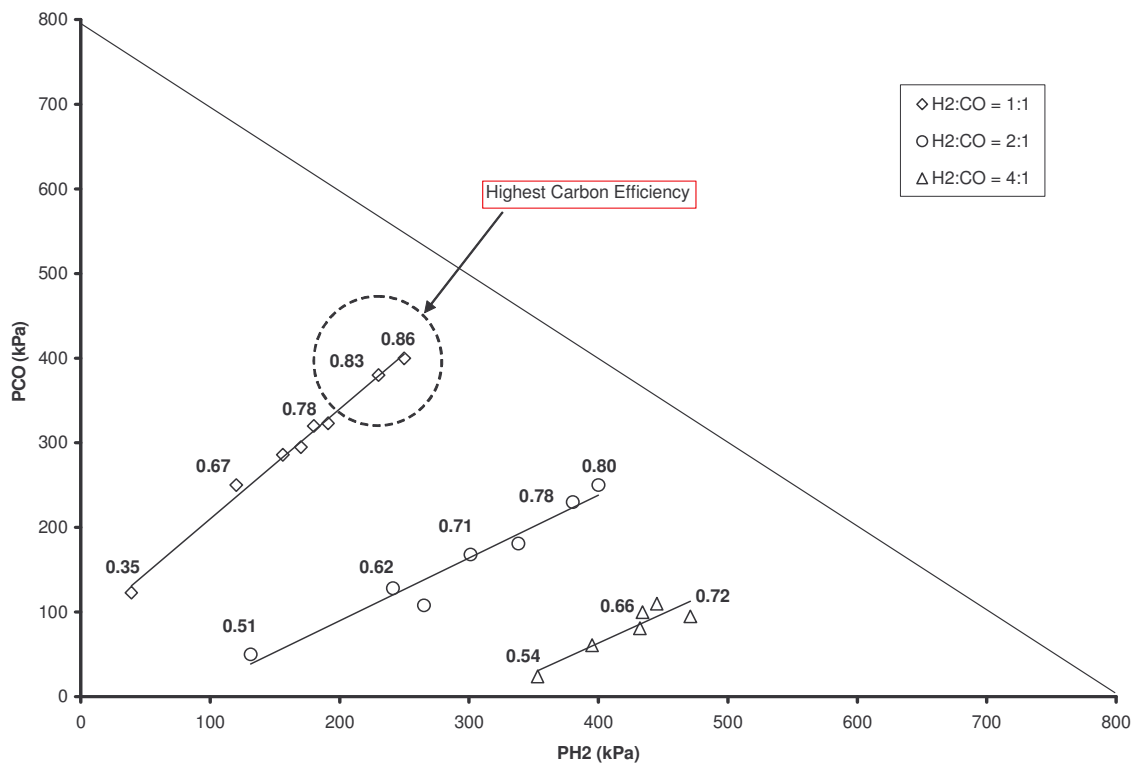


Figure 3.14 Carbon efficiency for the process with the incorporation of the CH₄/-CH₂- separation unit.

Figure 3.15 indicates the percentage energy requirements for the various operations which have been considered in the development of the alternative flow sheets. The flow sheet consisting of compression, air separation, ideal reforming and methane/hydrocarbon separation has been considered at various H₂: CO ratios, space velocities and CO conversions. From the graph it is seen that in areas of higher CO conversions most of the energy required goes to the steam reforming process and as the CO conversions decreases so does the reforming energy requirements. In the regions of lower CO conversions the air separator dominates in that its energy requirements surpass that of the reformer, compressors and the -CH₂/-CH₄ separator. The energy requirement for the -CH₂/-CH₄ separator is almost negligible as can be seen from the graph.

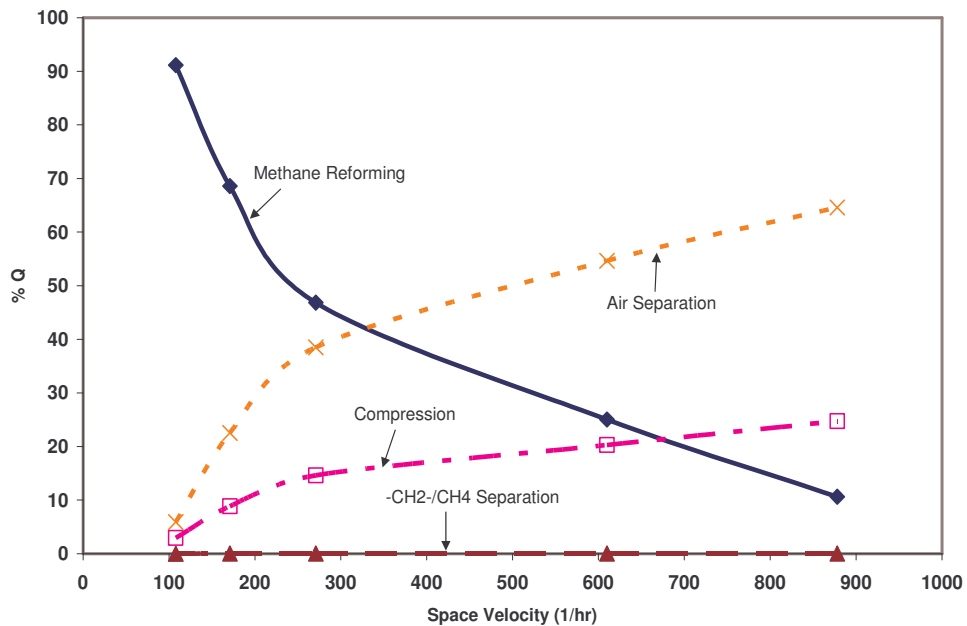


Figure 3.15 Percentage energy demands for the various operations at various space velocities, CO conversions and H₂: CO = 1:1 at 220 °C.

The carbon efficiency of the process declines with the increase in the amount of methane formed as can be seen in Figure 3.16. This is purely on the basis of the amount of energy consumed for reforming of the methane formed. As the system forms more and more methane, there will be a greater demand on the amount of methane to be burnt for the reforming process to take place.

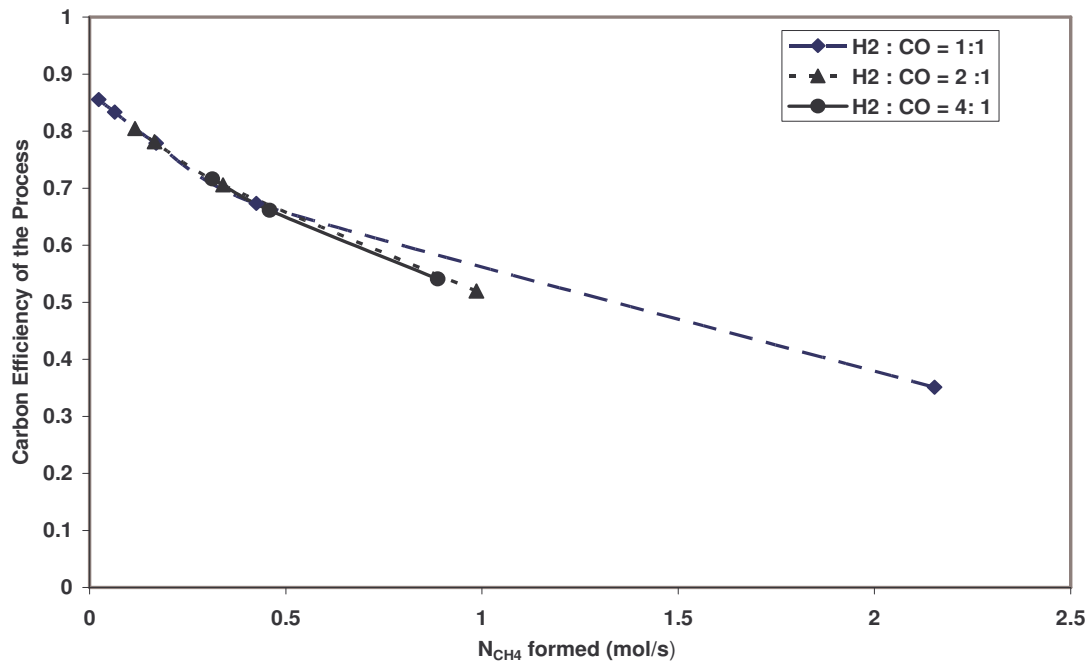


Figure 3.16 Carbon efficiency as a function of methane formation.

Inert gases in the feed gas to the reactor reduce the reactant partial pressures and this in turn reduces the FT selectivity towards hydrocarbons. The basis of the calculations was the production of a fixed amount of hydrocarbons and through mass balances the feed material was calculated that did not include the inerts assuming that the syngas coming to the reactor was free of inerts, however, an analysis was made to ascertain the cost of including a purge stream in the flowsheet on the overall process carbon efficiency should any inerts be present and this was found to have no effect on the overall carbon efficiency. Unlike other processes (e.g., ammonia synthesis) that are very sensitive to purge streams, it is not so for FT recycle processes. This does not mean that inerts they should be allowed in the feed stream as they can have a negative effect on the FT selectivity.

3.6 CONCLUSION

A method of developing an FT process flowsheet using experimental data has been presented. A systematic method of evaluating the flowsheet with a view of identifying the major drivers using carbon efficiency as a measure of plant performance has been developed. The method is quite general and can be used on other processes such as methanol and ammonia syntheses. The major purpose of the paper has been to show how a flowsheet can be synthesized in a systematic way using simple calculations and concepts (mainly thermodynamics). The purpose of the flowsheet, in the first instance, is to derive a meaningful objective, so that the laboratory experiments can be done under the “best” conditions. For this purpose it is not necessary to try and do sophisticated and complicated capital costing. The whole idea is to look for direction and factors that are the main drivers for the process. As the process of evaluating the results develops more accurate models can be applied. The time and effort to increase the accuracy at this early stage are however, not justified.

This approach allows for the identification of further laboratory experiments that need to be done and thus, making sure that the experimental results are useful for the design of an energy efficient process.

The analysis of the obtained experimental data for the process synthesis of an FT flowsheet has led to the conclusion that, for this catalyst, running an FT process at low conversions per pass (high recycle ratios) will give the highest carbon efficiency. This, interestingly enough, is typical of fixed-bed processes where low conversions per pass are used to control the highly exothermic FT reaction. In contrast, modern gas-to-liquid (GTL) processes are designed to operate at high conversions per pass using slurry reactors that have more favourable heat transfer properties. From our point of view, it would be interesting in future to identify the factors that have current GTL technology to run in an apparently reduced regime of carbon efficiency.

Unlike in other processes (for example, methanol synthesis) where a purge stream has a big impact on the process, it has been found in this study that this is not the case here. Carbon efficiency calculations with a 5% and 10% purge stream showed no tangible effect on the carbon efficiency of the entire process. This is on account of the low amount of carbon lost in the purge.

ACKNOWLEDGEMENTS

We would like to thank NRF for the funding that made this study possible. David Glasser thanks the Oppenheimer Trust for the award of the Harry Oppenheimer Memorial Fellowship that allowed the recipient to spend some time at the Chemical Engineering Department of the University of Sydney in Australia during which period some of this work was done.

3.7 REFERENCES

Bodke, A. S., Bharadwaj, S. S and Schmidt, L. D. (1998), The effect of ceramic supports on partial oxidation of hydrocarbons over Noble coated Monoliths, *Journal of Catalysis*, 179, 32-

Cerci, Y. (2002), The minimum work requirement for distillation processes, *Exergy*, 2, 15 – 23.

Espinoza, R. L., Steynberg, A. P., Jager, B and Vosloo, A. C. (1999), Low temperature Fischer-Tropsch synthesis from a Sasol perspective, *Applied Catalysis A: General*, 186, 13-26.

Iglesia, E., Reyes, S. C and Madon, R. J. (1991), Transport-enhanced α -olefin readsorption pathways in Ru-catalyzed hydrocarbon synthesis, *Journal of Catalysis*, 129, 238.

Jager, B and Espinoza, R. (1995), Advances in low temperature Fischer-Tropsch synthesis, *Catalysis Today*, 23, 17- 28.

Jess, A., Popp, R and Hedden, K. (1999), Fischer-Tropsch Synthesis and Nitrogen-Rich syngas. Fundamentals and Reactor Design aspects, *Applied Catalysis A: General*, 186, 321 – 342.

King, C. J., (1971), *Separation Processes*, McGraw-Hill Book Company, 634.

Kuipers, E. W., Scheper, C., Wilson, J. H and Oosterbeek, H. (1996), Non-ASF Product Distribution due to Secondary Reactions during Fischer-Tropsch Synthesis, *Journal of Catalysis*, 158, 288.

Lampert, A., Ericjson, J., Smiley, B and Vaughan, C. (1983), Fischer-Tropsch Synthesis of Hydrocarbon Report, MIT School of Chemical Engineering Practice, USA.

Larson, D. E and Jin, H. (1999), Biomass conversion to Fischer-Tropsch liquids: preliminary energy balances. In: R. Overend, E. Chornet, editors: *Proceedings of the Fourth Biomass Conference of the Americas*. Kidlington, UK: Elsevier Science, vol.1/2, 843-854.

Madon, R. J., Iglesia, E and Reyes, S. C. (1993), in *Selectivity in Catalyst*, American Chemical Society, Washington, DC, 382- 396.

Ngwenya, T., Glasser, D., Hildebrandt, D., Coville, N and Mukoma, P. (2005), Fischer-Tropsch results and their Analysis for reactor synthesis, *Industrial & Engineering Chemistry Research* 44, 5989 – 5994.

Process Design Centre (PDC), Process Synthesis Introduction, INTERNET. <http://www.process-design-center.com>. Cited 18 August 2004.

Rostrup-Nielsen, J.R. (2002), Syngas in Perspective, *Catalysis Today*, 71, 243-247.
Sie, S. T and Krishna, R. (1998), Process Development and scale-up: Part 2. Catalyst design strategy, *Reviews in Chemical Engineering*, 14, 109 – 157.

Vosloo, A. C. (2004), Conceptual design of a Fischer-Tropsch based GTL plant. INTERNET. http://www.sasolchevron.com/conceptual_design.html. Cited 14 October 2004.

4

A PROCESS SYNTHESIS APPROACH TO INVESTIGATE THE EFFECT OF THE PROBABILITY OF CHAIN GROWTH ON THE EFFICIENCY OF THE FISCHER-TROPSCH SYNTHESIS

This paper has been published in the *Industrial & Engineering Chemistry Research*, 2006, 45, 5928 – 5935. Part of this work was also presented at the following conferences:

- World Chemical Engineering Congress, Scotland, July 2005.
- AIChE Annual Meeting, Cincinnati, Ohio, USA, October 30 – November 4, 2005.

A Process Synthesis approach to investigate the effect of the probability of chain growth on the efficiency of the Fischer-Tropsch Synthesis.

Peter Mukoma, Diane Hildebrandt and David Glasser

COMPS, School of Chemical and Metallurgical Engineering,
University of the Witwatersrand, P/Bag 3, WITS 2050.

Abstract

To evaluate a process at the early stage of its development, one needs to be able to do simple calculations in order to compare all the alternatives. This must be done on a reasonably realistic basis, so that one can make credible decisions; however, the process should not be so detailed and laborious that it becomes too “expensive” to perform for alternatives that can ultimately be discarded. A methodology for performing these calculations has been developed and this will be illustrated with a case study on Fischer-Tropsch Synthesis.

The effect of designing a Fischer-Tropsch (FT) process targeting a particular value of the probability of chain growth (α) on the overall carbon efficiency has been studied using simplified FT synthesis flow sheet models. Two process configurations - namely; the once-through and recycle processes - have been compared and it is observed that, for a fixed production rate of liquid fuels at 100% CO conversion, the carbon efficiency for the process with a recycle stream is higher than the once-through process for all values of α . However, if the aim is to maximize diesel production by hydrocracking the waxes, it has been determined that an optimal α value should be sought to reduce the cost of hydrocracking very heavy waxes. The

incorporation of wax hydrocracking in the two processes reduces the carbon efficiency at all α values beyond 0.7, thereby making it uneconomical to produce very long chain hydrocarbons.

4.1 INTRODUCTION

Fischer-Tropsch Synthesis (FTS) is a process that produces liquid hydrocarbons from synthesis gas (CO , H_2) and is a promising option for the production of environmentally friendly chemicals and fuels from coal and natural gas.

Presently, Fischer-Tropsch (FT) catalyst/process technology suffers from the following limitations: (i) limited selectivity for premium products (e.g. light olefins, gasoline or diesel); (ii) catalyst deactivation; (iii) high capital cost; (iv) heat removal as reaction is highly exothermic; and (v) less than optimum thermal efficiency (Mills, G. A., 1988).

Several factors have led to renewed interest in the use of Fischer-Tropsch technology for the conversion of natural gas and coal to liquid fuels. Some of the major factors influencing this renewed interest include (i) an increase in the known reserves of natural gas; (ii) the need to monetize remote or stranded natural gas; (iii) environmental pressure to minimize the flaring of associated gas; and (iv) the need to reduce dependence on crude oil

Because of this renewed interest, more FT plants are likely to be built. Existing FT plants are very capital-intensive processes, so it is anticipated that future plants will be designed based on the available raw materials (coal or natural gas) and the specific needs of a particular economy. For this reason, it is appropriate to make a process evaluation by examining alternative process configurations at the early stage of design. Jess et al. (1999), in their paper, advocated the use of low-cost technology for countries in remote areas where the cost of natural gas is low as the only economical

solution for the conversion of natural gas to higher hydrocarbons using FT-Synthesis. This technology may not be highly efficient but it will bring benefits to the economy. This concept of a low-cost FT process is based on the use of a nitrogen-rich syngas which does not utilize a recycle loop (once-through process) to avoid any nitrogen build-up in the system.

To achieve a reasonable efficiency in a once through FT process of the type proposed by Jess et al. (1999), a reasonably high per pass CO conversion should be achieved. A possibility for achieving this is the use a number of reactors in series (Rage et al., 1997).

In contrast, the objective of the recycle process is to achieve higher reactor productivity using higher syngas flow rates because of the recycle and low single-pass CO conversion.

It is possible that, for the same reactor volume and catalyst loading, the recycle process could have a higher production rate of hydrocarbons than a single-pass operation. The drawback to the recycle process is the level of investment, which is likely to be higher due to the separation of hydrocarbon products, CO₂ and H₂O from the exit stream before syngas and the lighter gases can be recycled. The second choice of using reactors in series (especially if the same volume reactors are to be used) is complicated by the fact that additional fresh syngas might have to be added to the syngas leaving the previous reactor in order to obtain the required feed rate. However, in the case where catalyst activity is such that effectively 100% conversion can be achieved in a single per pass conversion, the once-through process should be the configuration of choice because it will not require any compression and reforming of the recycle stream and no air separation. This is especially true if the cost of methane and or coal is low. Even if 100% conversion is not achieved, if the reactor costs relative to the rest of the plant are relatively low, it may still be preferable to conduct a once-through process.

The FT process is also very interesting from the process synthesis point of view. The reaction produces a range of products and the product distribution is determined by the catalyst, operating conditions and reactor structure. In a recent paper (Ngwenya et al., 2005), the question of the optimal reactor structure and operating conditions for an FT reactor was considered. The rate of CO conversions and selectivity were measured at various CO/H₂ ratios at two different temperatures for a given catalyst. The question that was asked was, how could these data be used to determine the optimal reactor design and the optimal reactor configuration? In particular, the interaction between the experimental program and the process design was considered. It was shown that the optimal reactor design and operating conditions for Fischer-Tropsch reactor was dependent on the objective set, and the resulting reactor and operating conditions could be quite different for seemingly similar and reasonable objectives. An important insight was that the process in which the “optimal” reactor was embedded was far from optimal, in that the processes had large recycle flow rates and very low per pass conversions in common.

A subsequent paper then examined the use of a small set of experimental data to determine the reactor structure and operating conditions when optimizing the process (Mukoma et al., (2006). This was again done with the objective of understanding the interactions between the experimental program, the reactor structure, the process configuration and operating conditions. The concept of carbon efficiency was introduced, which will also be used in this work. Carbon efficiency is directly related to the running costs of the plant and indirectly to the capital costs of the plant. The carbon efficiency of a process is also directly related to the environmental impact that the process has on the environment and, as such, is a very powerful variable which incorporates aspects of running costs, capital costs and environmental impact. It was shown how simple calculations could be performed to evaluate various alternatives and how the outcomes from these calculations could be drivers for deciding plant operating conditions and, hence, guide the experimental program. It

was determined that, to maximize the carbon efficiency of the process, the methane production rate in the reactor had to be minimized

In the previous paper (Ngwenya et al., 2005), all hydrocarbon products, with the exception of methane, were considered to be equally valuable. In this paper, we extend the ideas to take into account the fact that not all products are equally desirable. In particular, we will investigate the effect of the probability of chain growth (α) on the production of diesel fuel. This study will not rely on experimental data, but rather ask the question backwards so to speak: What is the optimal α value for an FTS system that is producing diesel? Once we understand what range of α value we are targeting, we can decide on a suitable catalyst and operating conditions to achieve this.

Of all the products produced by the FT reactor, only a certain percentage of these will be in the diesel fraction. The longer-chain products must be cracked to produce diesel. Previously, we found that the optimal FT reactor did not necessarily translate into the optimal FT synthesis process; in other words, the optimization must consider the entire system. With this in mind, optimal α values for two different systems, namely the syngas production and the FT synthesis section as opposed to the system that includes the syngas production, the FT synthesis and the hydro cracking section, were compared. It is, again, determined that the optimal alpha is different for the two systems, and therefore, it is concluded that the latter system, which incorporates the hydrocracking units, gives the fuller description of the process and hence the more realistic optimal alpha value.

Another question that we can ask at the earliest stage of the process synthesis is what the effect of process configuration is on the objective function, namely achieving the highest carbon efficiency. Again, this can be done before laboratory data is available or, indeed, before a catalyst has been chosen. This furthermore can be done with relatively little effort using very simple models at the very earliest stage of the

process design. We will illustrate this by considering both a recycle and once-through process, as proposed by Jess et al., (1999).

An important parameter in determining the carbon efficiency of especially the once through process is the CO per pass conversion. The effect of varying this on the carbon efficiency of the process and the optimal level of the CO will also be considered.

We propose that process synthesis be used at the earliest possible stage of the design, to guide the experimental program. We claim that by using this approach, we are, in effect able to scan all possible catalysts and operating conditions to determine what the target carbon efficiency is and how sensitive it is to factors such as product selectivity and CO conversion. We are furthermore examining how the structure or configuration of the flowsheet interacts with the choice of catalyst and operating conditions. Lastly, we are able to set targets for the various process configurations, which are upper bounds on the carbon efficiency. Thus, one is able to determine quantitatively what the effect of structure and operating conditions is on the target carbon efficiency. This allows one to understand the impact of the configuration on the plant and, hence, to make decisions in this regard at the earliest possible stage of the process design.

Since the process will be set to maximize diesel production, the process will be evaluated from syngas synthesis right through to hydrocracking of the waxes to maximize diesel yield. The differences between the two processes, in terms of their chemical feedstock and energy requirements, and how these affect the carbon efficiencies will be analyzed. It is hoped that this study will show how a designer can identify major drivers in the two process options without performing any experiments or doing detailed process simulations. In particular, we believe that these simple calculations give insights that can inform both the design and the experimental program.

4.2 PRODUCT SELECTIVITY

The FTS produces a wide range of hydrocarbons, from light gases to heavy wax. By plotting the logarithms of the mole fractions of the various hydrocarbons against the number of carbon atoms, a straight line is often obtained representing the Anderson-Schulz-Flory (ASF) reaction mechanism. In some cases, more than one straight line may be found but we will not consider these cases in this paper. However the methods employed in this paper would be as applicable in these cases.

The slope of this straight line, which is called α , describes the product selectivity (this is also referenced as the probability of chain growth). A high α value implies a high yield of heavy hydrocarbons, whereas a low α value means greater production of lighter hydrocarbons. A current viewpoint seems to be that it is desirable to have a catalyst with selectivity towards high α values (Mills, G. A., 1988). The higher amounts of heavy hydrocarbons produced can be subsequently processed in a hydrocracking unit to produce diesel-range hydrocarbons as has been demonstrated in the Shell Middle Distillate Synthesis (SMDS) process (Eilers et al., 1990). The diesel yield is of high quality, bearing in mind the ever increasing demand for less noxious engine exhaust emissions.

The range of α is dependent on the reaction conditions and catalyst type. Typical ranges of α reported in the literature for ruthenium, cobalt, and iron are 0.85-0.95, 0.70-0.80, and 0.50-0.70, respectively (Dry, M. E., 1982). Figure 3.1 shows the distribution of hydrocarbons (in terms of wt %), as a function of probability of chain growth (α).

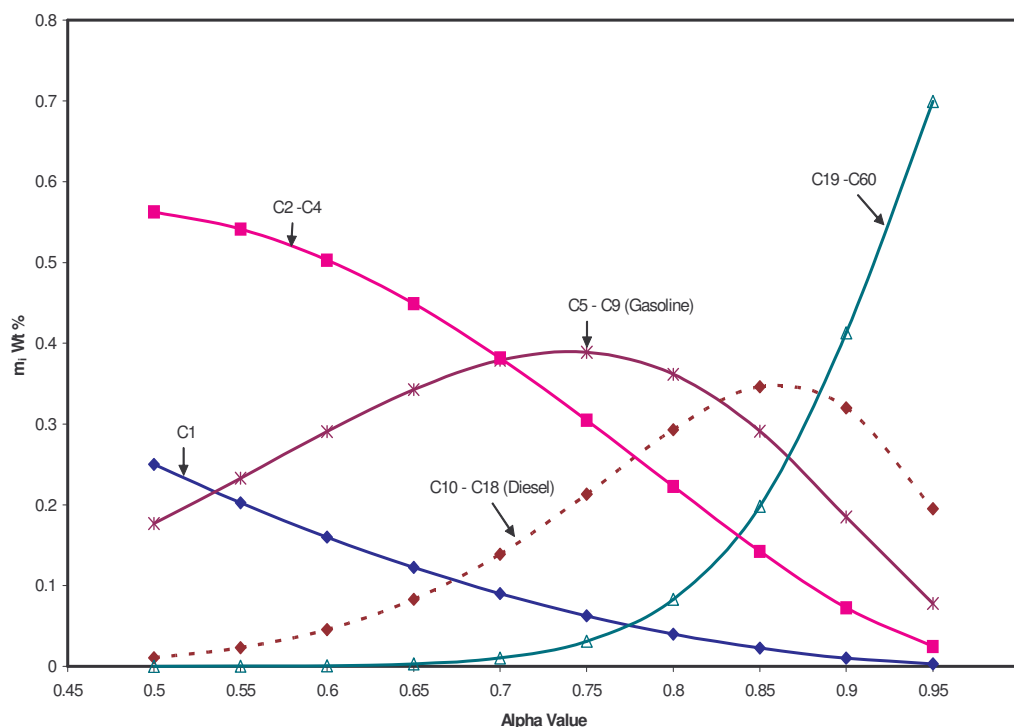


Figure 4.1 Probability of chain growth (α) as a function of the weight factor.

Using the current commercial catalysts available for FT, there are many factors that affect product selectivity. However, the overall product selectivity is controlled by the process operating temperature, reactant partial pressures, and, in the case of iron catalysts, the higher the alkali content, the greater the shift to higher carbon number products. For both Cobalt and iron catalysts targeting wax production at lower temperatures, the H_2 : CO ratio is a key factor. The operating pressure does not affect product selectivity for iron catalysts, whereas for Cobalt, there is a shift toward higher- molecular- mass products as the total pressure increases (Dry, M. E., 1982). It has been reported that, for FT Synthesis operating at high temperature, especially using iron catalyst, the situation is more complicated. Apart from the total pressure, product selectivity is also dependent on the partial pressures of H_2 , CO, H_2O and CO_2 (Dry, M. E., 2004).

Figure 4.1 shows that there is a great range of α value that is achievable. The product selectivity is dependent on the α value. Thus, once the optimal product selectivity and, hence, the desired α value has been decided, the catalyst and operating conditions would need to be chosen to achieve this value.

4.3 CO CONVERSION

It is important in every chemical reaction process to maximize the conversion of feed material into the desired product. In catalytic reactions such as FT, CO conversion rate is an easily measured indicator of catalyst activity, since the more active the catalyst, the higher the CO conversion at constant temperature and space velocity. To achieve a higher CO conversion, the space velocity has to be decreased, or equivalently, residence time increased. As the residence time increases, the probability of a CO molecule adsorbing on the catalyst surface and reacting increases as well and this results in higher conversions of CO (Lampert et al., 1983). There are practical limitations to achieving 100% CO conversion in FT processes, however, from a designer's point of view, a process could, in principle, be designed to operate at almost 100% conversion, because the reaction is not equilibrium limited. This assumption is made in this study. Possible process key drivers for such a process will be identified either in terms of material or energy consumption.

4.4 DESIGN BASIS

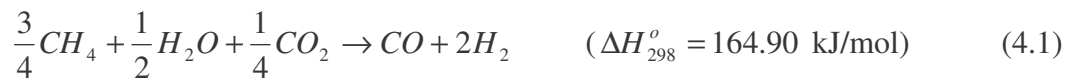
The basis for this process design and analysis is the production of a fixed amount of hydrocarbons from syngas obtained from natural gas (modeled as methane) in a once-through and recycles process. We assume a low-temperature FT synthesis process with no or very minimal CO₂ production.

The approach used in this work differs from that used traditionally for design, in that we are using simple models, which incorporate the major effects such as mass, energy

and entropy balances. We do this as we wish to compare the intrinsic target efficiencies of the processes. We do not wish, at this stage, to incorporate more complex models which look at the practical limitations (i.e. heat transfer, materials of construction etc.); however, this can be done in the next phase, if required, to compare the sensitivity of the processes to equipment inefficiencies. In effect, our underlying assumption at this stage is that the processes have similar sensitivities to inefficiencies as they mostly use similar equipment such as reformers, hydrocracking etc. Thus, the assumption at this stage is that, although more detailed models that incorporate equipment inefficiencies will reduce the target carbon efficiency of the processes, the ranking of the processes, in terms of carbon efficiency, will not be changed. This assumption is more likely to be valid if the carbon efficiencies of the processes are very different. If the processes have similar carbon efficiencies, then, the ranking of the process may be sensitive to equipment inefficiencies.

4.4.1 Reforming Model

All the models below reform the natural gas, which we assume to be methane. We have assumed that the composition of the syngas entering the FT section is stoichiometric, which corresponds to a H_2/CO ratio of ~ 2 . To illustrate the methodology, we will use a somewhat novel system with steam reforming of methane with the addition of CO_2 to obtain syngas of the required H_2 to CO ratio (reaction 3.1). This approach is possible with the stranded natural gas containing CO_2 or if a stream of pure CO_2 is available. The more conventional processes can be analyzed by a similar approach if required.



Reaction (4.1) is endothermic and the energy for syngas production will be derived from methane combustion shown in reaction (4.2):



We have, in this simple model, decoupled the reforming process and the energy providing step. The two reactions (eqs 4.1 and 4.2) may be conducted in one or more pieces of equipment; however, the overall process must be, at best, adiabatic. All the energy and work requirements for recycling and reforming of the lighter gases in the recycle process will be similarly obtained from the combustion of methane.

The quantity of methane to be combusted to meet the energy requirements for the reaction was calculated using the following equation:

$$N_{CH_4} = \frac{Q_{combustion}}{\Delta H_{combustion}} \quad (4.3)$$

Where N_{CH_4} is the number of moles of methane that are required to be combusted to provide the combustion energy $Q_{combustion}$. $\Delta H_{combustion}$ is the enthalpy of methane combustion (802.31 kJ/mol) as calculated in eq 4.2.

4.5 CARBON EFFICIENCY

Figure 4.2 is a simple model that is used to help understand the definition of carbon efficiency as it is applied in this work.

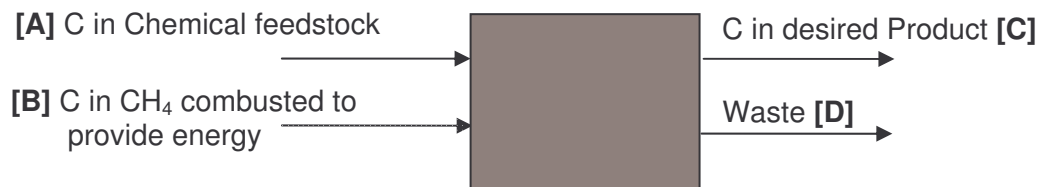


Figure 4.2 Simple model showing variables considered in carbon efficiency calculations.

We differentiate between process streams that provide chemical feedstock (stream A), and those that supply energy (stream B). We, in particular, determined the number of moles of carbon in these streams. Stream C refers to the desired product (for example diesel or C₅₊) whereas stream D is the waste or unwanted products as unconverted syngas, CO₂ and flared gases. The main energy supply that we consider for Stream B is to the reformers as the previous work (Mukoma et al., 2006) showed that these were, by far, the largest energy costs in the process.

Therefore, Carbon Efficiency (η) is defined as:

$$\eta = \frac{\text{Moles of carbon in [C]}}{\text{Moles of carbon in [A] + Moles of carbon in [B]}}$$

In all cases, we fixed the amount of the desired product, namely the quantity of stream C. To produce this fixed amount of desired product, different amounts of CH₄, were consumed (stream A), depending on the alpha values, configuration, etc., and, hence, different amounts of C₁–C₄ and other waste streams (Stream D) were produced.

The carbon efficiency takes the chemical feedstocks and energy streams into account. Thus, it is a good measure of plant operating economics, because the higher the carbon efficiency, the higher the usage of feed material and energy for the production of the desired product. It is also related to the capital costs, because the lower the carbon efficiency, the more material must be processed to produce the same quantity of products. Thus, the process equipment will be larger with correspondingly higher capital costs. It is also a good tool for evaluating the environmental impact that the process has. High carbon efficiency means that the process is environmental friendly, because its emission of CO₂ into the environment is low.

The design of modern chemical processes embraces the concept that decisions to protect human health and the environment can have the greatest impact and cost

effectiveness when applied early to the design and development phase of a process or product.

By tracking carbon efficiency in the early stages of process design, we will, in fact, be measuring the efficiency of the plant, in terms of its utilization of the raw material and energy and, at the same time, evaluate its likely impact on the environment. This allows for major process drivers influencing carbon efficiency to be identified earlier on and suggest modifications to traditional engineering practices and processes, the development of new catalytic processes and the use of sustainable resources (Keiski, R., 2004).

4.6 RESULTS

We will now examine the effect of the flowsheet configuration as well as the system definition on the carbon efficiency by examining various processes where we change both the configuration and system.

4.6.1 The Once Through Process consisting of reforming and FT synthesis Sections

In the once-through process, at each α value, the various fractions of liquid hydrocarbons and waxes produced were regarded as the desired products and the lighter gases (C_1 - C_4) were regarded as waste. Notice that, in principle, the (C_1 - C_4) products could be burnt to supply energy and the components such as C_2 - C_4 are potentially valuable chemical feedstocks. We did not incorporate this feature at this stage, and hence, the target carbon efficiency we are calculating for the once through process is fairly conservative.

The once through process consists of the reformer (syngas synthesis section) and the FT Synthesis section as shown in Figure 4.3. We first examine the effect of varying

the α value on the carbon efficiency of the overall process. We will also assume that, in this case, the desired product is the C_5^+ hydrocarbon products. We initially assume that the CO conversion in the FT reactor is 100 %; however, at a later stage, we will examine the effect of conversion on the overall carbon efficiency.

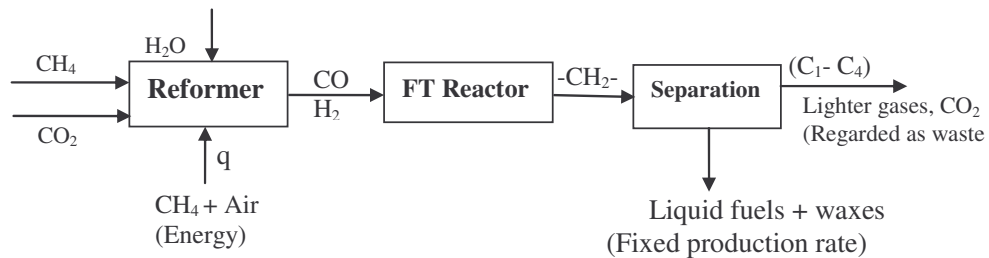


Figure 4.3 Fischer-Tropsch Synthesis (FTS) flowsheet in a once-through process with 100% conversion.

The results in Figure 4.4 show that there is an increase in carbon efficiency with an increase in α . The amount of lighter gases formed decreases with an increase in the α value and, because this is a once-through process operating at 100% CO conversion, the loss in terms of the amount of carbon wasted is therefore less at higher α values. Thus, as can be seen from Figure 4.4, the maximum possible carbon efficiency is 85% and corresponds to a value $\alpha = 1$. The 15% loss in carbon efficiency is due to the methane that is used to supply heat to the reformers only, and, under these conditions, there is no loss of carbon due to flaring of the C_1 - C_4 products.

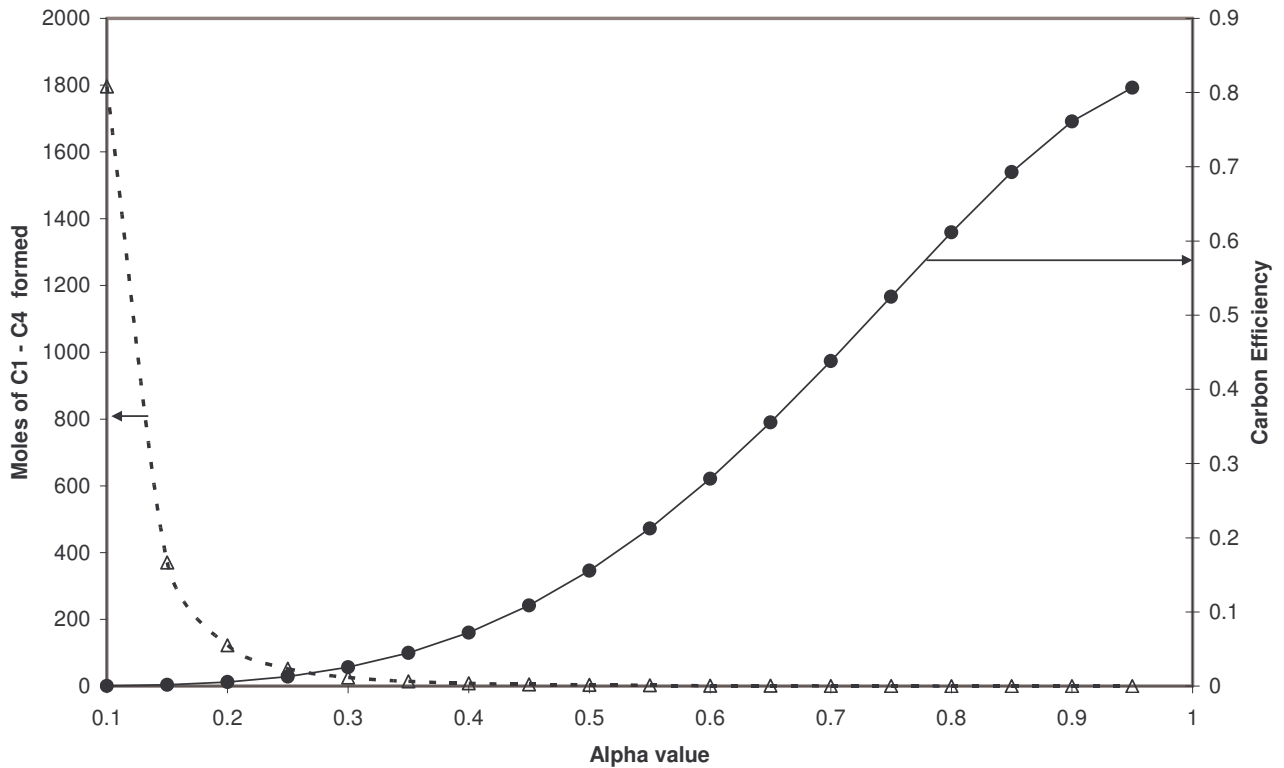


Figure 4.4 Carbon Efficiency and moles of lighter gases formed as a function of alpha for the once through process, 100 % overall carbon efficiency.

4.6.2 The Recycle Process

Standard FT plants operate with recycle streams; this is normally done to increase the overall syngas conversion, because the plants operate at low per-pass conversions. For the purpose of this study, it is assumed that the recycle stream will be composed of the lighter gases (C₁-C₄) and unconverted syngas (Figure 4.5). In principle, the recycled gases can be sent to a second reformer; however, in this study only one reformer has been used, since methane is being used as the primary feed stock.

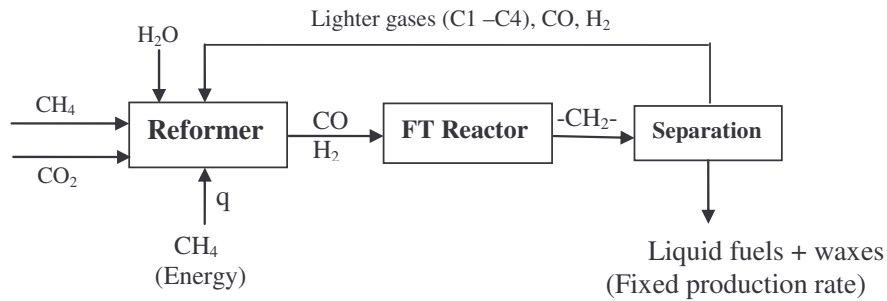


Figure 4.5 FTS flowsheet with a lighter gas recycle stream.

The results in Figure 4.6 show that, at intermediate α values, there is a big advantage in operating a process with a recycle stream as the recycled and reformed gases improve overall carbon efficiency through the utilization of the lighter gases, which are flared in the once-through process.

These results also show that the maximum carbon efficiency for both processes is the same at 85%, because at the highest alpha value of 1, there are no lighter gases produced. It is thus possible to achieve the same carbon efficiency by using either of the two processes; however, carbon efficiency values achieved in the process with a recycle stream at lower α values will only be achievable at higher α values in a once-through process. At $\alpha = 0.35 - 0.85$, there is a big difference in the value of carbon efficiency obtained in the two processes at the same α values. However, at $\alpha = 0.95 - 1$, it is apparent that it does not matter what process configuration is used to achieve this value of alpha because very similar carbon efficiencies can be achieved either way.

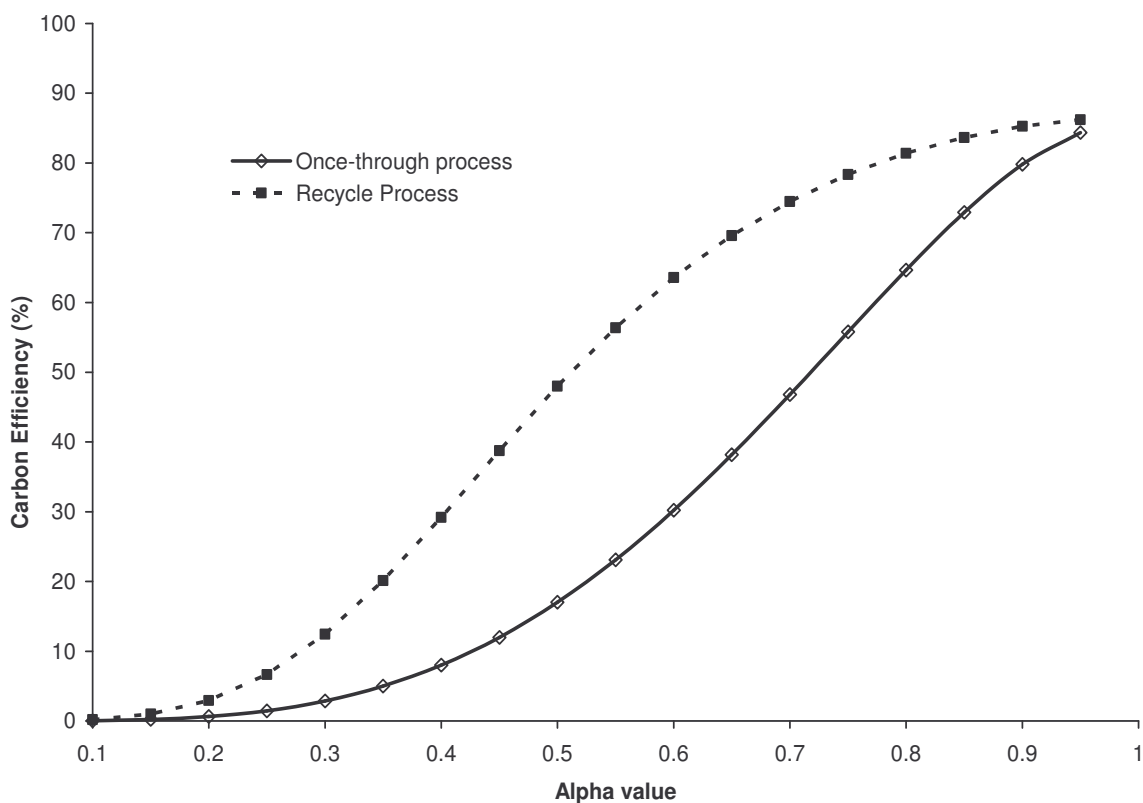


Figure 4.6 Comparison of carbon efficiencies at different α values in once-through and recycle processes at 100% conversion.

Any decrease in the rate of CO conversion affects the carbon efficiency of the once through process negatively. Since this analysis is based on production of a fixed amount of hydrocarbons, in a once-through process, any amount of carbon (moles) lost through unconverted syngas that was produced at great material and energy costs has to be compensated for by an increase in the feed materials required to maintain the production rate. In a recycled process, the unreacted syngas in the recycle loop that joins the feed stream improves and, hence, does not affect the overall conversion and carbon efficiency. Although there is an energy cost to recycling and reforming, this is smaller, compared to the cost of material lost in the once-through process.

We note that if we regard all C_5^+ products equally valuable, we would like to run both the once through and the recycle process at the highest possible α value. In this mode, the processes would be producing primarily waxes. We might now ask the question: if our desired product was diesel and gasoline, how would this change our answer? We would need to upgrade the products from the FT section by cracking them and we would need to look at the effect of this on the overall carbon efficiency of the process.

We will briefly look at the hydrocracking and a simple model that would incorporate the carbon efficiency.

4.7 WAX HYDROCRACKING

To increase the amount of diesel to be obtained from an FT synthesis process, the waxes (C_{19+}) must be hydrocracked into the diesel fraction at high temperatures and hydrogen pressure. This process has now been well established (SASOL as well as Shell, apply this hydrocracking technology in their processes to obtain diesel from coal and or natural gas). In the 1970s, SASOL investigated the selective hydrocracking of FT wax. The wax was cracked to extinction under mild conditions and recycling of the products heavier than diesel. The product distribution achieved was ~80% diesel, ~15% naphtha and ~5% C_1 - C_2 gas. Shell implemented the hydrocracking of FT wax to kerosene and diesel fuel at their plant in Malaysia in the 1990s, whereas EXXON also has now a process for hydrocracking/hydroisomerizing FT wax to liquid oils (Dry, M. E., 2001).

It has been observed from the results obtained so far that high carbon efficiencies are attained at high α values. At high α values, product selectivity favors the production of waxes and other heavier hydrocarbons. In this portion of the study, a simple model has been used to compute the cost of hydrocracking waxes into diesel.

Hydrocracking is a catalytic process that utilizes hydrogen at high pressure and temperature. The hydrogen reacts with the cracked products, thereby suppressing the formation of heavier compounds and increasing the diesel yield. In practice, since the conversion of syngas is not 100%, H₂ can be obtained from the unreacted syngas. However, in this study, hydrogen for hydrocracking was obtained externally using reaction 3.4 and then compressed from atmospheric pressure to 100 bars. Since every α value has its own inherent product distribution, this means that the quantities of wax obtained at different α will vary. These amounts of wax obtained are then cracked to diesel.



The energy for reaction 4.4 is supplied by the combustion of methane as described by eq 4.2. The compression work (W_s) was calculated by assuming that the compressor worked adiabatically (eq 4.5) and the energy for this compression work was obtained from combustion of methane (reaction 4.2). Equation 4.6 shows how the quantity of methane needed to provide this energy for compression work was calculated.

$$W_s = \left(\frac{\gamma}{\gamma - 1} \right) MRT_1 \left[\left(\frac{P_2}{P_1} \right)^{\frac{\gamma - 1}{\gamma}} - 1 \right] \quad (4.5)$$

where W_s is the adiabatic work (kW), T_1 is the compressor feed temperature (K), P_1 is the feed pressure to compressor, P_2 is the exit pressure from compressor, M is the molar flow rate of the gas to the compressor (kmol/s), $\gamma = C_p / C_v = 1.4$ (where C_p is heat capacity at constant pressure and C_v is heat capacity at constant volume).

The amount of methane needed for compression (cost of compression) is calculated in eq 4.6, which takes into consideration the maximum possible efficiency that can be

achieved when thermal energy is converted into mechanical energy ($\eta = ((T_H - T_C)/T_H)$). Thus, for a steam cycle, $T_H = 573$ K and $T_C = 298$ K, $\eta = 0.48$.

$$N_{CH_4}(Comp) = \frac{|W_s|}{\eta \Delta H_{combustion}}, \eta = 0.48 \quad (4.6)$$

where, N_{CH_4} is the number of moles of methane required for compression, W_s is the work of compression calculated in eq 4.5, η is the compression efficiency ($\eta = 0.48$) and $\Delta H_{combustion}$ is the enthalpy of methane combustion in reaction 4.2.

The average carbon number of the waxes used for calculations was 40; this number was determined from the assumption that the hydrocarbons to be formed will be up to C_{60} . It was assumed that these hydrocarbons were paraffins and that they will all be cracked to C_{10} s; therefore, the correct amount of H_2 required for this process was calculated based on the quantity of the C_{40} formed at that particular α value. This assumption will give us the lower bound on carbon efficiency in an FT synthesis process that incorporates hydrocracking because, in practice, during hydrocracking, some gases are formed. For this simple model, reaction 4.7 shows the hydrocracking reaction used in this study:



4.7.1 Carbon efficiency of the once trough and recycle FT processes with Hydrocracking of heavier products to diesel.

To try and answer the question of what the penalty on process carbon efficiency for hydrocracking waxes to diesel will be, a simple process model is shown in Figure 4.7,

which incorporates product work-up, and hydrocracking of the waxes (C_{19+}) has been presented.

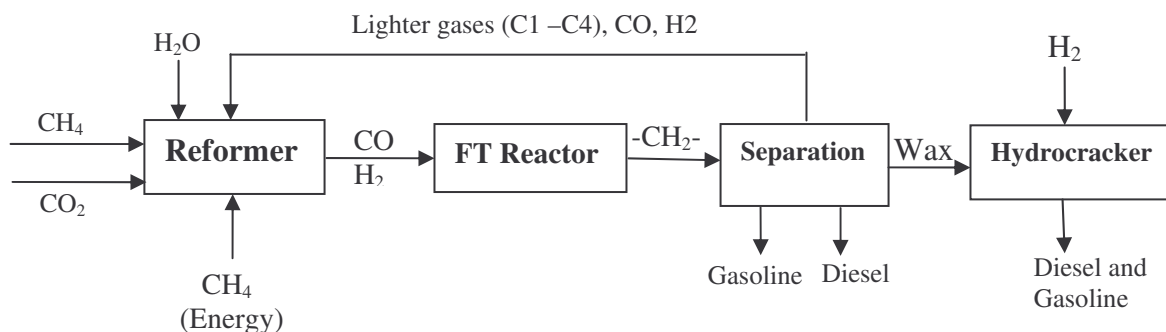


Figure 4.7 FTS flowsheet with a lighter gas recycle stream and wax (C_{19+}) hydrocracking.

The flowsheet for the once-through process will appear similar to Figure 4.7, except that the lighter gases (C_1-C_4) and unconverted syngas will be flared (regarded as waste, see Figure 4.3).

The effect of the α value of the FT process on the carbon efficiency of both the recycle and once through process is shown in Figure 4.8. In the once-through process, hydrocracking of waxes into diesel decreases the maximum carbon efficiency to 60%, and this correspond to an optimal value of $\alpha = 0.82$. In the recycle process the maximum carbon efficiency decreases to 75%, which occurs at an optimal value of $\alpha \approx 0.75$. This loss in carbon efficiency is purely due the increased requirement of methane for H_2 production and compression to process the heavier hydrocarbons to liquid fuels. The more waxes are formed, the more H_2 is needed to hydrocrack them. Because H_2 is produced from CH_4 , there will be an increase in C feedstock to the reactor for H_2 production.

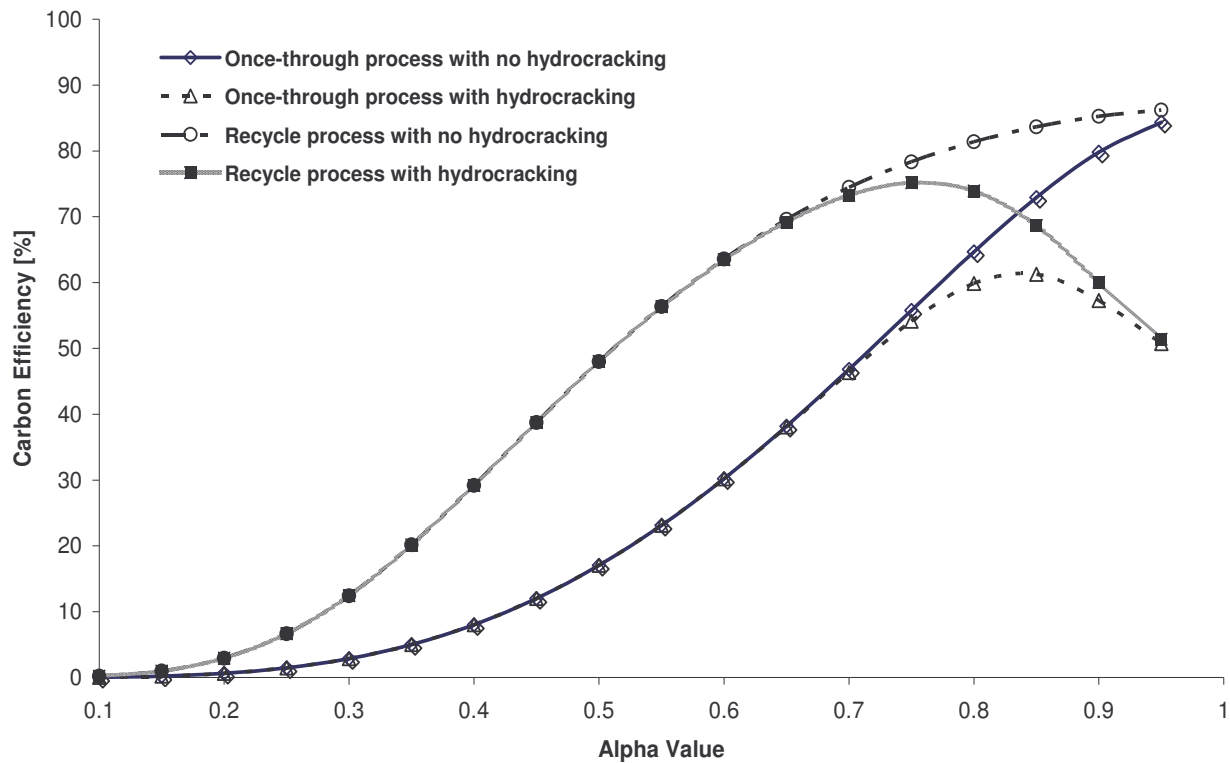


Figure 4.8 Carbon efficiency as a function of α in a once-through and recycle process.

The recycle process has 15 % higher maximum carbon efficiency than that of the once through process. The recycle process also achieves higher carbon efficiencies than the once-through process at the same α values. For example, at $\alpha = 0.7$, the carbon efficiency for the recycle process with hydrocracking is ~73% compared to ~46% obtained in the once-through process with hydrocracking.

The analysis of the two process configurations in this study has shown that the recycle process is more efficient at all α values. For as long as the CO conversion is the same for both process configurations, the amount of waxes produced in both the

once-through and recycle processes are the same at similar α values and, therefore, the energy and material requirements for both hydrocracking and H₂ production are the same. However, the difference in their carbon efficiencies arises mainly because of the fact that the carbon moles lost in the lighter gases flared in the once-through process are recovered in the recycle process and reformed to syngas. This syngas is fed to the FTS reactor and therefore improving on material utilization of the process

4.8 CONCLUSION

From the results in this study and what is already known about Fischer-Tropsch Synthesis (FTS) product distribution, we can conclude the following:

Using the process synthesis approach, a method of comparing two probable process configurations for FTS has been developed without any experimental data or any detailed and complicated modelling. Using the probability of chain growth (α) as a variable and the resultant carbon efficiency, we have established a basis for comparing the two operations.

This type of analysis has enabled us to examine with the issue of designing an environmentally friendly process that is, at the same time economically feasible, at least, from the material and energy utilization point of view, at an early stage of process design.

Designing an FTS process with recycling and reforming of the lighter gases, is very beneficial, especially if the reaction products are described by low to middle α values, because higher values of carbon efficiency (η) values are obtained and the amount of overall CO conversion is enhanced.

In both the once-through process and the recycle process, the trend should be to reduce the formation of lighter gases by increasing the α value because η increases as α increases.

Because CO conversion is a measure of catalyst activity, which is also closely linked to reaction residence time, experiments using different catalysts at various space velocities and other process conditions should be performed until the targeted CO conversion and higher α values are achieved. Laboratory experiments should be performed to obtain process operating conditions that will yield high α values at high conversion. The activity of the catalyst under different operating conditions and the effect of by-products such as water on product selectivity should be investigated.

However, if the aim is to maximize diesel production by hydrocracking the waxes, then an optimal alpha value should be sought, to reduce the cost of hydrocracking very heavy waxes. Compared with the processes without hydrocracking, the incorporation of wax hydrocracking in the two processes decreases the carbon efficiency η for $\alpha > 0.7$, thereby making it uneconomical to produce very long chain hydrocarbons.

The design and operating conditions for the two processes will be different. From the temperature point of view, the once-through process will be better-off as a low temperature FT process, whereas the recycle process will be a high temperature FT process. This is because the mean chain length, and, therefore, the hydrocarbon distribution of FT synthesis changes with temperature. At higher temperatures, the mean chain length is smaller, more methane and lighter hydrocarbons and less diesel and waxes are formed. A Cobalt-based catalyst that is used as a low temperature FT catalyst will be suited for the once-through process to maximize wax production, whereas the iron catalyst will be ideal for the high temperature process with a recycle stream.

This study has shown that it is possible to evaluate a process and its efficiency with a relatively small amount of information. From the calculations that are performed, it is possible to decide what the key drivers for the processes are and choose among various alternatives. Even though many simplifying assumptions are made, the results bear sufficient resemblance to the real situation to make valid comparisons between the different situations. In particular, as the same assumptions are made for the different alternatives, the accuracy of the assumptions is not particularly important.

4.9 REFERENCES

Dry, M. E. (1982), Catalytic aspects of industrial Fischer-Tropsch Synthesis, *Journal of Molecular Catalysis*, 17, 133-144.

Dry, M. E. (2001), High quality diesel via the Fischer-Tropsch process – a review, *Journal of Chemical Technology and Biotechnology*, 77, 43 – 50.

Dry, M. E. (2004), Present and future applications of the Fischer-Tropsch process, *Applied Catalysis A: General* 276, 1-3.

Eilers, J., Posthuma, S. A. and Sie, S.T. (1990), The Shell Middle Distillate Synthesis Process (SMDS), *Catalysis Letters*, 7, 253 -270.

Jess, A., Popp, R. and Hedden, K. (1999), Fischer-Tropsch synthesis with nitrogen-rich syngas: Fundamentals and reactor design aspects, *Applied Catalysis A: General* 186, 321-342.

Keiski, R. (2004), *Green Engineering Chemistry/Chemical Engineering for Sustainability*, University of Oulu, GSCE Course, Finland.

Lampert, A., Ericjson, J., Smiley, B and Vaughan, C. (1983), Fischer-Tropsch Synthesis of Hydrocarbon Report, MIT School of Chemical Engineering Practice, USA, September 1983.

Mills, G. A. (1988), Catalysts for Fuel from syngas, New Directions for Research, IEACR/09, IEA Coal Research, London.

Mukoma, P., Hildebrandt, D., Glasser, D and Coville, N. (2006), Fischer-Tropsch Results and their analysis for Process Synthesis, (Accepted for publication in Industrial & Engineering Chemistry Reserach).

Ngwenya, T., Glasser, D., Hildebrandt, D., Coville, N and Mukoma, P. (2005), Fischer-Tropsch results and their Analysis for reactor synthesis, Industrial & Engineering Chemistry Research, 44, 5989 – 5994

Raje, A., Inga, J, R. and Davies B. H. (1997), Fischer-Tropsch synthesis: process considerations based on performance of iron-based catalysts, Fuel, 76 (3), 273-280.

**A COMPARISON OF COAL AND NATURAL GAS FEED
MATERIAL FOR FISCHER-TROSCH SYNTHESIS**

This paper has been submitted for publication to the *Industrial & Engineering Chemistry Research*.

A comparison of coal and natural gas as feed material for Fischer-Tropsch Synthesis

Peter Mukoma, Diane Hildebrandt and David Glasser

COMPS, School of Chemical and Metallurgical Engineering,
University of the Witwatersrand, P/Bag 3, WITS 2050.

Abstract

A method of analyzing a process at a conceptual stage using simple models has been developed using minimal information. . This procedure allows one to investigate the impact of design drivers at the early stage of process development. Fischer-Tropsch Synthesis processes based on two different feed stocks (coal and natural gas) have been studied. Carbon efficiency at various values of the probability of chain growth has been used to compare the two processes. Simple process flow sheet models were synthesized and analyzed.

The recycle of lighter hydrocarbons and wax hydrocracking was used to increase diesel yields and maximize the usage of the feed synthesis gas. Generally speaking, processes based on natural gas were found to be more carbon efficient than the coal-based ones.

5.1 INTRODUCTION

The conversion of synthesis gas (syngas) via Fischer-Tropsch (FT) synthesis to liquid fuels and chemicals is attracting a lot of interests mainly because of unstable prices of crude oil and environmental concerns with regard to the use of fuels obtained from crude oil. Stringent environmental regulations is pushing conventional refineries to use more costly deep hydrogenation technologies to remove impurities that cause environmental pollution from the feed (crude oil) in order to improve fuel quality. This is more so for diesel fuels, which has successfully been combined with modern diesel engine technology, gaining benefits from both high energy efficiency and improved environmental effects.

Syngas can be produced from a variety of carbon-bearing feedstocks such as coal, natural gas and biomass and the resulting high-quality crude oil can be further processed to specific boiling-point fractions. In an FT production complex the production of purified syngas normally accounts for 60-70% of the capital and running costs of the entire plant. The selection of the right syngas production process is based on the available raw material and the desire to ensure the correct CO: H₂ ratio while simultaneously minimizing certain inherent inefficiencies of the selected technology. Natural gas is preferred to coal for syngas production because the capital cost is normally about 30% lower and the process is more efficient. In natural gas reforming, about 20% of the carbon is converted to CO₂ compared to coal gasification where it is about 50% due to coal's much lower hydrogen content (Higman, C., 1990).

Since the cost of syngas is high, it is important that its downstream conversion to liquid fuels and chemicals is as efficient as possible. It goes without saying, therefore, that, depending on the source of syngas, the efficiencies of the FT processes are likely to be different. It is important for process developers to be able to assess the efficiencies of these processes earlier on using very little information available to

them without doing very detailed, time, and money consuming studies. The aim of such an assessment is not to find the best option but to eliminate bad alternatives. By so doing, key process drivers will be identified and then a more detailed analysis can be done. To allow for a comparison of these processes, it is very important that this comparison is done on the same basis.

In this study, a comparison has been made between two FT Synthesis processes, one based on the coal feed and the one based on natural gas feed. The products made by the FT reaction are hydrocarbons of different chain length. The FT reaction follows a chain-growth mechanism in which the product spectrum adheres to an Anderson-Schulz-Flory (ASF) distribution characterized by the probability of chain growth (α). The ASF distribution describes the molar yield in carbon number as:

$$C_n = \alpha^{n-1}(1-\alpha) \quad (5.1)$$

where α is the chain growth probability and n the length of the hydrocarbon, making $1-\alpha$ the chance that the chain growth will terminate.

The Carbon Efficiency (CE) of the processes has been compared at the same values of chain growth probability (α). It has been assumed that the entire range of α values can be achieved. No particular catalyst was chosen for this study. Some researchers have recommend the use of iron-based catalysts for both natural gas and coal feed stocks while cobalt-based catalysts are recommended for natural gas feed (Tijm, P. J. A., 2001).

The issue at hand is to develop a method of screening α values in FT synthesis processes based on two different feed stocks. The study will examine how the two processes compare if production of a fixed amount of hydrocarbons with a certain α value is targeted and whether it matters if the process is coal or natural gas based.

From an FT synthesis point of view, it doesn't really matter the source of syngas as long as the syngas coming to the FT reactor is clean and in the right CO: H₂ proportion, the end products will depend on the catalyst used, type of reactor and operating conditions. This method will also enable us to determine possible regions of optimal energy efficiencies where the plant should operate.

The two processes will be compared on the basis of their carbon conversion efficiency (η) which is defined as:

$$\text{Carbon Conversion Efficiency} = \frac{\text{Carbon (moles) in product produced}}{\text{Carbon (moles) fed to process} + \text{carbon (moles) used for equivalent energy}}$$

The carbon efficiency takes the chemical feedstocks and energy streams into account. Thus, it is a good measure of plant operating economics because the higher the carbon efficiency the higher the usage of feed material and energy for the production of the desired product. It is also related to the capital costs, as the lower the carbon efficiency the more material needs to be processed in order to produce the same quantity of products. Thus, the process equipment will be larger with correspondingly higher capital costs. It is also a good tool for evaluating environmental impact that the process has. High carbon efficiency means that the process is environmental friendly as its emission of CO₂ into the environment is low.

The design of modern chemical processes embraces the concept that decisions to protect human health and the environment can have the greatest impact and cost effectiveness when applied early to the design and development phase of a process or product.

By tracking carbon efficiency in the early stages of process design, we will, in fact, be measuring the efficiency of the plant in terms of its utilization of the raw material and energy and at the same time evaluate its likely impact on the environment. This allows for major process drivers influencing carbon efficiency to be identified earlier on and suggest modifications to traditional engineering practices and processes, the development of new catalytic processes and the use of sustainable resources (Keiski, R., 2004).

This kind of an analysis is particularly necessary in the early stages of plant design and can be very beneficial in the choice of technology. Some people may not agree that an analysis of the plant based on its carbon conversion efficiency is a good measure of plant economics, more emphasis is put on the Capital/Project costs, however, from a process design point of view, especially in the early stages, Capital/Project cost may not be the most economic sensitive parameter over the life of a project. However, the Capital and Operating costs can always be included as the design develops. Issues of accessibility to raw materials (most of the natural gas is stranded in remote areas) and proximity to the market for the targeted product will have to be considered once the decision on what process to go with has been made.

5.2 PROCESS FLOWSHEET DESCRIPTION

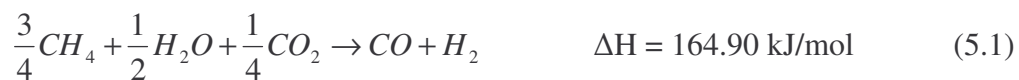
The two design options described in the preceding sections are based on simplified generic models. No specific choice of technology is made, apart from what is generally known about the Fischer-Tropsch Synthesis. The material balance data based on the production of a fixed amount of hydrocarbons and maximizing diesel production has been used to generate the resource consumption and yield data presented here. The basis for these calculations is the feedstock and energy to be consumed for the production of 1 ton per day of liquid fuels (gasoline and diesel) and hydrocracking of all the waxes to maximize diesel production. While the design for the two options may differ slightly in detail, they can all be broken down into three

main process sections, namely; the Syngas Generation section, which depends on the nature of the feedstock, the FT Conversion (in practice, this may vary depending on the nature of the catalyst and operating conditions) and the FT Product Upgrading area targeting a fixed amount of liquid hydrocarbons and wax hydrocracking to maximize diesel production (this in practice may depend on the nature of the final products desired).

In this study, the design options will be based on the generation of syngas from coal and natural gas. Comparisons will be made between running a once-through process and a recycle process. The FT Conversion area will have the same details in both cases. The desired final products will be diesel and so the Product Upgrade area will constitute of the wax hydrocracking unit with a hydrogen feed from outside. In the designs without recycle (once-through), the lighter gases produced will be flared and considered as a waste (in practice, this may be used to meet the energy needs of the plant by generating power).

5.2.1 Natural gas based Design

Synthesis gas derived from natural gas typically has a much higher H₂: CO ratio than that produced from coal and biomass; this is because of the higher hydrogen content of methane (CH₄), the primary component of natural gas. Natural gas is converted to syngas either by partial oxidation, steam reforming, or a combination of both called autothermal reforming. In this study, the process with a natural gas feed has been studied using two syngas production processes. The first one is a steam reforming process with an addition of CO₂ to the feed (equation 4.1). This process is particularly important if a source of CO₂ is available (or for a CO₂ rich natural gas).



The reaction shown in eq 5.1 is endothermic and the energy for syngas production will be derived from methane combustion. All the energy and work requirements for recycling and reforming of the lighter gases in the recycle process will also be obtained from the combustion of methane shown in equation 5.2:



The second syngas production process is the partial oxidation of methane (equation 5.3). This is non-catalytic exothermic reaction with the desirable composition of the syngas from a mass balance point of view, corresponding to a ratio H₂: CO of ~ 2.



We know that CO₂ is produced in this technology, but we are separating the energy production step from the syngas production step, however, this will be included in the energy balance. The reaction in eq 5.2 takes place either with enriched air or pure oxygen supplied from an air separation unit (ASU). The two options have been studied and compared. The effect of air separation and compression of air on the carbon efficiency of the whole process based on eq 5.3 has also been studied.

The syngas production process with air has been studied as a once-through process to avoid the accumulation of nitrogen in the loop and reduce compression costs of the large recycles whilst the processes in eqs 5.1 and 5.3 have been studied in both the once-through and recycle processes. Figure 5.1 is a simple process flowsheet with syngas obtained from the process represented by eq 5.1. Natural gas (CH₄) is feed to the reactor together with CO₂ and steam. Since the reaction is not spontaneous, energy to drive the reaction is provided for by methane combustion.

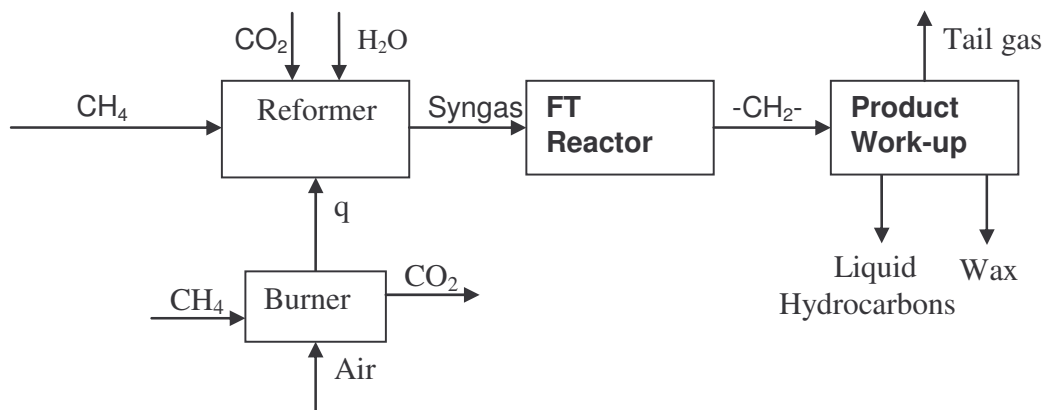


Figure 5.1 A once-through FT Process flowsheet utilizing syngas from steam reforming of natural gas with a CO_2 feed without wax hydrocracking.

The process in Figure 5.1 focuses on the recovery of liquid hydrocarbons, flaring of all gaseous product including unreacted CO and H_2 .

The process in Figure 5.2 is based on the syngas obtained by the partial oxidation of the natural gas using compressed air. Both syngas production processes (eqs 5.1 and 5.3) give the H_2/CO ratio of 2.

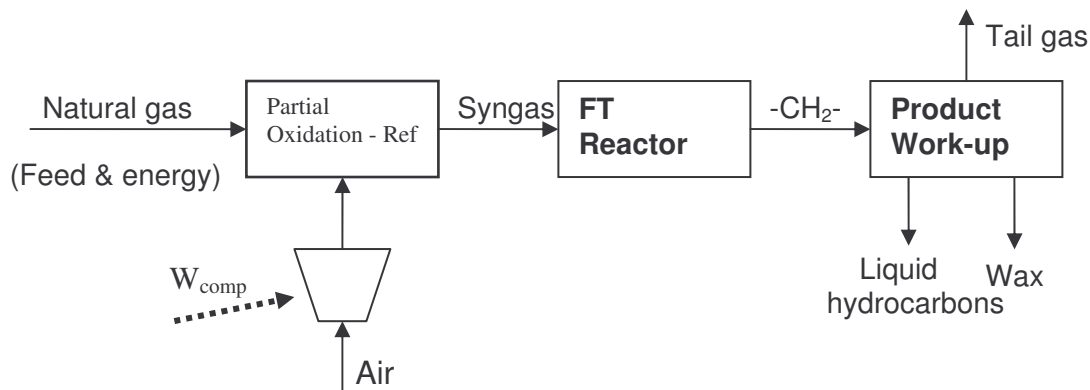


Figure 5.2 A once-through FT process model based on syngas obtained from the partial oxidation (POX) of natural gas using compressed air with out wax hydrocracking.

Just like in chapters 3 & 4, the work of air compression (W_{comp}) has been calculated using equation 5.4 by assuming that the compressor worked adiabatically and the energy to provide this work was obtained from natural gas combustion:

$$W_{comp} = \left(\frac{\gamma}{\gamma-1} \right) MRT_1 \left[\left(\frac{P_2}{P_1} \right)^{\frac{\gamma-1}{\gamma}} - 1 \right] \quad (5.4)$$

where W_{comp} is the adiabatic work of compression (kW), T_1 is the compressor feed temperature (K), P_1 is the feed pressure to compressor, P_2 is the exit pressure from compressor, M is the molar flow rate of the gas to the compressor (kmol/s), $\gamma = C_p / C_v = 1.4$ (where C_p is heat capacity at constant pressure and C_v is heat capacity at constant volume). The exit pressure from the compressor (P_2) depends, among other things, on the operating pressure of the reformer, which in this case was taken to be 25 bar.

The amount of methane needed for compression (cost of compression) is calculated in eq 5.5, which takes into consideration the maximum possible efficiency that can be achieved when thermal energy is converted into mechanical energy ($\eta = (T_H - T_C) / T_H$). Thus, for a steam cycle, $T_H = 573$ K and $T_C = 298$ K, $\eta = 0.48$.

$$N_{CH_4} (Comp) = \frac{|W_s|}{\eta \Delta H_{combustion}}, \eta = 0.48 \quad (5.5)$$

where, N_{CH_4} is the number of moles of methane required for compression, W_s is the work of compression calculated in eq 4.4, η is the compression efficiency ($\eta = 0.48$) and $\Delta H_{combustion}$ is the enthalpy of methane combustion in reaction 5.2.

The carbon efficiencies for the two processes (Figures 5.1 and 5.2) at various α values were calculated by taking into account all the carbon that has gone into the process against the liquid hydrocarbon products and waxes.

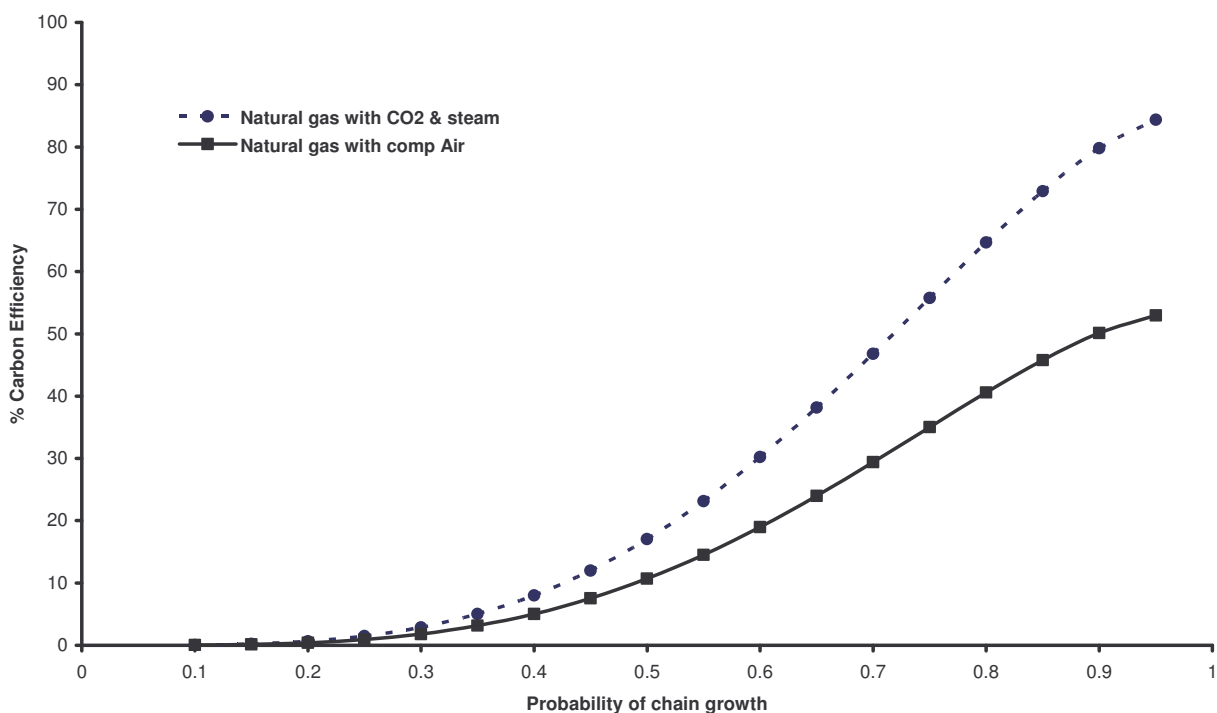


Figure 5.3 Carbon efficiencies at various α values in a once-through FT process based on syngas production from natural gas using two different processes at 100% CO conversion.

The results in Figure 5.3 clearly favor the production of syngas using steam reforming with the addition of CO₂ to the reformer. At all the α values where the amount of liquid hydrocarbons and waxes are more than the lighter gases (C₁-C₄), carbon efficiency for the process utilizing CO₂ and steam is higher than the process utilizing compressed air for syngas production.

If the main objective for the above described processes was to maximize diesel production by product upgrading (wax hydrocracking), the process models (flowsheets) will look very similar to Figures 5.1 and 5.2 except that there will be an addition of the wax hydrocracker and a source of compressed hydrogen. Product upgrading has been simplified to wax hydrocracking only. No other refining process is used to upgrade the products. This design is indicative of a situation that might arise where the size of the plant and the economy of the country where the plant is located do not warrant the addition of capital intensive refinery processing. In this section, the FT wax stream from the recovery plant will be cracked at high pressure and temperature in the presence of hydrogen. In practice, catalytic hydrocracking is used in the petroleum refinery industry to produce a wide variety of products that includes light hydrocarbon gases, naphtha, distillates and lubricating oils. This process converts the high molecular weight components in heavy petroleum distillates by a complicated sequence of reactions involving hydrogenation and carbon-carbon bond cleavage. Sulphur, nitrogen and oxygen compounds are removed at the same time, and olefins are saturated. Parameters of a hydrocracking process can be optimized to give a 100% conversion of the feedstock to a certain product, for example, diesel fuel. In this study, an assumption has been taken that the average chain length of the wax feedstock to the hydrocracker is 40 and this is hydrocracked to C_{10} in a 'once through' hydrocracking unit using an external hydrogen source.

Figure 5.4 shows a simplified once-through FT process flowsheet with hydrocracking based on steam reforming of natural gas with CO_2 as a source of syngas. The results shown in Figure 5.5 show a substantial decrease in the carbon efficiencies of both processes resulting from the addition of hydrocracking units, this is even more pronounced in the process utilizing CO_2 and steam for syngas synthesis whose carbon efficiency decreased from ~ 84% to 61% at $\alpha = 0.95$. It is interesting to note that both cases have maximum α values beyond which the processes start to become less efficient. Carbon efficiency for the process utilizing steam and CO_2 for syngas

production reaches its maximum at $\alpha = 0.85$ ($\eta = 61$) and then drops to $\sim 51\%$ at $\alpha = 0.95$.

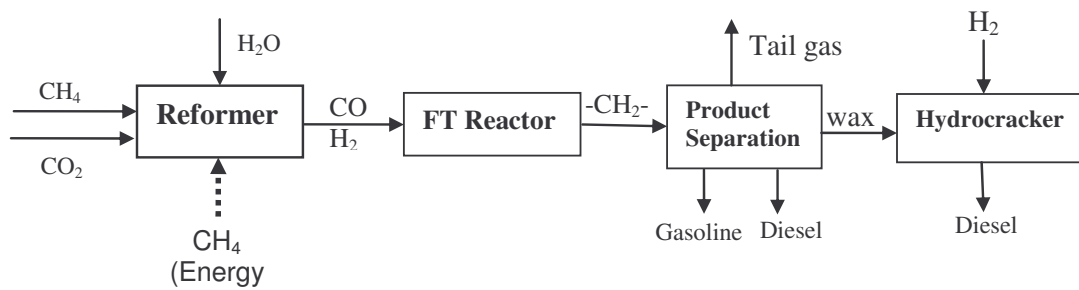


Figure 5.4 A once – through FT Synthesis process flowsheet with wax (C₁₉₊) hydrocracking.

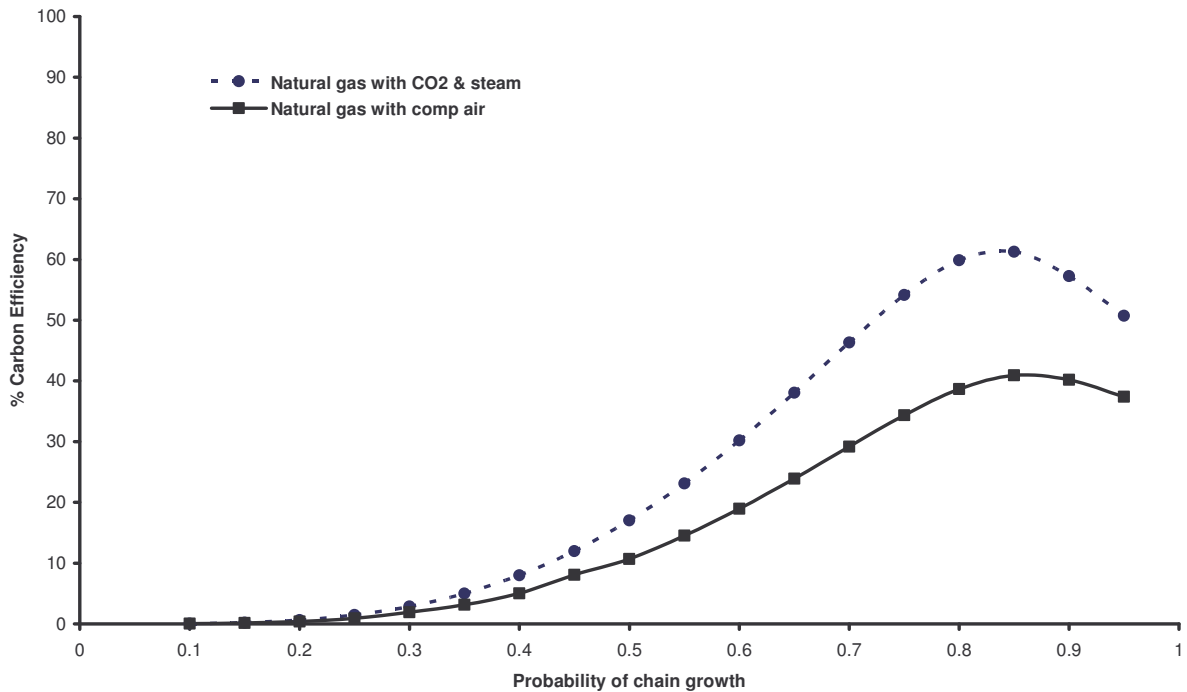


Figure 5.5 Carbon efficiencies at various α values in a once-through FT process based on the two syngas production processes at 100% CO conversion.

Up to 40% of the main costs of a syngas plant based on partial oxidation (POX) and autothermal (ATR) are related to the oxygen plant. There have been suggestions of using air directly for syngas generation thereby eliminating the cryogenic air separation plant, however, the use of air in the process stream is only feasible in once-through synthesis schemes in order to avoid the accumulation of nitrogen. The use of air instead of oxygen will result in big reformer volumes and consequently big feed/effluent heat exchangers and compressors. This may also result in big purge gas streams leading to energy and material waste (Jess et al., 1999). Since this study is comparing the efficiencies of two FT process configurations (once-through and

recycle process), the use of an Air separation Unit (ASU) to obtain oxygen for syngas synthesis in the partial oxidation process has to be considered.

In spite of the information on the work of air separation and its efficiency being readily available in public domain, we have decided to apply the thermodynamic principles used in chapter 3, to obtain the minimum work of separation. This minimum work of separation represents a lower bound on the energy that must be consumed by a separation process. This is very important at the early stages of process design because it gives an indication of the relative difficulties of the separation. In some processes the separation must be carried out with energy consumption close to the minimum work of separation in order to be economical.

As in any commercial cryogenic Air Separation Units (ASU), separation of O₂ from N₂ is achieved by distillation because these gases have different boiling points. In this study, we propose to thermodynamically model distillation as a set of heat engines because distillation is a separation process driven by heat input (King, C. J., 1971). Often the energy to drive a separation process is supplied in the form of heat rather than mechanical work.

To illustrate this further, a separation process shown in Figure 4.6 will be discussed as a reversible heat engine driven by heat Q_H entering the system at a temperature T_H . An amount of heat Q_C leaves the system at a temperature T_C . If Q_H was supplied to a reversible heat engine rejecting heat at T_0 , an amount of work equal to $Q_H \frac{T_H - T_0}{T_H}$, could be obtained. Similarly an amount of work equal to

$Q_C \frac{T_C - T_0}{T_C}$, could be obtained from Q_C .

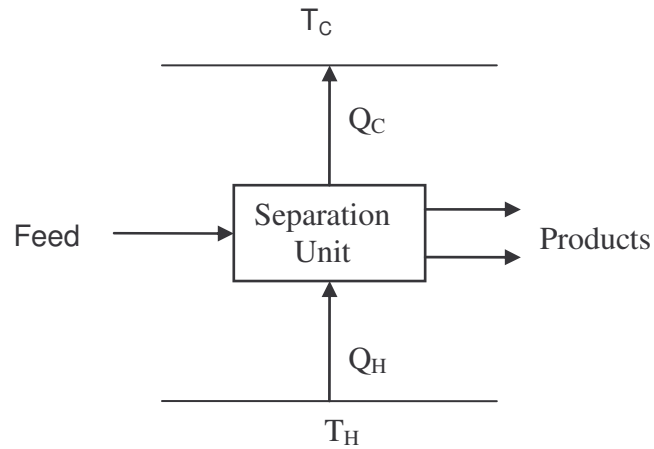


Figure 5.6 A separation process driven by heat input

The net work consumption of the process W_n is: $W_n = Q_H \frac{T_H - T_0}{T_H} - Q_C \frac{T_C - T_0}{T_C}$

In an ordinary distillation process, an amount of heat equal to Q_R enters at the reboiler at temperature T_R and heat Q_C is removed in the condenser at a temperature T_C . If no mechanical work is involved in the separation process and the enthalpy difference between feed and product is negligible compared to the heat input, then $Q_H = Q_C = Q$. For $T_H = T_R$ and $T_L = T_C$, the net work of consumption for the separation process will be:

$$W_n = Q \left[1 - \frac{T_C}{T_R} \right], \text{ for } T_L > T_0 \quad (5.6)$$

In this study, this separation principle has been applied.

The minimum isothermal work of separation is also equal to the increase in Gibbs free energy (G) of the products over the feed. The Gibbs free energy is defined as $G = H - TS$.

Therefore,

$$\Delta G = W_{\min,T} = \Delta H - T\Delta S \quad (5.7)$$

Where T is the absolute temperature, ΔH is the enthalpy of the products less the enthalpy of the feed and ΔS is the entropy of the products less the entropy of the feed. For the isothermal separation of a mixture of ideal gases $\Delta H = 0$ and therefore the minimum work for a reversible separation process separating products at the same temperature and pressure as the feed is:

$$W_{\min,T} = -T\Delta S = -RT \sum_{i=1}^N x_i \ln(x_i) \quad (5.8)$$

Where, $W_{\min,T}$ is the reversible work of separation (kJ/Kmol) at temperature T , R is the gas constant (kJ/Kmol), T is the ambient temperature (K) and x_i is the mol fraction of component i in the mixture (in this case O_2 and N_2 only).

For a fixed production rate of hydrocarbons per day, the daily oxygen requirements will be calculated from the following overall reaction:



The boiling points for oxygen and nitrogen are 90 and 78 K, respectively. Therefore, for the distillation process, heat will be supplied to the reboiler of the column at 90 K and then removed from the condenser at 78 K. The removal of heat from the condenser at 78 K will be done by refrigeration and reject it to the atmosphere at 298 K.

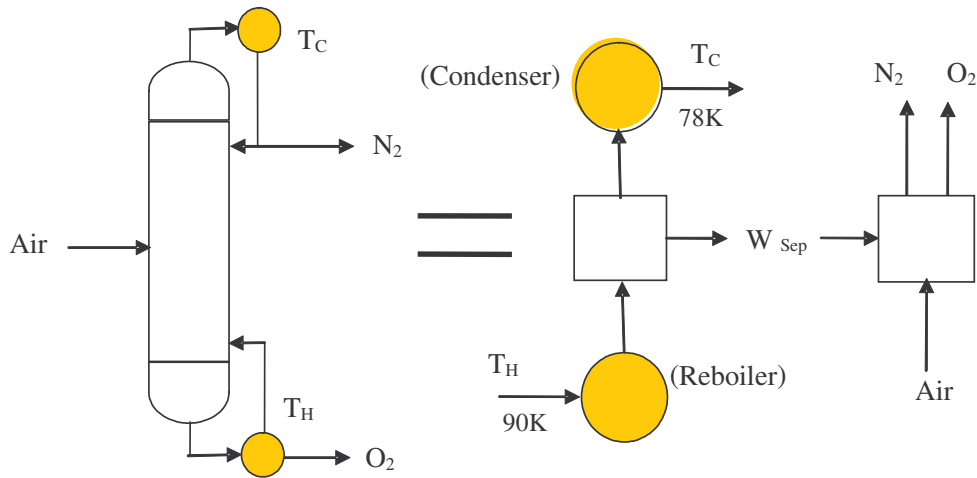


Figure 5.7 A distillation process modelled as a heat engine.

For the refrigeration purposes, work will be supplied by a Carnot engine which burns methane (natural gas) to supply heat and rejects heat to the surroundings (eq 5.2). The heat will be converted to work using a normal steam power cycle.

Steam that will be generated in a turbine at 573 K will generate energy for refrigeration work. This turbine (modelled as a heat engine) will take in heat at 573 K and release it to the atmosphere at 298 K. The three processes (Distillation, Refrigeration and Power generation) needed for air separation have been modelled as thermodynamic engines.

A comparison of the carbon efficiencies obtained in the process using O_2 from an ASU instead of compressed air show that air separation is a cost that affects carbon efficiency of the plant. This is shown in Figure 5.8.

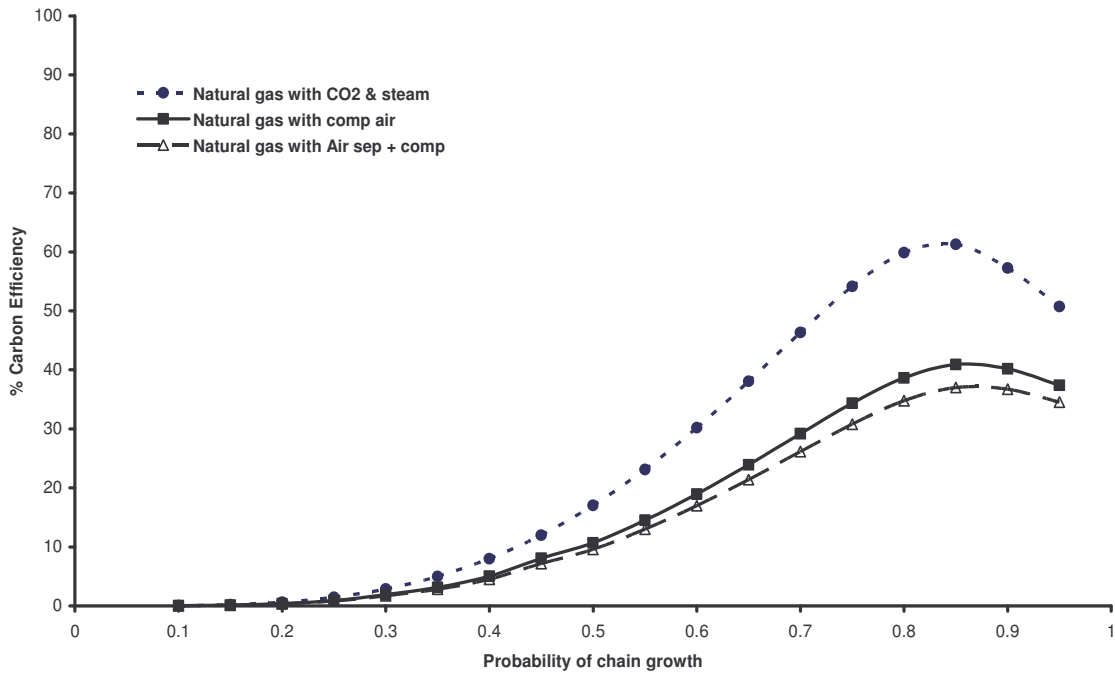


Figure 5.8 Carbon efficiency at various α values for a once-through FT process with wax hydrocracking at 100% CO conversion.

For as long as there is no inert in the feed gas the most sensible thing to do is to recycle the gaseous products and the unconverted syngas. Therefore, the next process to be considered will be a recycle process. The unreacted syngas is recycled to the FT reactor and the tail gas is reformed in reformer 2 to syngas and fed to the FT reactor. Reformer 2 is assumed to be a perfect reformer. This is a steam reformer making use of the water produced during the FT synthesis reactions. Figure 5.9 gives a flowsheet for a recycle process with syngas obtained from steam reforming of natural gas with CO₂ addition.

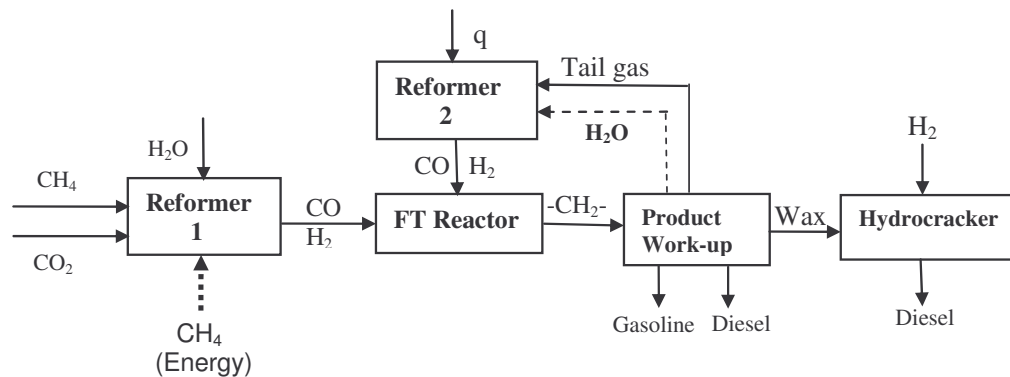


Figure 5.9 An FT synthesis process flowsheet for a recycle process with syngas obtained from steam reforming of natural gas with CO_2 .

Carbon efficiency of the process shown in Figure 5.9 has been compared with the carbon efficiency obtained from a recycle process with syngas obtained via partial oxidation of natural gas using O_2 obtained from an ASU (Figure 5.10) and the results of the recycle process without hydrocracking are shown in Figure 5.11.

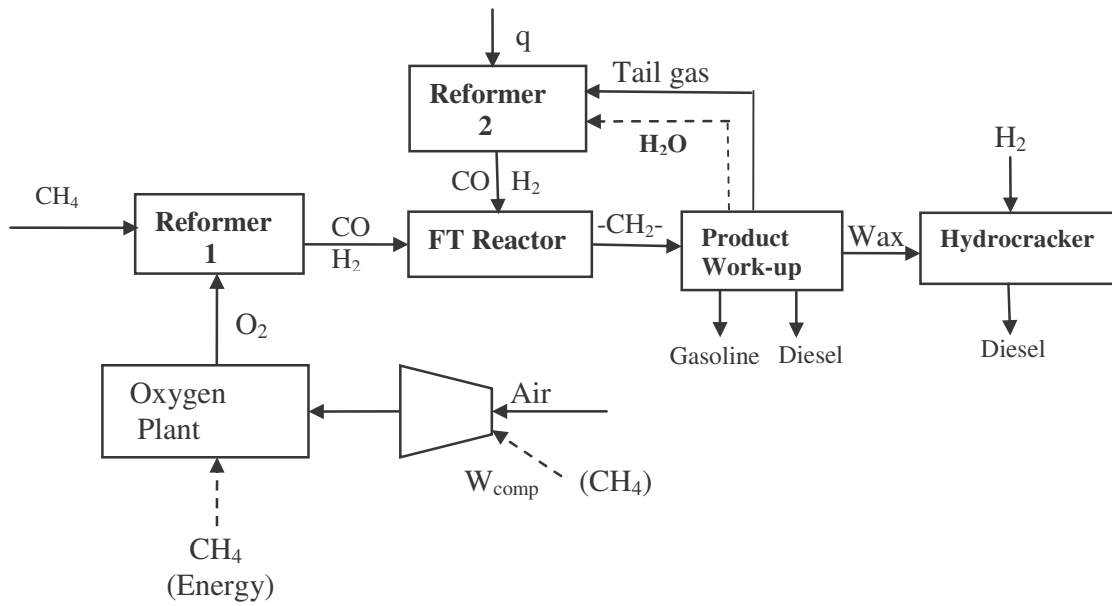


Figure 5.10 FT synthesis process flow model for a recycle process with syngas obtained by partial oxidation of natural gas using oxygen obtained from an oxygen plant.

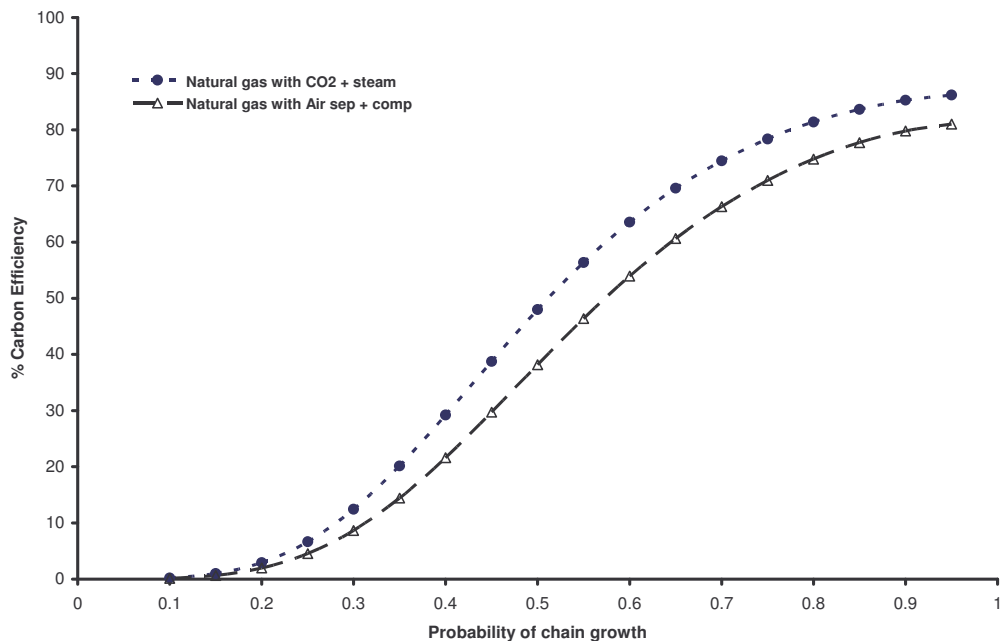


Figure 5.11 Carbon efficiency at various α values for the recycle FT process without hydrocracking.

From Figure 5.11, it can be seen that the carbon efficiency of the recycle FT process based on syngas obtained from steam reforming with an addition of CO_2 increases with α values without wax hydrocracking and this was also observed in the once-through process (Figure 5.3). The major difference is that in the recycle process, the process using syngas obtained by partial oxidation with oxygen obtained from an ASU has a much improved carbon efficiency of $\sim 81\%$ at $\alpha = 0.95$ compared to 53% at the same α value in the once-through process. This shows that there are huge benefits in using a recycle stream. We shall see what effect wax hydrocracking has on the carbon efficiency has on the recycle process (Figure 5.12).

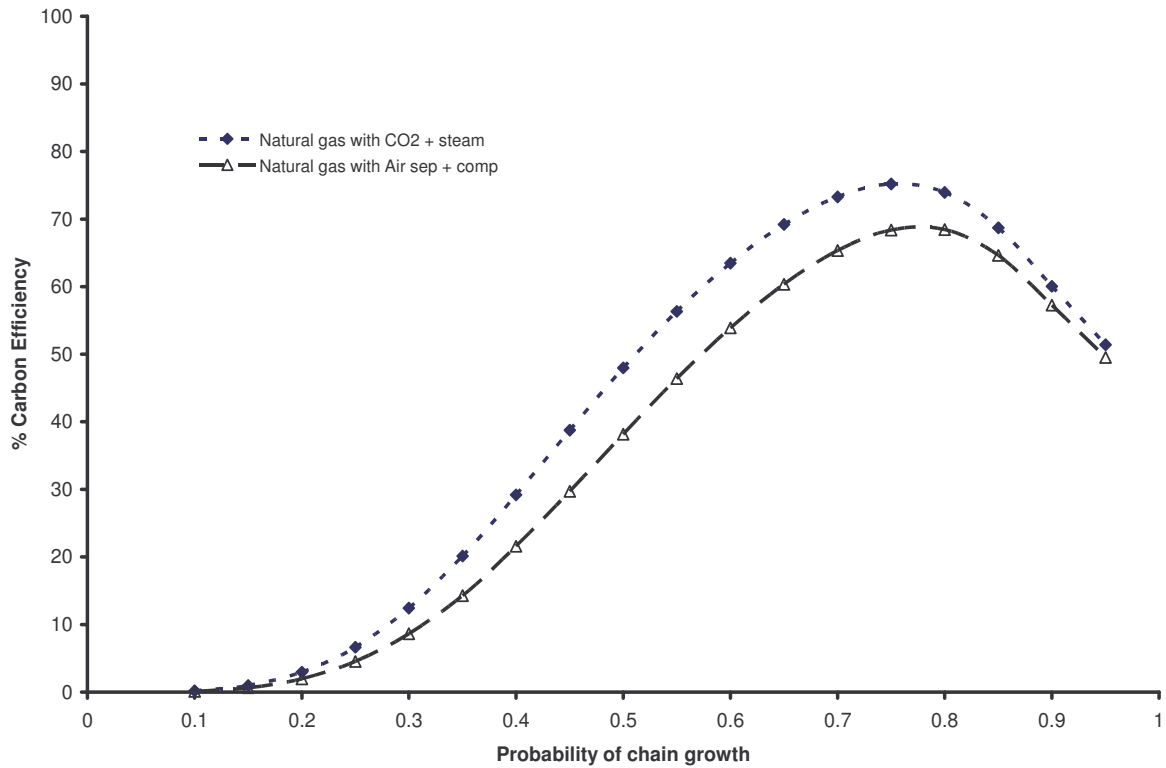


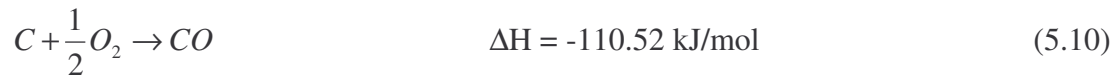
Figure 5.12 Carbon efficiency at various α values in the recycle process with wax hydrocracking at 100% CO conversion.

The recycle process with wax hydrocracking drops carbon efficiency at all alpha values in all the processes under consideration; this is, on account of the energy consumed in the wax hydrocracking process. Carbon efficiency reaches a maximum in both processes at $\alpha = 0.75$ beyond which the energy for hydrocracking the longer chain hydrocarbons start having a major impact on the overall carbon efficiency reducing it by ~30% in both cases at $\alpha = 0.95$.

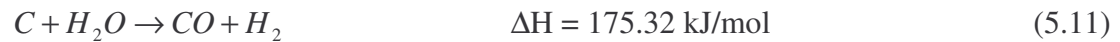
5.2.2 Coal based Design

Synthesis gas is obtained from coal through gasification. Coal gasification is a process where coal is reacted with water and an oxidant (air or O₂). In gasification, the oxidant is used for partial oxidation rather than complete combustion with synthesis gas (H₂ and CO) as the main products. The products of complete coal combustion are mainly H₂O and CO₂ instead of syngas.

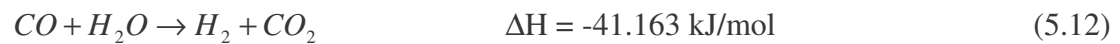
The three main reactions of coal gasification are (William, R. H., 2001):



Reaction 5.10 is a partial oxidation reaction which is highly exothermic, it provides heat for coal devolatilization and various endothermic reactions involved in gasification.



Reaction 5.11 is a water gas reaction which is highly endothermic.



Reaction 5.12 is a water-gas-shift reaction which is mildly exothermic.

The overall endothermic reaction for coal gasification is:



The analysis of carbon efficiency in coal-based FT processes has been done in the once-through processes utilizing compressed air and then compared to processes utilizing oxygen obtained from an Air Separation Unit (ASU) with and without wax hydrocracking. Air separation has been achieved by distillation as described in the

natural gas based processes (section 5.2.1). The amount of oxygen for the process has been worked out from the following overall reaction:



All the heat, energy and work requirements for this process are met by coal combustion shown in reaction 5.15 as:

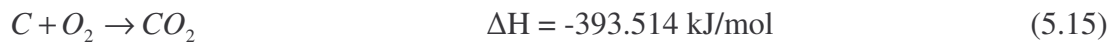


Figure 5.13 is a simple once-through process flow model of a coal-based FT synthesis process utilizing compressed air as the source of the oxidant. Just like with the once-through process based on natural gas, the unreacted syngas and the light hydrocarbon gases (tail gas) from the FT reactor are flared and considered as waste. The light and heavy waxes are hydrocracked to diesel at high temperature and pressure using hydrogen from an outside source.

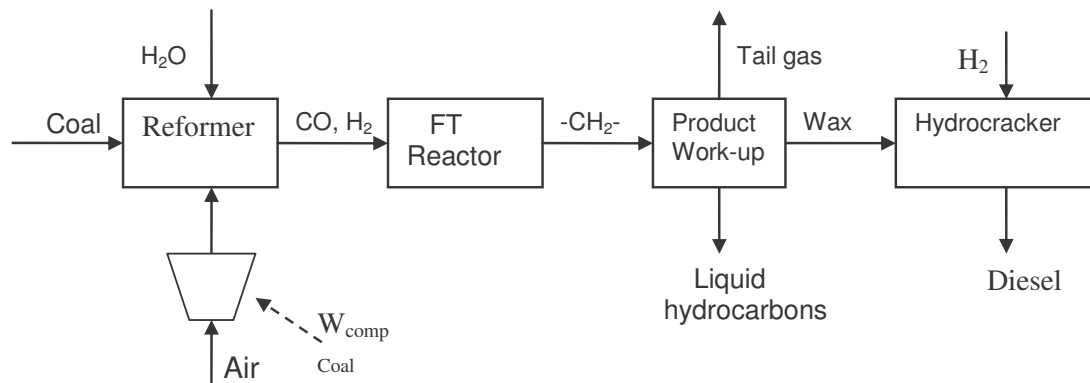


Figure 5.13 Process flow model for a once-through FT synthesis process based on syngas obtained by coal reforming with compressed air.

The process flowsheet for a recycle process based on coal gasification is very similar to Figure 5.10. The only difference is that coal instead of natural gas has been the feed with water and oxygen. This is shown here in Figure 5.14.

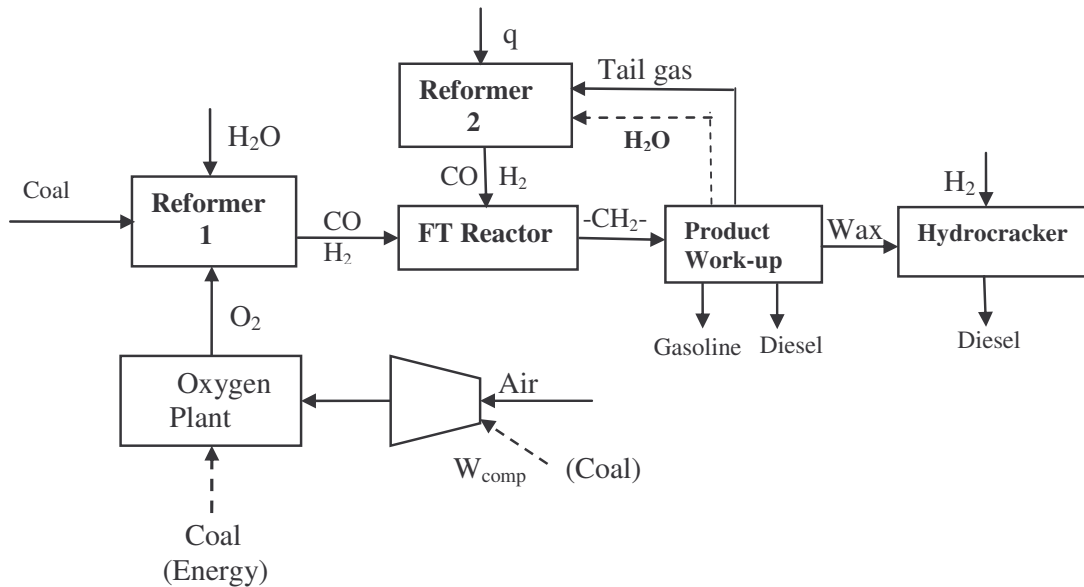


Figure 5.14 FT synthesis process flowsheet for a recycle process with syngas obtained by steam reforming of coal using oxygen obtained from an oxygen plant.

In this study, the catalyst has been assumed not to be active for the Water-gas-shift (WGS) reaction and there is consensus in literature that carbon dioxide does not have any inhibiting effect on the rate of FT synthesis for catalysts that are not active for the WGS reaction (Espinoza et al., 1999). CO_2 removal requires a lot of energy (about 0.68 GJ/ton CO_2 for the process based on absorption/stripping using methyldiethanolamine) (Desideri & Palucci, 1999) and since CO_2 removal does not influence the rate of FT synthesis, it has not been included in the process flow sheet.

All the results obtained from the various processes based on natural gas and coal in a once-through process without hydrocracking have been put together in Figure 5.15. It

is worthy noting that the process based on steam reforming of natural gas with the addition of CO₂ is by far the most efficient process ($\eta_{\max} \sim 84\%$) at the highest value of $\alpha = 0.95$ whereas, the most inefficient process ($\eta_{\max} \sim 29\%$) is the coal-based process that utilizes water and oxygen obtained from an air separation unit. It is also important to mention that both processes that incorporated oxygen plants had their carbon efficiencies decreasing by $\sim 6\%$ compared to those utilizing compressed air.

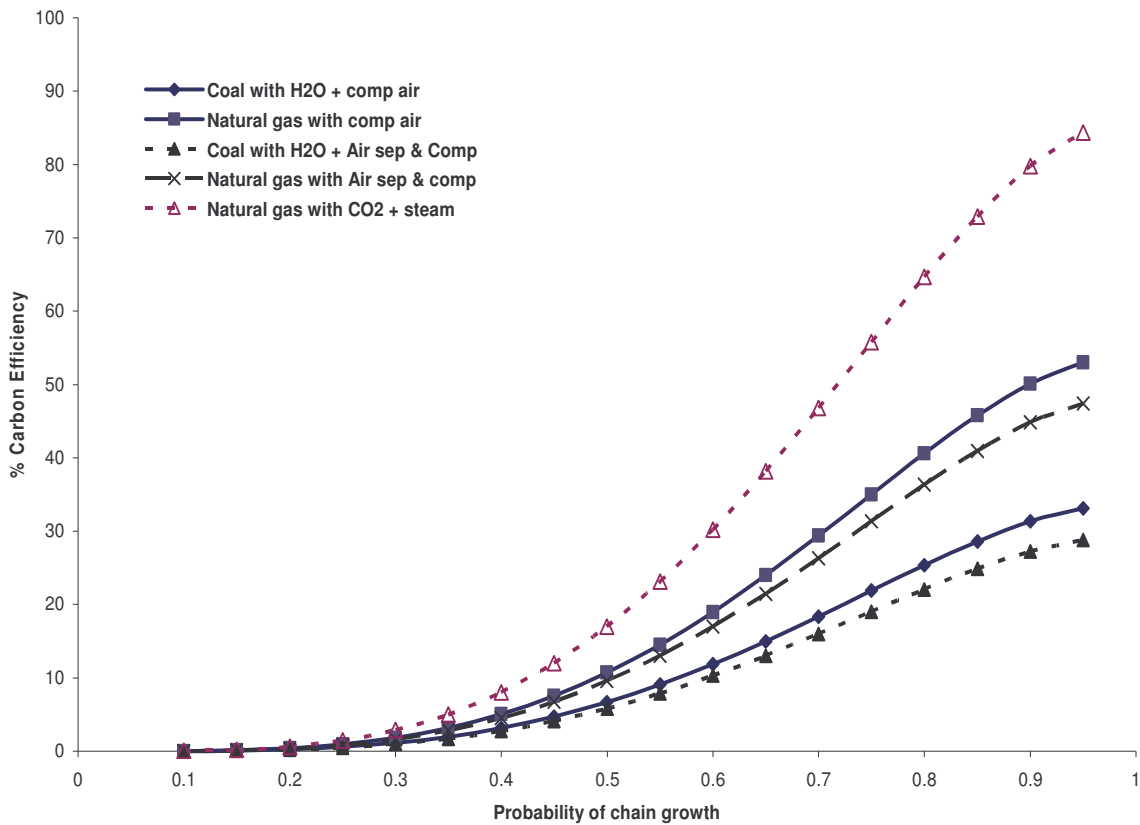


Figure 5.15 A comparison of carbon efficiencies at various α values in the once-through FT process based on coal and natural gas reforming without wax hydrocracking.

Wax hydrocracking has been incorporated in the once-through process and again a comparison has been done between the various FT synthesis processes with sources of syngas based on coal and natural gas in Figure 5.16.

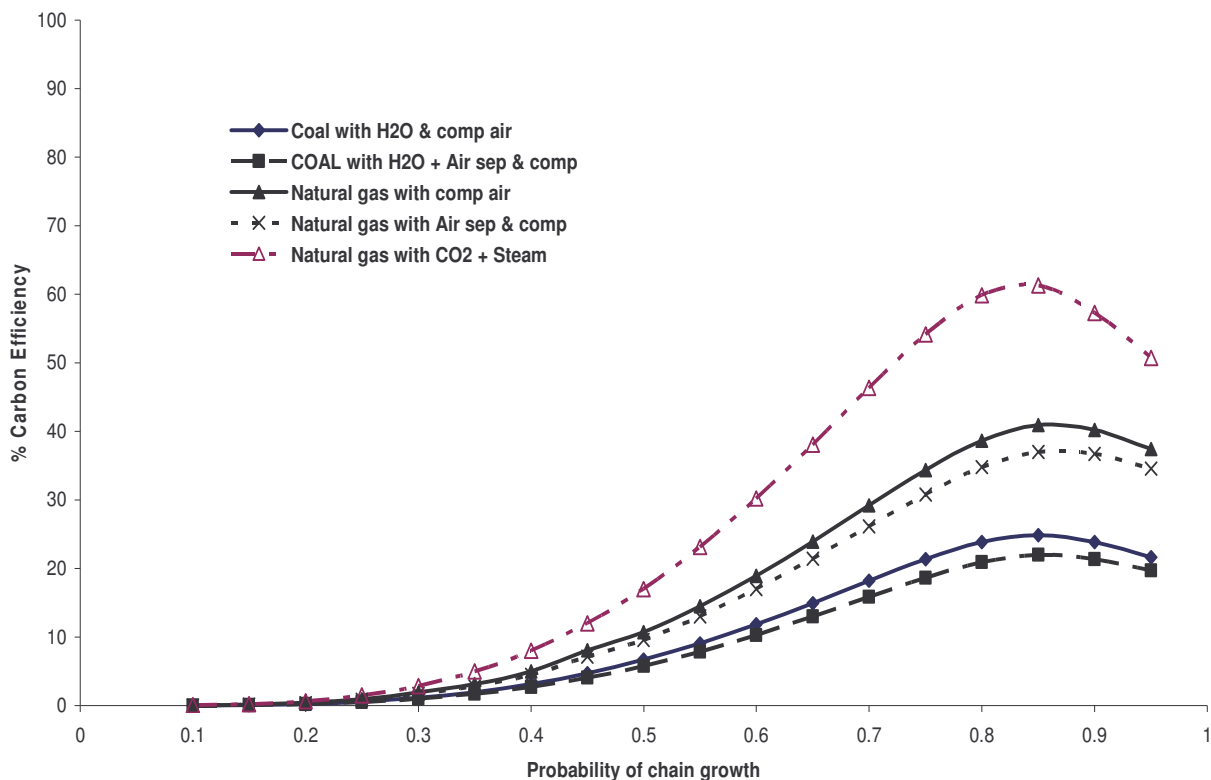


Figure 5.16 A comparison of carbon efficiencies at various alpha values in the once-through FT process based on coal and natural gas reforming with wax hydrocracking.

The carbon efficiency in the process based on steam reforming of natural gas with CO₂ is still the highest. The same observation made in other cases where wax hydrocracking was incorporated in the processes and optimum carbon efficiency was reached at some alpha values, has also been made here.

For all the various FT processes shown in Figure 5.16, the highest carbon efficiency is achieved at alpha value $\alpha \sim 0.85$, thereafter, the hydrocracking processes become very energy intensive. This is more prominent in processes based on natural gas. At $\alpha \sim 0.85$, the carbon efficiency reduces from $\sim 72\%$ in Figure 5.15 for the process with the highest carbon efficiency to $\sim 61\%$ in Figure 5.16. This 11% drop is attributed to the energy consumption of the wax hydrocracking. The process with the lowest carbon efficiency in Figure 5.15 (without hydrocracking) had the lowest drop in carbon efficiency at $\alpha = 0.85$ after the incorporation of a wax hydrocracking unit ($\sim 3\%$). This is the coal-based process featuring an air separation unit.

The recycling of the tail gas that has been regarded as waste in the once-through processes is, however, only feasible if pure oxygen is used instead of compressed air in the syngas generation section to avoid the build up of the inert N_2 in the recycle loop.

The carbon efficiencies of three recycle processes that uses oxygen plants without wax hydrocracking have been shown in Figure 5.17. It can be seen from the results that carbon efficiency for the process based on natural gas with an air separation and compression as a source of syngas has greatly improved from $\sim 47\%$ at $\alpha = 0.95$ in Figure 5.16 to 81% at the same α value in Figure 5.17. Marginal increases in the carbon efficiency of the other two processes have been noticed. The carbon efficiency for the recycle process based on natural gas with CO_2 and steam is $\sim 86\%$ at $\alpha = 0.95$ compared to $\sim 84\%$ at the same α value in the process shown in Figure 5.15. The recycling of the tail gas in the process based on coal gasification with air separation and compression has only increased carbon efficiency by $\sim 4\%$ compared with the once-through process based on the same source of syngas.

Between the two processes based on natural gas the difference in the recycle process without hydrocracking is very small. At the maximum $\alpha = 0.95$, the carbon efficiency for the process based on natural gas with air separation and compression is 86%

compared to the process based on natural gas with CO₂ and steam of 81%. Therefore, in this process it does not matter how syngas is obtained from natural gas.

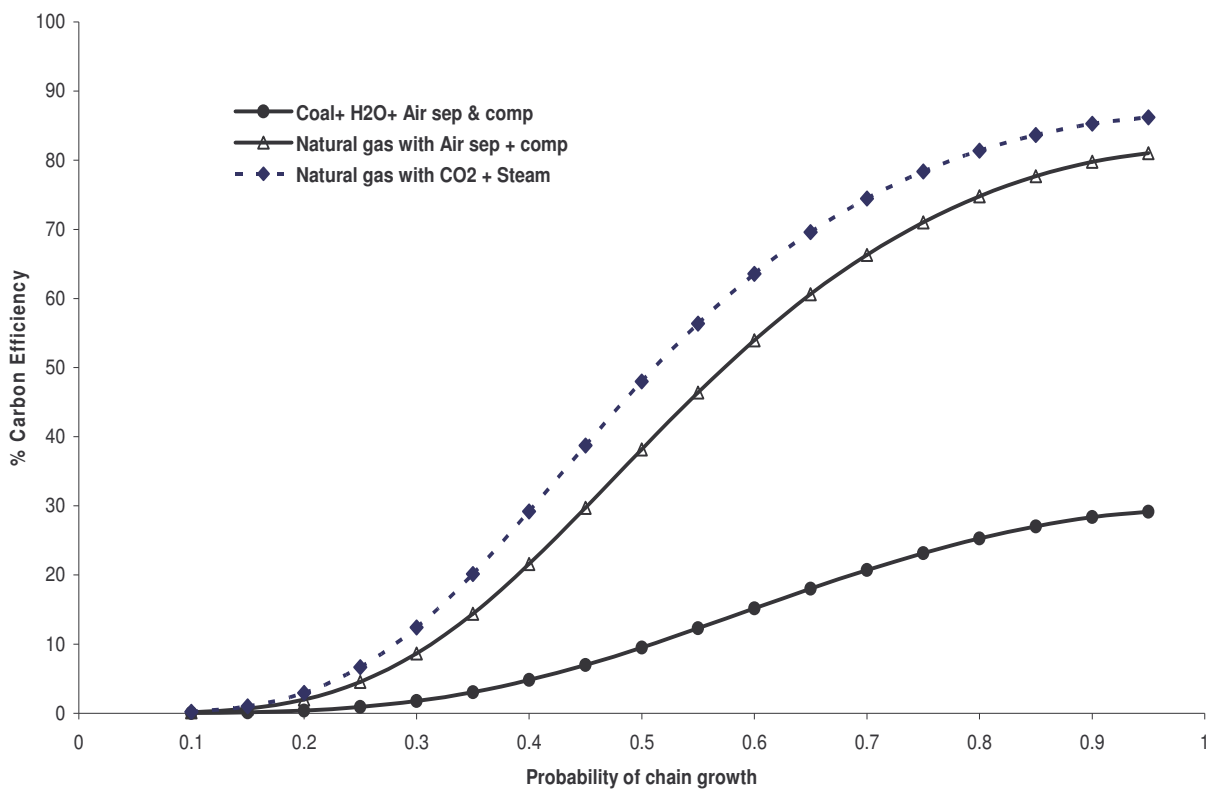


Figure 5.17 A comparison of carbon efficiencies at various α values in the recycle FT process based on coal and natural gas reforming without wax hydrocracking.

Figure 5.18 shows the carbon efficiencies of recycle FT processes incorporating wax hydrocracking based on natural gas and coal reforming. Compared to the same processes without wax hydrocracking, hydrocracking, generally, reduces carbon efficiency; however, this is more prominent in the processes based on natural gas. At the highest $\alpha = 0.95$, hydrocracking reduces carbon efficiency by ~35% (from 86% to 51%) for the process based on natural gas steam reforming with CO₂, while the process based on natural gas with air separation and compression had its carbon

efficiency by ~31% (from 81% to ~50%). The coal based process had the least carbon efficiency drop at $\alpha = 0.95$ by the addition of hydrocracking (from ~29% in the process without hydrocracking to almost 20% by the addition of the hydrocracking process). The highest carbon efficiency for the natural gas based processes was attained at $\alpha = 0.75$. The process based on natural gas steam reforming with CO_2 had carbon efficiency ~ 75% at $\alpha = 0.75$ while the other one based on natural gas with air separation and compression had carbon efficiency ~ 68% at $\alpha = 0.75$. In the coal based process the highest carbon efficiency ~23.8% was attained at $\alpha = 0.8$.

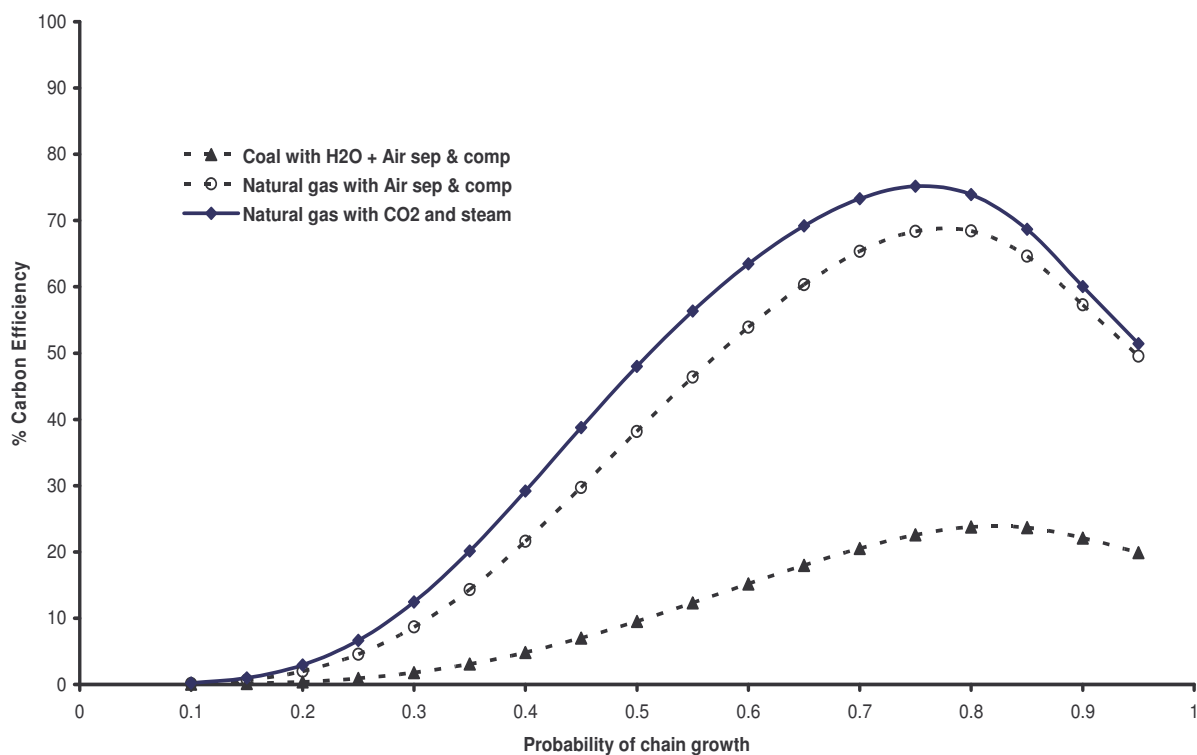


Figure 5.18 A comparison of CE at various alpha values in the recycle FT process based on coal and natural gas reforming with wax hydrocracking.

5.3 CONCLUSION

It has been reported that synthesis gas generation may account for approximately 60% of the required investments in large scale gas conversion plants based on natural gas. The choice of the syngas generation technology and the size of the syngas plant will have a direct impact on the carbon efficiency of the entire plant. It is, therefore, important that the choice of the syngas reforming technology be made by taking into consideration the effect it will have on the rest of this multi-step operation. For this purpose, it is important for the economics of an individual project to tailor the syngas synthesis process to the needs of subsequent processes.

Through out this study, it has been established that processes based on steam reforming of natural gas with CO₂ addition give the highest carbon efficiencies and so it can be a technology of choice especially in situations where CO₂ is readily available. It has been well established in literature and this study has also shown that natural gas based processes are more efficient than coal based ones (Benham & Bohn, 1999).

There are many possible options for the usage of FT tail gas comprising of the unconverted syngas, CO₂, and light hydrocarbons produced from the FT reactor. The optimum usage will depend on the process scheme and the desired products, which can also vary with locations. In this study, it is evident that recycling the tail gas allows for increased conversion and liquid hydrocarbon production, thereby increasing the overall carbon efficiency of the process.

FT synthesis technology flexibility allows for the choice of the most efficient conversion of the available feedstock into target products.

5.4 REFERENCES

Benham, C. B and Bohn, S. M. (1999), Maximization of diesel fuel product from an iron-based Fischer-Tropsch catalyst, Rentech Inc., 1999 AIChE Spring National Meeting, Houston, Texas, March 14 -18

Desideri, U and Palucci, A. (1999), Performance modeling of a carbon dioxide removal system for power plants, *Energy Conversion and Management* 40, 1899.

Dry, M. E. (2002), The Fischer-Tropsch process: 19500 – 2000, *Catalysis Today* 71, 227 – 241.

Espinoza, R. L., Steynberg, A. P., Jager, B and Vosloo, A.C. (1999), Low temperature Fischer-Tropsch synthesis from a Sasol perspective, *Applied Catalysis A: General* 186, 13.

Jess, A., Popp, R & Hedden, K. (1999), Fischer-Tropsch Synthesis and Nitrogen-Rich syngas. Fundamentals and Reactor Design aspects, *Applied Catalysis A: General* 186, 321 – 342.

King, C. J. (1971), *Separation Processes*, McGraw-Hill Book Company, 634.

Tijm, P. J. A. (2001), Assessment of Different feedstocks for Synthesis Gas Production and Fischer-Tropsch (F-T) Conversion, Gas to Liquids Viability, Economics and Strategy, Omni Hotel, Houston Texas, September 29 – 30.

William, R. H. (2001), Toward zero emissions from coal in China, *Energy for sustainable Development*, Volume 5, No.4.

6

OVERALL CONCLUSION

This work has shown that it is possible to use the Process Synthesis approach and limited experimental data and simple calculations to quickly synthesize a process flowsheet and investigate various alternatives at an early stage of process development. Using carbon efficiency as a measure of process efficiency, the methodology presented here identifies the key areas of further experimentation and other process development efforts away from dead-ends.

It has been established that when choosing the optimal region for the operation and design of an FT Synthesis process, the influence of the system parameters must be well understood. This is only possible if the kinetics, reactor, and process design are done iteratively. It is recommend not optimizing the reactor independent of the process in which it is going to be used without understanding the impact of its operating conditions on the entire plant.

Using data from an FT experiment and literature, various process configurations have been developed. The results were evaluated with a view of identifying major process drivers and it was observed that it is beneficial to run an FT reactor at low CO conversion to avoid higher methane formation. Whether the process is run as a once-through or recycle process, the trend should be to minimize the formation of lighter gases by obtaining high α values because carbon efficiency increases as α values increase. It is recommended that experiments should be performed to obtain operating conditions that will yield high α values. However, if the aim is to maximize diesel production by hydrocracking the waxes, then an optimal α value should be targeted to avoid the hydrocracking very heavy waxes.

The choice of the syngas generation technology has a direct impact on the carbon efficiency of an FT synthesis plant. Processes based on natural gas feed are more efficient than coal based ones. This study has established that running an FT synthesis process with syngas obtained by steam reforming of natural gas with CO₂ addition can yield high carbon efficiencies especially in situations where CO₂ is readily available. It is known that CO₂ is produced in FT synthesis, especially during energy production and in this study, the reaction that incorporates the use of CO₂ was aimed at showing that CO₂ can be used as a reactant and by so doing help in the reduction of CO₂ emission into the environment. If the addition of CO₂ to methane steam reforming is to be considered as one of the alternate ways of syngas gas production and CO₂ sequestration then I recommend that the question of the break even point in CO₂ production and usage can be investigated in a future process integration study.

APPENDIX I

Fischer-Tropsch synthesis: A study of the effect of water on the catalytic activity of a cobalt-alumina catalyst

Peter Mukoma¹, Gary Jacobs², David Glasser¹, Diane Hildebrandt¹, Burtron H. Davis.²

¹COMPS, School of Chemical and Metallurgical Engineering,
University of the Witwatersrand, P/bag 3, WITS 2050.

²Center for Applied Energy Research, University of Kentucky, 2540 Research Park Drive, Lexington, KY 40511, USA.

Abstract

Degussa C γ -alumina has been modified (wetted, dried, calcined) and used as a wide pore ($d \approx 25.5$ nm) support to prepare a 12% Co/Al₂O₃ catalyst. The influence of water on this alumina-supported cobalt catalyst during Fischer-Tropsch synthesis was investigated in a continuously stirred tank reactor (CSTR) at 493 K and 20 atm by adding water to the synthesis gas feed, the added water replaced an equivalent amount of inert gas leaving all the other reaction conditions the same before, during and after water addition. Water addition had a negative effect on the catalytic activity. The extent of loss in catalytic activity depends on the amount of water feed. The addition of water amounts <25 vol. % decreased CO conversion slightly and the effect was mostly reversible, suggesting a kinetic effect of water, possibly due to adsorption of inhibition. However, the catalytic loss observed after the addition of 25 vol. % water was more permanent. The steady increase in CO₂ selectivity indicated that an oxidized type of cobalt species (e.g., cobalt oxide or cobalt support

compounds like cobalt aluminate) active for the water-gas shift reaction was formed under high water partial pressure. C_{5+} selectivity was mostly unchanged at about 86%.

1 INTRODUCTION

Supported Fischer-Tropsch synthesis (FTS) cobalt catalysts have been found to be well suited for the conversion of high H_2 : CO ratio syngas derived from natural gas to liquid fuels. This is mainly due to their low water-gas shift rates, good activity and selectivity towards high molecular weight hydrocarbons. Various supports such as SiO_2 , TiO_2 , Al_2O_3 , etc have been used to prepare these catalysts. It has been found that the support has a significant influence on the catalyst reducibility, activity, and selectivity properties of the active phase (Reuel & Bartholomew, 1984), thereby, making the choice of catalyst support very important.

Among the supports used in the preparation of cobalt-based catalysts, alumina (Al_2O_3) is known to have high resistance to attrition in slurry reactors (Espinoza et al., 1998). It has been reported that in cobalt-alumina catalysts, there is a strong interaction between the support and the cobalt oxide phase (Chin & Hercules, 1982). Therefore, the activity and selectivity of the Fischer-Tropsch synthesis are influenced by the surface properties of the Al_2O_3 support and the nature of the species formed after preparation.

Oxygen is mainly removed as water during cobalt catalyzed FTS. In fixed bed reactors this tends to create high partial pressures of water at the reactor exit. Ideally, in slurry reactors or CSTRs high water concentrations and low reactant concentrations will exist throughout the entire reactor as a result of extensive back mixing. The use of cobalt-based catalysts in Fischer-Tropsch synthesis on a commercial basis requires that the catalysts withstand long-term use at high CO conversions. High CO conversions are feasible in slurry reactors because of their

favourable heat transfer properties (Fox, 1993). High CO conversions result in high water production. Condensation of water in the pores of the catalyst support may occur when this high water concentration reaches saturation levels. In spite of the many studies that have been conducted on the effect of water on the activity of the cobalt-based FTS catalysts, there has been little consensus on the findings. This is probably due to the different support materials, promoters, cobalt precursors and preparation methods that are used by various researchers (van Berg et al., 2000; Hilmen et al., 1999; Li et al., 2002; Jacobs et al., 2004). Although the effect is not very well understood, it is evident that Al₂O₃-supported cobalt catalysts deactivate faster with water addition. Analysis of the reaction products indicates that this deactivation was most likely due to the oxidation of the cobalt metal clusters. The studies conducted by Bolt (1994) on the formation of metal-alumina spinel at high temperatures found that water increased the rate of metal-aluminates formation. He also found that the reaction rate for aluminate formation increased in the order Fe<Ni<Co<Cu. It is also understood that the extent of deactivation depends on water partial pressure in the reactor. Low water partial pressures are associated with temporal catalyst activity loss and high water partial pressures are associated with more permanent catalyst activity loss.

Schulz et al (1995) did not find any changes in the activity of a Co/Zr/aerosol catalyst even when it was exposed to high water partial pressures; however, he reported a decrease in methane selectivity and an increase in C₅₊ selectivity with a high content of olefins in the products. Model studies carried out by Schanke et al (1995) on Co/Al₂O₃ catalysts using H₂O/H₂ feeds in conjunction with XPS and gravimetry showed that reoxidation of cobalt can occur in H₂O containing mixtures and that the extent of reoxidation depends on the partial pressure of water and the H₂O/H₂ ratio. Based on SSITKA results, Rothaemel and co-workers (1977) reported a decrease in catalyst activity after exposing both Co/Al₂O₃ and Co/Re/Al₂O₃ catalysts to water. They concluded that the catalyst surface available for methane formation and reversible CO adsorption decreased after water addition. They proposed that the

water treatment of the Co catalyst leads to an oxidation of exposed Co atoms, thus decreasing the available active surface.

This study was undertaken to ascertain the effect of water on a cobalt catalyst supported on modified Degussa C- Alumina. This support has not been widely studied. The catalyst was characterized using standard techniques (BET, TPR, H₂ Chemisorption by TPD, XRD). The study was more focused on the effect of water on the activity and product selectivity of the catalyst.

2 EXPERIMENTAL

2.1 Catalyst preparation

Two alumina supported catalysts were prepared and characterized. Cobalt nitrate was used as the precursor while modified Degussa C γ - Alumina was used as support. Degussa C γ - Alumina is a narrow particle size material with a high surface area. When wetted by water to the incipient wetness point, dried in air at 375 K for 24 hours and calcined at 623 K for 5 hours, the material is transformed. The particles agglomerate into small “clusters” and this result in a sponge-like structure characterized by cages with an average diameter of 25.5 nm.

A novel slurry phase impregnation method based on a Sasol patent (Espinoza et al., 1998) was used to prepare the catalysts. Two catalysts with different metal loadings (12% and 25%) were prepared. For the slurry phase method, the ratio of the volume of loading solution used to the weight of alumina was 1:1, such that approximately 2.5 times the pore volume of solution was used to prepare the catalyst. Multiple impregnation steps were used to load the total weight % cobalt metal to the support. Between each step the catalyst was dried under vacuum in a rotary evaporator at 333K and the temperature was slowly increased to 373K. After the final impregnation/drying step, the catalyst was calcined at 623K.

2.2 Catalyst characterization

The structural studies of the prepared alumina-supported cobalt catalysts were studied by using the following techniques: BET, Temperature Programmed Reduction (TPR), H₂ Chemisorption by Temperature Programmed Desorption (TPD) with O₂ Pulse reoxidation, and X-ray Diffraction.

2.2.1 Surface areas and pore size measurements

Surface area and pore size measurements were carried out by N₂ adsorption on a Micromeritics Tri-Star system on both the supports and the calcined catalysts. Prior to measurements, the samples were evacuated at 433 K to approximately 50 mTorr for 4 hours. The surface area was calculated as the Brunauer-Emmet-Teller (BET) surface area. Total pore volume and pore size distribution were calculated from the nitrogen desorption curve using the Barrett-Joyner-Halenda (BJH) method.

2.2.2 Temperature Programmed Reduction

Temperature programmed reduction (TPR) of catalysts was conducted utilizing a Zeton-Altamira AMI-200 unit. First, calcined samples were purged in flowing Ar to remove traces of water. A liquid nitrogen trap was used to prevent water generated by reduction from interfering with the signal of the thermal conductivity detector (TCD). TPR was performed using a 10% H₂/Ar mixture at a flowrate of 30 cm³/min using Ar as the reference to maximize the signal to noise ratio. The sample was heated from 323 K to 1073 K using a heating ramp of 10 K/min.

2.2.3 H₂ Chemisorption by TPD

Chemisorbed hydrogen was quantified using the Zeton-Altamira AMI-200 unit. The sample weight was kept at 0.220 g. Catalysts were reduced using hydrogen at 623 K

for 10 hours and cooled under flowing hydrogen to 373 K. The sample was held at 373 K under flowing argon to remove weakly bound species, prior to increasing the temperature slowly to 623 K. The catalyst was held at 623 K under flowing argon to desorb the remaining chemisorbed hydrogen until the TCD signal returned to the baseline condition. The TPD spectrum was integrated and number of moles of desorbed hydrogen determined by comparing to the areas of calibrated pulses of hydrogen in argon. The sample loop was previously calibrated with pulses of nitrogen in helium flow and compared against a calibration line produced from using gas tight syringe injections of nitrogen into helium flow. Assumptions of a spherical cobalt cluster morphology and a 1:1 H: Co stoichiometric ratio were made.

2.2.4 Pulse oxidation

The extent of reduction was determined by pulse oxidation with O₂ of reduced samples at 623 K. After TPD of hydrogen, the samples were reoxidized at 623 K by sending pulses of pure O₂ in helium carrier. Complete oxidation of the cobalt metal clusters was the condition whereby the entire O₂ pulse was observed by the TCD. After reoxidation, the number of moles of O₂ consumed was determined, and the extent of reduction calculated assuming that the Co⁰ reoxidized to Co₃O₄ (Jacobs, et al., 2000; Vada et al., 1995).

2.2.5 X-Ray Diffraction (XRD)

Powder diffractograms on calcined catalysts were recorded using a Philips X'Pert diffractometer. Long scans were made over the intense peak at 36.8° corresponding to (311) so that estimates of Co₃O₄ cluster size could be assessed from line broadening analysis.

2.3 Reaction system and procedure

Prior to loading into the reactor (CSTR), the calcined catalyst (ca. 12 g) was reduced ex-situ in a fixed bed reactor at 623 K for 10 hours in hydrogen at a flow rate of 1L/min. The catalyst was then transferred to the CSTR under the protection of helium to mix with Ethylflow 164 Oil (C₃₀ oil) as a start up media. To facilitate the transfer, the fixed bed reactor was connected to the CSTR using a transfer tube with a ball valve. The fixed bed reactor was pressurized with argon forcing the catalyst powder out of the reactor through the valve. The reactor was weighed before and after the transfer of the catalyst to ensure that all the catalyst powder was transferred to the CSTR. The catalyst was then reduced in situ with hydrogen at a flow rate of 59 SL/h at atmospheric pressure. With the temperature controller in a ramp/soak mode, the reactor temperature was ramped up to 553 K at a rate of 2 K/min and held at 553 K for 24 hours.

The reactor system used for the slurry FTS reaction was a 1 liter CSTR. Separate mass flow controllers were used to deliver hydrogen, carbon monoxide and the inert gas at the calculated rate to a mixing vessel. Carbon monoxide passed through a vessel containing lead oxide-alumina to remove iron carbonyls. The mixed gases entered the CSTR below the stirrer which was operated at 750 rpm.

After the activation period, the reactor temperature was decreased to 453 K, synthesis gas (H₂: CO = 2:1) was introduced to the reactor and the pressure was increased to 20.7 atm (2.03 MPa). The reactor temperature was increased to 493 K at a rate of 1 K/min and the space velocity was maintained at 5 SL/h/gcat.

The reaction liquid products were continuously removed from the vapor and passed through two traps, a warm trap maintained at 373 K and a cold trap held at 273 K. The uncondensed vapour stream was reduced to atmospheric pressure through a letdown valve. The gas flow was measured using a wet test meter and analyzed in an

online GC. The accumulated reactor liquid products were removed every 24 hours by passing through a 2 μm sintered metal filter located below the liquid level in the CSTR. The contents of the 273 and 373 K traps were combined; the hydrocarbon and water fractions were separated and then analyzed using a GC. The reactor wax, which was collected in a third trap maintained at 473 K, was analyzed using a high-temperature GC to obtain a carbon number distribution of high molecular weight hydrocarbons.

In all experiments, the pressure of CO and H₂ in the feed remained constant at 70 % of the total pressure, while argon was used to make up the balance before, during, and after H₂O addition experiments. Therefore, when water was added, a fraction of the argon was replaced by water. The amount of water added was calculated based on the amount of argon to be replaced, thus ensuring that the sum of the water and argon partial pressures remained at 30 % of the total pressure. Water addition was done using a high precision, high pressure ISCO syringe pump. The added water, together with the water produced by the reaction was collected in the warm and cold traps and the fractions were combined to ensure an accurate water balance.

3 RESULTS AND DISCUSSION

3.1. Characterization

To determine if there was any structure modification to the Degussa C $\gamma\text{-Al}_2\text{O}_3$ support after wetting and drying, adsorption/desorption isotherms obtained before and after modifications were compared. The results in Figure 1 are in agreement with previous reports in the literature (Brenner et al., 1995). That is, the as-received Degussa C $\gamma\text{-Al}_2\text{O}_3$ yields a type II Brunauer's adsorption isotherm without leveling off. The wetted/dried/calined Degussa C $\gamma\text{-Al}_2\text{O}_3$, on the other hand, yields a type IV adsorption isotherm indicating a porous structure.

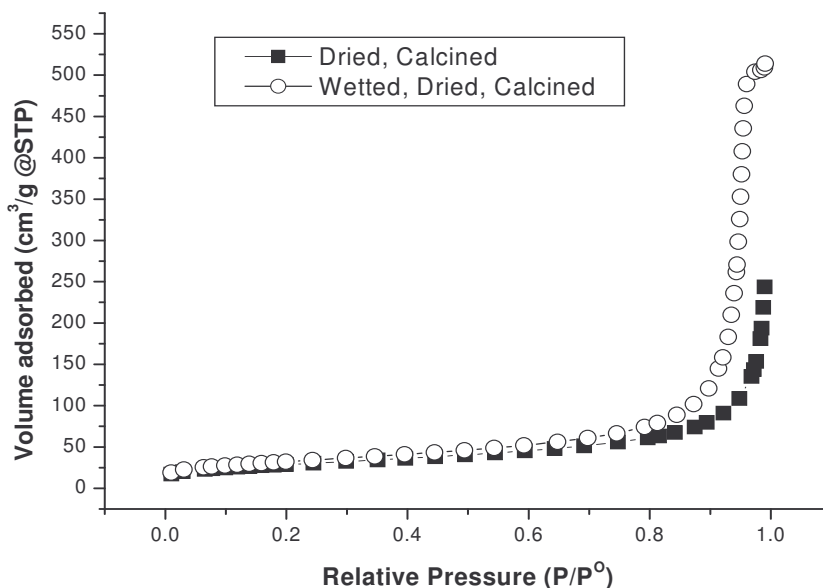


Figure 1. N₂ adsorption isotherms for the as-received and modified Degussa C γ -Al₂O₃ support.

The results of the BET surface area, pore volume and diameter measurements are shown in Table 1. The average pore volume of the modified Degussa C γ -Al₂O₃ is twice that of the as-received material and this is also shown in Figure 2.

Table 1: BET surface area and BJH pore size measurements of the Degussa C γ -Al₂O₃ supports and the supported catalysts calcined at 623 K.

Material description	Measured surface (m ² /g)	BET area	BJH Des Pore Vol (cm ³ /g)	BJH Des Pore Diam (nm)	Ave
Degussa C γ -Al ₂ O ₃ Dried, Calcined	103.4		0.3835	15.68	
Degussa C γ -Al ₂ O ₃ , Wetted, Dried, Calcined	116.9		0.7966	25.50	
12% Co/Al ₂ O ₃ Degussa C γ -Al ₂ O ₃ , Wetted, Dried, Calcined	89.1		0.4212	15.32	
25% Co/Al ₂ O ₃ Degussa C γ -Al ₂ O ₃ , Wetted, Dried, Calcined	76.9		0.3939	19.43	

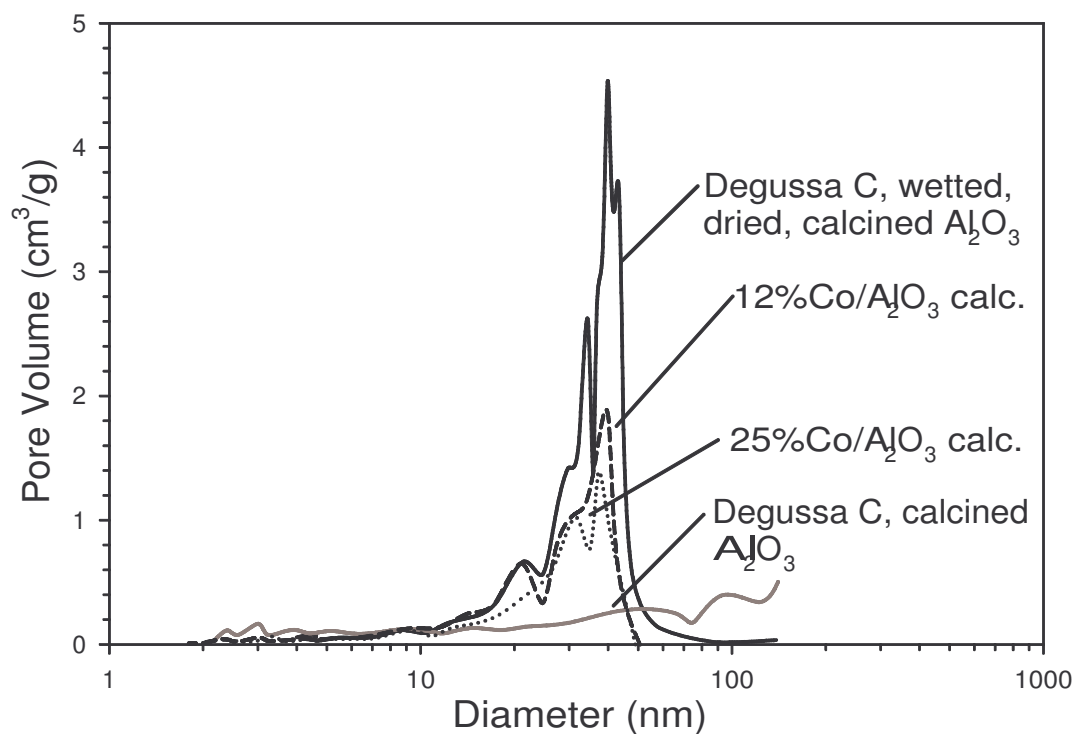


Figure 2. Pore size distributions by BJH adsorption of nitrogen for the modified alumina supports and catalysts.

Cobalt catalysts supported on alumina have limited reducibility due to a strong interaction between the support and cobalt oxides. Calcined Co/Al₂O₃ catalysts have a complicated composition on the surface of the support and this can be a mixture of Co₃O₄ and cobalt-support complexes such as cobalt aluminates (Wang & Chen, 1991). To calculate the cluster size and the degree of reduction by chemisorption, a method in which the amount of oxygen consumed by the metallic component to be reoxidized after a reduction procedure, has been employed to estimate the metallic fraction of the cobalt (Jacobs et al., 2000). The extent of reduction is included in the denominator of the dispersion equation so that a much more accurate estimate of the true dispersion of the metallic fraction (and therefore, cluster size) can be obtained.

After calcination, the catalysts were scanned by XRD to give another estimate of the cobalt metal cluster size. The XRD was able to detect the spinel crystalline phase of Co_3O_4 . From Table 2, it can be seen that results from XRD are not very different from those obtained through calculations from chemisorption after taking into account percentage reduction. The average cluster diameter for the 25% $\text{Co}/\text{Al}_2\text{O}_3$ is almost double that of the 12% metal loaded catalyst. It can be assumed therefore, that for the 12% $\text{Co}/\text{Al}_2\text{O}_3$, nearly all of the cobalt metal particles are present in the pores of the support.

Table 2: Co^0 particle size and dispersion from H_2 chemisorption, and Co_3O_4 particle size from XRD.

Catalyst	Dispersion (H_2 - ads.)(%) ^a	Reduction (H_2 - ads.) (%) ^b	Co^0 particle size (H_2 -ads.) (%) ^c	Co_3O_4 particle size (%) ^d
12% $\text{Co}/\text{Al}_2\text{O}_3$ (Degussa C)	8.4	67.8	12.2	13.3
25% $\text{Co}/\text{Al}_2\text{O}_3$ (Degussa C)	5.3	60.1	19.5	23.2

^a Co^0 dispersion from H_2 chemisorption, assuming adsorption on Co atoms only.

^b The reduction of Co_3O_4 to Co^0 by TPR.

^c Co^0 particle size calculated from H_2 chemisorption.

^d Co_3O_4 particle size calculated from XRD of calcined catalysts using the most intense peak located at $2\theta = 36.8^\circ$.

3.2 Effect of water addition on catalyst activity

The experiments to determine the effect of water on the activity and selectivity of the 12% Co/Al₂O₃ Fischer-Tropsch catalyst were carried out in the reaction system described in section 2.3. Different amounts of water (5 - 25 vol. %) were added to the feed gas replacing argon by the same amount to maintain constant syngas partial pressure and space velocity. The partial pressures of the inlet H₂ and CO were kept unchanged during all the runs. After each run with water addition, the conditions were adjusted by switching off the water so as to obtain conditions similar to those obtained before water addition. The results in Figures 3 and 4 show the effect of water on CO conversion and FTS rate as a result of catalyst deactivation.

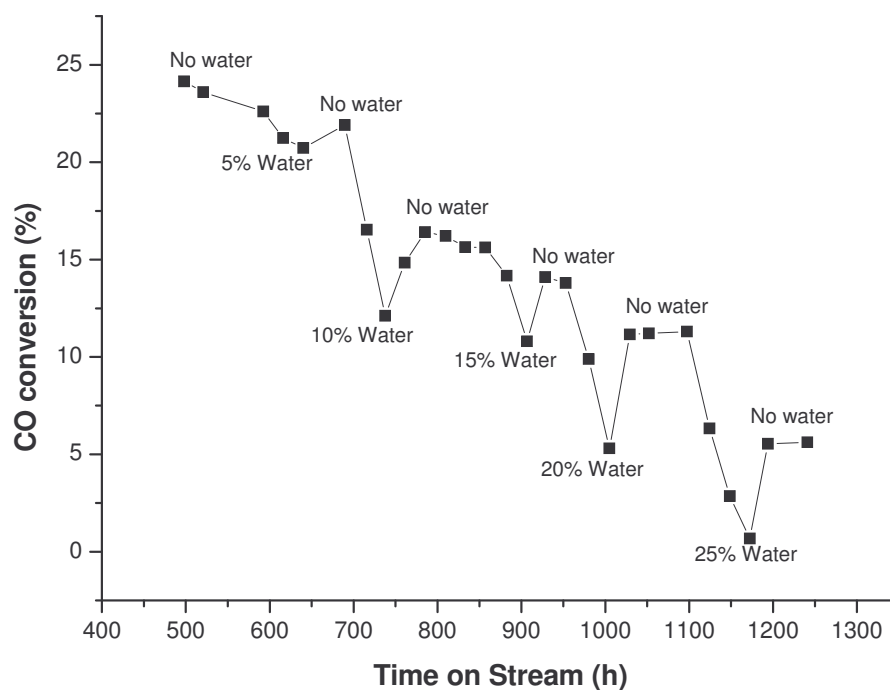


Figure 3 Effect of water on CO conversion for 12% Co/Al₂O₃ catalyst.

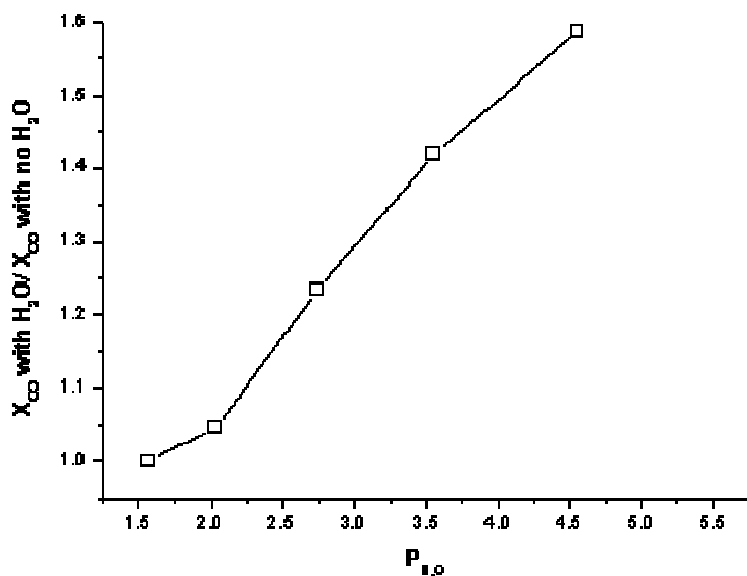


Figure 4. The effect of water addition on the rate of 12% Co/Al₂O₃ catalyst deactivation.

Whenever water was added to the feed, there was a loss in catalyst activity which was more temporal in the 5 – 20 vol. % range. The catalyst activity recovered after water addition was terminated. With 25 vol. % water addition, the loss in catalyst activity was severe and this was not fully recovered after the termination of water addition, an indication that the deactivation was more permanent. Although, it is evident from thermodynamic calculations that the oxidation of bulk phase metallic cobalt to either CoO or Co₃O₄ is unlikely (Van Berg et al., 2000), previous investigators (Hilmen et al., 1999; Jacobs et al., 2004; Schanke et al., 1995) found that the irreversible deactivation of Fischer-Tropsch cobalt catalyst was likely to be a result of an oxidative process caused by the presence of a high partial pressure of water, and may be attributed to cobalt-support complex formation.

Figure 5 shows the effect of water addition on CO₂ and CH₄ selectivity. It is seen that CO₂ selectivity increased steadily with the increase in the vol. % water added to the feed. This is a further confirmation that some surface cobalt atoms were re-oxidized to form cobalt oxide or some other oxidized form of cobalt (i.e., cobalt-support complex) active for water-gas shift reaction. Some studies found unreduced Co-Pt/Al₂O₃ catalyst to be active for water-gas shift reaction when a feed of CO/H₂O in the ratio 1:1 (without hydrogen) was introduced in the reactor at FTS conditions (Li et al., 2002).

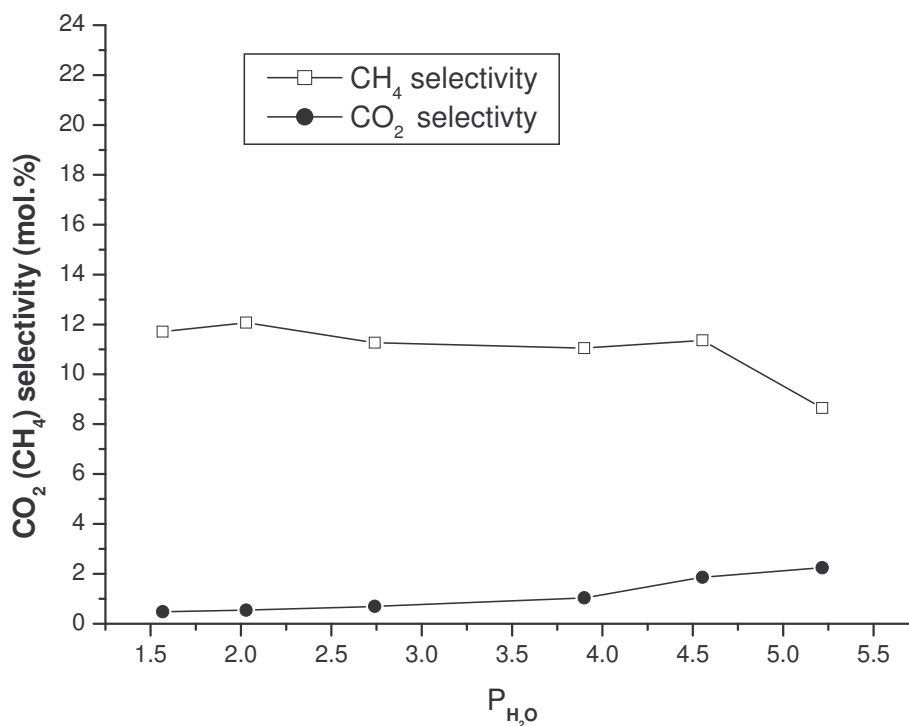


Figure 5. The effect of water addition on the CH₄ and CO₂ selectivity using Co/Al₂O₃ catalyst.

Although it has been reported by other researchers (Hilmen et al., 1999; Bertole et al., 2002; Krishnamoorthy et al., 2002; Shulz et al., 1994) that water increases C₅₊ selectivity and reduces CH₄ selectivity for all Co catalysts, the results presented in Table 3 show that when 5 – 20 vol.% water was added to the feed, C₅₊ selectivity remained almost unchanged, it increased slightly when 25 vol. % water was added.

Results shown in Figure 6.5 indicate no change in CH₄ selectivity for 5- 20 vol. % addition. An increase in water addition to 25 vol. % saw a reduction in CH₄ selectivity.

The P_{H₂}/P_{H₂O} ratios shown in Table 3 are higher than the thermodynamic equilibrium constants for $\text{Co} + \text{H}_2\text{O} \leftrightarrow \text{CoO} + \text{H}_2$ and $3\text{Co} + 4\text{H}_2\text{O} \leftrightarrow \text{Co}_3\text{O}_4 + 4\text{H}_2$ under FTS conditions (Van Berg et al., 2000) and since these are supposed to be the reactions between cobalt and water resulting in an oxidized form of cobalt, it can be assumed that the reduction of either CoO or Co₃O₄ by hydrogen are spontaneous during the slurry phase FTS under realistic conditions. However, the oxidation of bulk phase metallic cobalt to either CoO or Co₃O₄ does not happen.

Table 3: Effect of water on C₅₊ selectivity for 12% Co/Al₂O₃ catalyst (reaction condition: T = 220°C, P = 20 atm, H₂/CO = 2 with 30% Ar, SV = 5 SL/h/g_{cat})

H ₂ O (vol.%)	added	TOS (h)	CO (%)	conv.	P _{H₂O} (atm)	P _{H₂O} /P _{H₂}	C ₅₊ sel. (%)
0		498	24.2		1.6	0.249	85.7
5		616	21.2		2.0	0.314	85.0
10		716	16.5		2.7	0.400	86.1
15		857	15.6		3.9	0.562	85.7
20		980	9.9		4.6	0.617	85.1
25		1124	8.2		5.1	0.682	87.4

4 CONCLUSION

Wetting and drying transforms the non-porous Degussa C γ -Al₂O₃ into a porous alumina support. This is evidenced from the N₂ adsorption results. The modified Degussa C γ -Al₂O₃ has been used as support to prepare a 12% Co/Al₂O₃ catalyst and the catalyst showed good stability.

The results from water addition experiments are consistent with results of the other alumina-supported Fischer-Tropsch cobalt catalysts tested and reported in literature (Hilmen et al., 1999; Li et al., 2002; Jacobs et al., 2004; Schanke et al., 1995; Jacobs et al., 2000; Krishnamoorthy et al., 2002). The addition of water to the feed has a negative effect on the activity of the catalyst. Catalyst deactivation increased from 0.3% per day without water to 0.45% per day with water addition. The decrease in catalytic activity that was noticed when water below 25 vol. % was added, was mostly recovered after water addition was stopped, consistent with kinetic effect of water, probably due to adsorption inhibition. Very little catalyst activity was recovered after 25 vol. % water was added indicating that the high extents of Co oxidation were related to high water partial pressures.

CH₄ and C₅₊ selectivities remained almost unchanged until 25 vol. % was added when there was an increase in C₅₊ selectivity and a reduction in CH₄ selectivity because of the irreversible effect on CO conversion. CO₂ selectivity increased steadily with the increase in the amount of water addition. This indicated that there maybe the formation of oxidized form of cobalt, which most likely involves the formation of an irreducible cobalt-support compound causing a decrease in the active metallic surface.

5 REFERENCES

- Bertole, C. J., Mims, C. A and Kiss, G. (2002), *Journal of Catalysis* 210, 84.
- Bolt, H. (1994), Transition metal-aluminate formation in alumina-supported model catalysts, Ph.D. Thesis, University of Utrecht, The Netherlands.
- Brenner, A. M., Adkins, B. D., Spooner, S and Davis, B. H. (1995), *Journal of Non-Crystalline Solids* 185, 73.
- Chin, R. L and Hercules, D. M. (1982), *Journal of Physical Chemistry* 86, 360.
- Espinoza, R. L., Visagie, J. L., van Berg, P. J and Bolder, F. H. (1998), US Patent 5,733,839.
- Fox, J. M. (1993), *Catalysis Reviews – Science and Engineering* 35, 169.
- Hilmen, A. M., Schanke, D., Hanssen, K. F and Holmen, A. (1999), *Applied Catalysis A* 186, 169.
- Jacobs, G., Das, T. K., Zhang, Y., Li, J., Racoillet, G and Davis, B. H. (2000), *Applied Catalysis A* 233, 263.
- Jacobs, G., Patterson, P. M., Das, T. K., Luo, M and B. H. Davis, B. H. (2004), *Applied Catalysis A* 270, 65.
- S. Krishnamoorthy, S., Tu, M., Ojeda, M. P., D. Pinna, D and Iglesia, E. (2002), *Journal of Catalysis* 211, 422.
- Li, J., Zhan, X., Zhang, Y., Jacobs, G., Das, T and Davis, B. H. (2002), *Applied Catalysis A* 228, 203.

- Reuel, C. R and Bartholomew, C. H. (1984), *Journal of Catalysis* 85, 78.
- Rothaemel, M., Hanssen, K. F., Blekkan, E. A., Schanke, D and Holmen, A. (1977), *Catalysis Today* 38, 79.
- Schanke, D., Hilmen, A. M., Bergene, E., Kinnari, K., Rytter, E., Adnanes, E and Holmen, A. (1995), *Catalysis Letters* 34, 269.
- Shulz, H., van Steen, E and Claeys, M. (1994), *Studies in Surface Science and Catalysis* 81, 455.
- Shulz, H., Claeys, M and Harms, S. (1995), 4th Int. Natural gas Conversion Symp., Krugger National Park, South Africa..
- Vada, S., Hoff, A., Adnanes, E., Schanke, D and Holmen, A. (1995), *Topics in Catalysis* 2, 155.
- Van Berg, P. J., van de Loosdrech, J., Barradas, S and van der Kraan, A. M. (2000), *Catalysis Today* 58, 321.
- Wang, W. J and Chen, Y. W. (1991), *Applied Catalysis A*. 77, 223.

APPENDIX II

Efficiencies of the Thermodynamic Engines

The separation of air can be modelled as a heat engine with a heat input at 90 K and heat removal at 78 K. Substituting these temperature values in eq 1 gives the separation work with a Carnot engine efficiency of 0.13.

$$\eta_{work(sep)} = \frac{T_H - T_C}{T_H} = \frac{T_{O_2} - T_{N_2}}{T_{O_2}} \quad (1)$$

A refrigeration process is required to remove energy from the reboiler. The process must remove energy at 78 K and reject it to the atmosphere at 298 K.

$$\eta_{refrigeration} = \frac{T_C}{T_H - T_C} = \frac{T_{N_2}}{T_{ambient} - T_{N_2}} \quad (2)$$

The amount of heat required in the hot reservoir, Q_H is given by

$$Q_H = \frac{W_{separation}}{\eta_{separation}} \quad (3)$$

The energy rejected from the engine Q_C is given by

$$Q_C = Q_H - W_{separation} \quad (4)$$

For the refrigeration system, the energy required for the process ($W_{refrigeration}$) is given by

$$W_{refrigeration} = \frac{Q_C}{\eta_{refrigeration}} \quad (5)$$

For the power cycle, the energy required to provide the separation work, $Q_{\text{combustion}}$ is given by

$$Q_{\text{combustion}} = \frac{W_{\text{refrigeration}}}{\eta_{\text{generation}}} \quad (6)$$

Where

$$\eta_{\text{generation}} = \frac{T_H - T_C}{T_H} = \frac{T_{\text{steam}} - T_{\text{ambient}}}{T_{\text{steam}}} \quad (7)$$

The efficiency of the power cycle was calculated to be 0.66.

The quantity of methane required to produce energy $Q_{\text{combustion}}$ is given by

$$N_{\text{CH}_4} = \frac{Q_{\text{combustion}}}{\Delta H} \quad (8)$$

Where ΔH is enthalpy of the combustion reaction of methane. The value is - 802.3kJ/mol.